THE UNIVERSITY OF ALBERTA

RELEASE FORM

NAME OF AUTHOR   W. S. KENDAL

TITLE OF THESIS   OSCILLATORY MOTION OF INTRAAXONAL

                       ORGANELLES FOLLOWING INHIBITION OF THEIR

                       RAPID TRANSPORT

DEGREE FOR WHICH THESIS WAS PRESENTED MASTER OF SCIENCE

YEAR THIS DEGREE GRANTED   FALL 1982

THE UNIVERSITY OF ALBERTA

OSCILLATORY MOTION OF INTRAAXONAL ORGANELLES FOLLOWING

INHIBITION OF THEIR RAPID TRANSPORT

by

©   W. S. KENDAL

A THESIS

SUBMITTED TO THE FACULTY OF GRADUATE STUDIES AND RESEARCH

IN PARTIAL FULFILMENT OF THE REQUIREMENTS FOR THE DEGREE

OF MASTER OF SCIENCE

IN

EXPERIMENTAL SURGERY

DEPARTMENT OF SURGERY

EDMONTON, ALBERTA

FALL 1982

THE UNIVERSITY OF ALBERTA

FACULTY OF GRADUATE STUDIES AND RESEARCH

The undersigned certify that they have read, and
recommend to the Faculty of Graduate Studies and Research,
for acceptance, a thesis entitled OSCILLATORY MOTION OF
INTRAAXONAL ORGANELLES FOLLOWING INHIBITION OF THEIR RAPID
TRANSPORT submitted by W. S. KENDAL in partial fulfilment of
the requirements for the degree of MASTER OF SCIENCE in
EXPERIMENTAL SURGERY.

ABSTRACT

To clarify the dynamics of axonal transport, two
features of this process were studied: (1) The motion of
intraaxonal organelles after inhibition of rapid axonal
transport, and (2) the fine structure of axons after
freezing and thawing.

Axons from *Xenopus laevis* were treated in solutions of
colchicine, dinitrophenol, or dimethylsulfoxide. Other axons
were treated with hypertonic potassium glutamate, heavy
water, or were frozen in liquid nitrogen and then rapidly
thawed. The movements of intraaxonal organelles were
observed in all preparations with dark-field microscopy.
Film records of the movements were made and the data were
compiled by computer. The analysis of data consisted of
calculating: the standard deviations of positional
fluctuations, instantaneous velocities, velocity
distributions, and periodograms. In addition, specimens of
thawed nerve were examined with electron microscopy.

In all of the preparations, transport of organelles was
inhibited. However, many organelles moved back and forth
about fixed positions with a frequency of about 0.1 Hz. The
standard deviations of these movements were maximally five
micrometers. Also the movements were aligned with the
longitudinal axis of each axon. Similar positional
fluctuations were found superimposed on the linear
displacements of transporting organelles.

ACKNOWLEDGMENTS

Table of Contents

List of Tables

List of Figures

List of Plates

1. INTRODUCTION

1.1 The Problem

An intracellular movement of material occurs between
nerve cell bodies and the distal reaches of their axons.
This movement is called axonal transport. Under a high
powered microscope, transport appears as a longitudinally
directed movement of intracellular particles (Cooper and
Smith 1974). The movements of individual particles are
complex. While they move predominantly in retrograde or
anterograde directions, they may temporarily reverse
direction.

Under certain conditions axonal transport is inhibited,
and the previously translating particles then oscillate back
and forth about fixed positions (Hammond and Smith 1977). It
is not known whether these oscillations are a residual
component of an impaired transport process, or if they
result from an unrelated process.

The oscillatory motion can only be driven by thermal or
active forces. Thermal forces result from surrounding
molecular motions as with Brownian motion, while active
forces result from processes requiring energy from
metabolism. If the motion is thermally driven, then it is
possible to infer from the character of the motion the
viscosity and other properties of the axonal microstructure.
If instead the process is active, then it is likely related

to the mechanisms which drive axonal transport.

This thesis contains a study of several aspects of the oscillatory motion of intraaxonal particles. First, the conditions causing the residual oscillations are investigated. Second, the action of a metabolic blocker on this motion is examined in an attempt to distinguish between active and thermal forces. Third, the motion is quantitatively analysed and calculations are made of the standard deviations of the displacements, instantaneous velocities, velocity distributions, and periodograms. These calculations are then compared to predictions from Brownian theory, and to similar calculations obtained from transporting particles. By these means, it is possible to conclude whether the oscillatory motion results from thermal motion or if it is a component of axonal transport.

In addition to the study of oscillatory motion within axons, axonal microstructure is examined to see what effect this has on particle motion. For this purpose, axons were rapidly frozen and thawed, and then either the particle movements were observed with light microscopy, or the structural changes were studied with electron microscopy.

The final aim was to attempt to characterize the motion of intraaxonal particles. By means of the quantitative methods used in this study it was hoped that the results would allow a critical examination of the prevailing theories of axonal transport, and perhaps allow a better understanding of the mechanisms involved.

In the remaining introduction, the subject of axonal transport is reviewed. Particular emphasis is placed on the motion of optically detectable organelles within cells, and the conditions which produce oscillatory motion within neurons. Because the cytoplasmic medium which contains these organelles also affects their motion, the physical properties of axoplasm are reviewed. Finally, several postulated mechanisms for fast axonal transport are presented and criticized.

1.2 Axonal Transport

1.2.1 General Features

Axonal transport is a large and complex subject. In this review only areas pertinent to this thesis are discussed. The reader is referred to other reviews for a more general coverage (Ochs 1974; Schwartz 1979; Grafstein and Forman 1980).

Axonal transport can be classified into two broad categories based on the speed of transport (Grafstein and Forman 1980). The first is slow transport, or axonal flow. It occurs at speeds of 0.4 to 5 mm/d. The major structural components of axons: microtubules, neurofilaments, and actin filaments are transported at these speeds.

This study deals primarily with the second category—fast axonal transport. In fast transport the speeds may

.

reach 500 mm/d. A wide variety of materials such as proteins, lipids, synaptic transmitters, and various enzymes are transported via the fast system. (Grafstein and Forman 1980). Table 1.1 contains a list of some of these materials. Many diverse materials are transported at similar rates (Sabri and Ochs 1973).

Rapid axonal transport is bidirectional. Materials, originating in the cell body, are transported to the terminal axon where they may reverse direction and be transported back. This reversal of transported material was well demonstrated in studies of [^{14}C] leucine transport in leghorn chickens (Bray *et al.* 1971). Exogenous material, such as [^{125}I] labeled tetanus toxin, may also be taken up at the axonal terminal and be transported to the cell body at speeds of 264 ± 33 mm/d (Shield *et al.* 1977). Generally, the speed of retrograde transport is slower, but it is still within the same order of magnitude as anterograde transport. Retrograde transport is affected by the same agents that inhibit anterograde transport (Grafstein and Forman 1980). These similarities between retrograde and anterograde transport suggest that they both depend on equivalent mechanisms.

The form of the material transported within axons has been studied. Sabri and Ochs (1973), working with the transport of [^{3}H] leucine in cat sciatic nerves, homogenized and then centrifuged the transported material. They found a small proportion of the transported material was soluble

TABLE 1.1

Substances Transported By Fast Axonal Transport

<u>Membrane</u> <u>Constituents</u>

proteins
glycoproteins
lipids

<u>Synaptic</u> <u>Transmitters</u>

norepinephrine
acetylcholine
serotonin
dopamine

<u>Transmitter</u> <u>Related</u> <u>Enzymes</u>

choline acetyltransferase
dopamine β-hydroxylase
monoamine oxidase
catecol o-methyltransferase

<u>Retrograde</u> <u>Transport</u> <u>Of</u> <u>Exogenous</u> <u>Materials</u>

nerve growth factor
horseradish peroxidase
tetanus toxin
cholera toxin
herpes simplex virus
rabies virus
varicella zoster virus
polio virus

while most was particulate. In another study, Elam and
Agranoff (1971) analysed transported [^{3}H] proline and [^{3}H]
asparagine from goldfish optical nerves. In this study, 80%
of the protein transported was associated with particles. In

a third study, Cancalon and Beidler (1975), working with
[^{3}H] leucine in garfish olfactory nerve, noted that most of
the rapidly transported material was associated with
constituents of cell membranes. These findings have been
confirmed by many investigators. Transported materials are
generally particulate and are associated with membranes
(Rambourg and Droz 1980).

The classification of axonal transport into fast and
slow components has been disputed by some researchers. *In
vivo* experiments with the transport of [^{3}H] leucine in
rabbit hypoglossal nerve have shown four separate groups of
materials moving along nerve at different rates (Appeltauer
and Korr 1975). In other experiments, with [^{35}S] methionine
and rabbit optic nerve, Lorenz and Willard (1978) claimed to
find five groups of transport:

1. polypeptides transporting at greater than 240 mm/d that
   were associated with membranous material,
2. proteins transporting at 34 to 68 mm/d that were
   associated with mitochondrial material,
3. actin binding polypeptides, actin, and tubulin
   transporting at 4 to 8 mm/d,
4. similar material as in item 3 transporting at 2 to 4
   mm/d,
5. high density materials such as neurofilaments
   transporting at 0.7 to 1.1 mm/d.

While the classification of axonal transport into several
distinct components remains controversial, these findings do

indicate that different materials are transported at different speeds.

1.2.2 Methods Of Observing Axonal Transport

Many different techniques have been used to study axonal transport. In an early experiment, Weiss and Hiscoe (1948) found that nerve became distended just proximal to a constricting lesion. They postulated a distally directed flow of axoplasm towards the lesion. Later experiments demonstrated accumulation of radiolabeled material at distal sites. One example of these later experiments involved the accumulation of [³H] leucine in the optic tectum of goldfish, after being transported along the optic nerves (McEwen and Grafstein 1968). By means of biochemical assay this accumulation can also be confirmed. For example, Lubinska and Niemierko (1971) found that acetylcholin-esterase accumulated at the ends of transected dog nerves. These accumulation studies provided a way to confirm the transport of materials within axons.

The transported material can be analysed by additional techniques. Cell fractionation and gel electrophoresis are useful methods. Cell fractionation has been mentioned previously (Elam and Agranoff 1971). Willard and associates (1974) studied the transport of [³⁵S] methionine in rabbit retinal neurons using gradient gel electrophoresis and autoradiography. They found 43 different polypeptides in the transported material. Both cell fractionation and gel

electrophoresis demonstrate the heterogenous composition of transported materials.

Radioisotope techniques have been very important in studying axonal transport. Autoradiography and liquid scintillation counting are the main techniques. Droz and Leblond (1962) used autoradiography to find that [³H] leucine moved as a distally-directed front within rat sciatic nerve at a speed of 1.5 mm/d. Moreover, it is possible to infer the progression of radiolabel within axons by using liquid scintillation counting. Lasek (1968) treated the ganglia of cat sciatic nerves with [³H] leucine. He then incubated nerves for sequentially longer periods of time before segmenting each nerve and analysing the amount of radioactivity in each segment. Lasek concluded that transport occurred at speeds of 500 mm/d and 1.3 mm/d. A newer technique even allows the measurement of radioactivity as it is transported within living and intact nerves. This newer technique employs a radiation imaging device (Snyder et al. 1976).

Another method of observing axonal transport involves dark-field, phase contrast, or Nomarski microscopy (Allen et al. 1969). By these optical methods, organelles were observed to transport longitudinally within axons (Cooper and Smith 1974; Forman et al. 1977a). Optical methods were used in the present study and are discussed in greater detail in a following section.

1.2.3 Inhibitors Of Fast Axonal Transport

Many different agents will inhibit fast axonal transport (Table 1.2). For some of these agents the mechanism of inhibition is not clear (Grafstein and Forman 1980). The inhibitory agents used in this study are discussed in the following text.

Colchicine inhibits axonal transport (Edstrom and Mattsson 1972; Hanson and Edstrom 1977). Colchicine also depolymerizes microtubules (Margolis and Wilson 1981). These two actions of colchicine suggest that intact microtubules are required for axonal transport. However, Byers (1974) reported the continuation of transport of [³H] proline in rabbit vagus nerves despite depleted numbers of microtubules. Thus a dependence of fast axonal transport on microtubules remains controversial (Grafstein and Forman 1980).

Low temperatures also inhibit rapid transport. Brimijoin and associates (1979) observed inhibition of transport at temperatures below 13°C in rabbit nerve and 10°C in frog nerve. Other workers have noted similar temperature effects (Grafstein and Forman 1980). Low temperatures also cause microtubules to depolymerize (Rodriguez-Echandia and Piezzi 1968). Indeed, Brimijoin's group found a decreased density of microtubules in cooled axons. However, they also noted that transport continued despite 35% fewer microtubules in rabbit nerve and 65% fewer in bullfrog nerve. If microtubules are necessary for

TABLE 1.2

Inhibitors Of Fast Axonal Transport

Agent	Postulated Mechanism
colchicine	destruction of microtubules
vincristine	
vinblastine	
podophyllotoxin	
griseofulvin	
high $[Ca^{+2}]$	
low temperature	
heavy water	stabilization of microtubules
dimethylsulfoxide (DMSO)	
dinitrophenol (DNP)	blocked oxidative metabolism
sodium cyanide	
100% nitrogen	
calcium chelators	removal of calcium
batrachotoxin	sodium flux into cells

transport, then normal nerve must contain more microtubules than are necessary for transport.

High calcium ion concentrations will inhibit transport. Edstrom (1974) noted such an effect with 15 to 20 mM Ca^{+2}: this was concurrent with decreased microtubule numbers on electron microscopy. Also, microtubules are depolymerized by high calcium ion concentrations (Schliwa *et al.* 1981). While these results suggest a dependence of transport on microtubules, they have been contested. Brady and associates (1980) claimed that fast transport of [^{3}H] proline persisted in rat sciatic nerves exposed to 75 mM Ca^{+2}, despite a

complete loss of microtubules. Not only has the dependence of transport on microtubules been disputed by Brady, but also the inhibitory action of high calcium ion concentrations on transport has been questioned.

Heavy water inhibits axonal transport (Anderson *et al.* 1972). While heavy water stabilizes microtubules and increases the consistency of cytoplasm, its action on axonal transport is not fully understood. An effect purely from the increased viscosity of heavy water (1.26×10^{-3} Pa$\bullet$s) versus that of water (1.01×10^{-3} Pa$\bullet$s) should not be enough to account for inhibited transport.

Dimethylsulfoxide, in 10% concentration, also blocks rapid transport (Donoso *et al.* 1976). This effect may be secondary to DMSO preventing microtubules from depolymerizing. If this stabilizing action of DMSO is responsible for inhibition of transport, then this could imply that microtubules must be able to depolymerize in order to function. Donoso's group also noted that DMSO caused marked changes in cross-sectional area of axons. These area changes may result from alterations in the axonal microstructure. Perhaps, structural changes unrelated to microtubules are what allows DMSO to inhibit transport.

Dinitrophenol inhibits transport within fifteen minutes of its application to nerves (Ochs and Hollingsworth 1971). Since DNP is known to block oxidative phosphorylation, a reasonable conclusion is that transport critically depends upon oxidative metabolism.

1.3 Organelle Transport

1.3.1 General Description

The irregular motion of organelles within living cells has intrigued many investigators. Rebhun (1959; 1972) used the term *saltatory* to describe this motion. In order to differentiate saltatory motion from Brownian motion he devised several criteria based on the characteristics of motion. These criteria were:

1. intermittent and variable jumps of several microns,

2. velocities of several micrometers per second,

3. discontinuous changes in velocity, and

4. a discontinuous and non-Gaussian distribution of lengths of jumps.

Rebhun concluded that the fourth point best differentiated saltations from Brownian motion, since Brownian displacements have a Gaussian distribution. He also estimated that the lengths of saltatory displacements could possibly be within the probable range for Brownian motion; thus this feature was of limited usefulness.

Saltatory movements occur within a variety of cells. In this work, the movements of particles within axons are studied. The motion of intraxonal particles has been labeled saltatory (Rebhun 1972). This motion is discussed in greater detail here.

Organelles may be observed transporting within living axons by means of dark-field or Nomarski microscopy. Cooper

and Smith (1974) observed organelles that were 0.2 to 0.5 micrometers in diameter moving in both directions, longitudinally, within axons of *Xenopus laevis*. The ratio of the number of particles travelling distally to those travelling proximally was ten to one. Individual particles exhibited unexpected stops, starts, and partial reversals in direction. The velocities of individual particles varied with time but were generally around one micrometer per second. These observations of organelle movements have been reproduced by other workers using different preparations (Breuer *et al.* 1975; Forman *et al.* 1977a; Leestma and Freeman 1977).

The type of organelles involved in transport has been recently studied (Smith 1980). By means of electron microscopy of axons from *Xenopus laevis*, these organelles have been identified as dense lamellar bodies, membranous vesicles, multivesicular bodies, and small mitochondria. Clearly, transport is not specific to one type of organelle.

While radioisotope studies have demonstrated a significant transport directed towards the axonal terminal, optical studies have shown predominantly retrograde transport. It has been proposed that most anterograde moving particles are too small to be resolved by light microscopy (Forman *et al.* 1977a). Indeed, electron microscopy of axons has shown an accumulation of organelles on both sides of constricting lesions (Smith 1980). On the distal side of a constricting lesion the organelles were larger and

resolvable by light microscopy. On the proximal side, membrane bounded organelles of about 50 nm diameter accumulated. The inference here was that these smaller organelles accumulated as a result of axonal transport. Thus, it is reasonable to assume that anterograde transport involves particles too small for optical resolution.

Several other characteristics of optically detectable movement within axons have been documented:

1. Both Cooper and Smith (1974) and Breuer et al. (1975) noted that individual organelles moved independently of other organelles.

2. Forman et al. (1977a) noted that while organelles moved predominantly along the longitudinal axis, there was no evidence that particle motion was restricted to specific channels within axons.

3. Leestma and Freeman (1977) found that some particles moved back and forth several times over short distances before passing nonmoving organelles or obstructions.

From these observations it is evident that organelle movements within axons are complicated.

How well does the term saltatory describe the motion of intraaxonal particles? While the irregular movement of organelles in some preparations grossly fits this description (Leestma and Freeman 1977; Forman et al. 1977a), Cooper and Smith (1974) noted that most organelles showed "an almost continuous motion which took place in what appeared to be major periods of acceleration and retardation

of about ten micrometers length". A more sophisticated
analysis of movements within axons of *Xenopus laevis* (Koles
et al. 1982a), clearly showed that particle velocity was a
smooth, continuous function of time. Velocity did, however,
change more abruptly with position. When displacements of
particles were analysed with respect to time, significant
low frequency variations in position were found superimposed
on linear trends. Since saltatory motion, by definition, is
characterized by abrupt changes in velocity and position,
the movement of organelles within axons from *Xenopus laevis*
does not seem to be saltatory.

1.3.2 Inhibitors Of Organelle Transport

If the transport of optically detectable organelles
within axons corresponds to the transport of radioactive
labels in nerves then agents affecting transport of
radiolabel should also influence organelle transport.
Indeed, studies done with dinitrophenol (Kirkpatrick *et al.*
1972), colchicine (Hammond and Smith 1977), and with low
temperature (Forman *et al.* 1977b) demonstrated inhibition of
organelle transport. There are no reports on the effect of
dimethylsulfoxide, heavy water, or high calcium ion
concentrations on organelle movements. It is, however,
reasonable to conclude that optically detectable transport
and radioisotope transport are different aspects of the same
process.

1.3.3 Oscillatory Motion Of Organelles

In unimpaired nerve, most intraaxonal particles will transport in one net direction. Reversals in direction are infrequent, occur over distances of less than one micrometer, and are transient. Particles have a strong tendency to move in one direction (Cooper and Smith 1974; Breuer *et al.* 1975; Leestma and Freeman 1977; Forman *et al.* 1977a). In only 4 of 1000 particles tracked by Forman's group did particles reverse their net direction. A small number of particles will move back and forth about fixed positions. Leestma and Freeman (1977) observed this fixed motion in 5 of 272 particles using cultured murine spinal chord. Thus a general tendency for particles to move in one net direction is clearly evident, but there is also some capability for a particle to reverse its direction.

Certain agents will inhibit organelle transport, leaving a residual back and forth motion about fixed positions. Hammond and Smith (1977) observed a one micrometer wobble of organelles about fixed positions within axons of *Xenopus laevis* that were exposed to colchicine. This effect was observed during a phase of partial inhibition of transport of organelles. Similarly, Horie and associates (1981) observed a fixed wobble of organelles within cultured nerve of chick embryos that were treated with colchicine. Another observation of back and forth organelle movement was made in association with constricting axonal lesions in *Xenopus laevis* (Smith 1980). In this

preparation some particles moved back and forth over distances of up to twenty micrometers. No other conditions producing back and forth motion within axons have been described. Neither is it known whether the wobble produced by certain inhibitory agents is related to the transient back and forth motion observed in unimpaired nerve. In this thesis, the conditions producing this oscillatory motion are investigated.

The significance of the residual wobble is unknown. This wobble may be a residual component of unimpaired transport. It could be an exaggeration of the propensity for transporting particles to reverse direction. On the other hand, this wobble may be a form of Brownian motion. This present study is an investigation of this residual wobble.

1.4 Physical Properties Of The Cell Interior Affecting Transport

1.4.1 Intraaxonal Structure

Axons contain an abundance of submicroscopic structures. Besides mitochondria, smooth endoplasmic reticulum, and organelles moved in transport, there is an abundance of fibrillar elements (Table 1.3). Microtubules and neurofilaments are the principal fibrillar elements (Bray and Gilbert 1981). These fibrils extend longitudinally within axons. Weiss and Mayr (1971) found an orderly

TABLE 1.3

Main Fibrillar Constituents Of Axons

Structure	Properties
Microtubule	long cylinder composed of tubulin 25 nm in diameter
Neurofilament	long linear polypeptide rod 10 nm in diameter the commonest constituent of axons
Microfilament	actin composed fiber 7 nm in diameter

arrangement of fibrillar components within rat nerve. Neurofilaments were evenly spaced 0.04 micrometers apart, and microtubules extended along the axon's length. The role of these fibrillar elements is unclear (Bray and Gilbert 1981). These elements may have a role in maintaining cell form, and in intracellular transport.

Porter, Byers, and Ellisman (1979) proposed a more definite role for these fibrillar constituents. They based their speculations on the results of high-voltage electron microscopy. In their model, a "three dimensional lattice" was constructed from the fibrils. Enveloping this "cytoskeleton" was an aqueous phase. Extending from the framework were "microtrabeculae", linking the framework to vesicles, plasma membrane, smooth endoplasmic reticulum, and multivesicular bodies. This framework could constrain the

Brownian motion of particles contained within, and local conformational changes could induce saltatory motion of these particles. However, even if the structures observed were not artifactual, their dynamic properties and function remain hypothetical.

There are several ways that intraaxonal structure could affect transport. First, it is reasonable to assume that one or more of the structures, seen with electron microscopy, are involved in the mechanism for axonal transport. Second, the fibrillar elements may constrain organelle motion to certain directions or regions within axons. Third, these fibrillar structures may alter the viscoelastic properties of their surrounding axoplasm thus affecting resistance to organelle motion.

1.4.2 Axoplasmic Viscosity

The viscous resistance of axoplasm likely influences the transport of organelles. Biondi and associates (1972) measured the viscosity of frog axoplasm by its flow through a microcapillary tube. They found a viscosity of 10^3 Pa•s. Also, they noted that axoplasm was pseudoplastic, that is, viscosity decreased with increased rate of shear. In another experiment, Rubinson and Baker (1979) forced axoplasm from squid giant axons through a cellulose acetate tubule. The squid axoplasm had a viscosity of 15 Pa•s, and a yield stress of 11 Pa. Treatment of squid axoplasm with millimolar calcium solutions reduced its viscosity markedly.

Different techniques produce different viscosity values. Using the electron spin label, Tempone, Haak and associates (1976) found a viscosity of 5×10^{-3} Pa•s within cat sciatic nerve. Also Arhem (1975), with his current clamp method on *Xenopus laevis* axons, observed that diffusion coefficients for small ions were similar to those in water. This implied a viscosity similar to that of water.

Two conclusions can be drawn from the viscosity data:
1. The difference between the bulk viscosities of Biondi and Rubinson and the microscopic viscosities of Haak and Arhem arises from structures within the axoplasm.
2. Viscous resistance to a particle's movement depends upon the particle's size in relation to the microstructure.

1.4.3 Brownian Motion Of Organelles

Brownian motion may occur within cells (Shea and Karnovsky 1966). It is difficult, however, to distinguish between Brownian motion and the motion caused by metabolic processes. It was for this reason that Rebhun (1972) defined his criteria for saltatory movements. Generally small, rapid, and randomly directed movements can be attributed to Brownian motion. Taylor (1965) observed two types of movements of particles in cells of *Tritus viridescens*. One consisted of twenty micrometer displacements occurring in up to three second intervals. The second consisted of finer random displacements. Taylor designated these movements as saltatory and Brownian respectively. Piddington (1976) was

able to distinguish between saltatory and Brownian motion within cells of *Nitella* by using laser light scattering. The photon correlations Piddington obtained had different forms, depending on the manner in which particles moved with respect to each other. In both of these experiments the distinction between Brownian and active processes was based on plausibility arguments.

Within cells of highly developed organisms, Brownian motion is not easily observed (Shea and Karnovsky 1966). This is probably due to a more structured cytoplasm constraining any organelle movement.

1.5 Postulated Mechanisms Of Fast Transport

The mechanism of axonal transport is unknown. Several models have been proposed (Table 1.4). Models for axonal transport can be classified into three groups:

1. ratchet mechanisms,

2. fluid flow mechanisms,

3. smooth endoplasmic reticulum mechanisms

(Grafstein and Forman 1980). Particles are transported in the ratchet mechanisms by a series of incremental forces exerted by a motionless structure. In the fluid flow models, material is transported within a stream of axoplasm. The final group involves transport within a continuous system of smooth endoplasmic reticulum. Current examples of each mechanism are discussed in the following text.

TABLE 1.4

Models For Fast Axonal Transport

Ratchet Mechanisms

Schmitt 1968	particle microtubule interaction
Ochs 1971	transport filament
Samson 1971	particle-anionic polyelectrolyte interaction
Kerkut 1975	coded vesicles on transport filament
Goldberg 1978	reversible particle-carrier binding
Rubinow 1980	reversible particle-carrier binding

Fluid Flow Mechanisms

Weiss 1970	peristalsis in microtubules
Gross 1977	microstream flow
Odell 1976	flow induced by oscillating filaments

Smooth Endoplasmic Reticulum (SER)

Droz 1975	transport within SER

Other Mechanisms

Hejnowicz 1970	longitudinal electro-osmotic forces

1.5.1 Ratchet Mechanisms

In Schmitt's (1968) model, particles are transported by a series of incremental forces exerted by microtubule tracks. Each particle successively binds to a microtubule and is released as a new bond forms further along the microtubule. Schmitt did not explain the mechanism of microtubule binding. However, Samson (1971) provided a

further modification of this theory that did. Samson proposed that microtubules are coated with a layer of anionic polyelectrolytes. These polyelectrolytes, by means of sequential binding of particles followed by conformational changes and release of particles, provide the mechanism to move particles.

The problem of how a diverse variety of materials— vesicles, macromolecules, and soluble material— could be transported at the same speed, led Ochs (1974) to propose a transport filament model. In this model, the material transported is bound to actin-like filaments. Crossbridges are continually formed and broken between the filaments and microtubules. Motion occurs in analogy to the sliding filament theory of muscle. A transport filament thus slides along its microtubule guide under the control of a Ca^{+2} and Mg^{+2} dependent ATPase.

Kerkut (1975) developed his "coded vesicles theory" of axonal transport in order to explain how so many different materials could transport with different speeds and directions. In this theory, the transported material is contained within a vesicle. On the vesicle's surface is a specific protein, coding the type of material, rate, and direction of transport. To each vesicle a specific myosin-like filament is bound. The filament then slides along a framework of actin fibers within an axon, and carries the vesicle in the required direction and speed as determined by the coded instructions. Vesicles may transfer

from transport filament to filament, and may even reverse
direction.

Two additional models deal with particles binding to a
carrier system. In the first model, Goldberg and associates
(1978) proposed that particles could alternate between
stationary and moving states by reversibly binding to a
carrier system. The carrier transports particles at a
constant speed, and the fraction of time a particle spends
moving depends on the concentration of particles. The net
speed of transport thus depends on concentration.

In the second model, Rubinow and Blum (1980) assumed
reversible binding of particles to a carrier system and then
derived a travelling wave solution. The carriers transport
at a constant group speed, and by allowing different binding
constants for different materials, a wide spectrum of
transport speeds results. Rubinow's theory has been shown to
be similar to Goldberg's theory (Mackey *et al.* 1981).

1.5.2 Fluid Flow Mechanisms

Three examples of fluid flow mechanisms are discussed
here. In the first example, Weiss (1970) proposed that
materials may be transported within the core of microtubules
by a peristaltic mechanism. Axoplasm is propelled by
conformational constrictions propagating along each
microtubule.

The second example is Gross's and Weiss's (1977)
microstream model. Here transport occurs within microstreams

that flow in the vicinity of microtubules. Microtubules, by exerting longitudinal shear forces on their surrounding axoplasm, cause the thixotropic axoplasm to liquefy and flow. Larger particles are swept along within microstreams while soluble material diffuses out of these streams. There are thus two phases of axoplasm:

1. a stationary gel, and

2. a flowing sol.

Particles may reversibly bind to this gel (Gross and Weiss 1981) with different affinities depending on the chemical nature of each particle. The result is a variety of transport velocities, depending on the affinity of the specific material for the gel. With both anterograde and retrograde microstreams, bidirectional transport can occur.

The last example of a fluid flow model was proposed by Odell (1976). In his model, a group of longitudinally orientated intraaxonal filaments induce their surrounding axoplasm to flow by periodic contractions and relaxations. Material is then transported within this flowing axoplasm. For soluble material, its speed of transport is proportional to the cube root of its molecular mass.

1.5.3 Transport Within The Smooth Endoplasmic Reticulum

Droz and Rambourg (1975) proposed that transport occurred within a system of smooth endoplasmic reticulum. This system, they postulated, extended continuously throughout axons. Various materials are transported distally

within this system. At the distal reaches of axons, vesicles
that contain transported material then bud off the
endoplasmic reticulum and migrate to the cell membranes. A
retrograde system for transport also exists, but it moves
material contained within vesicles back to the cell body
(Rambourg and Droz 1980). The actual mechanism for transport
was not elaborated on for either the anterograde or
retrograde systems.

The final model discussed here does not fit into the
above classification. In this model Hejnowicz (1970)
proposed that particles are moved by longitudinal
electrophoretic forces propagating along intracellular
fibrils. Each fibril maintains a concentration gradient of
ions across its surface. A conformational change within each
fibril propagates along its length, releasing its stored
ions. The resulting variations in the surrounding electric
fields cause charged axonal particles to move along adjacent
fibrils.

1.6 Critique Of Mechanisms

The variety of postulated models for fast axonal
transport indicates that no particular model is generally
considered to be satisfactory. In this section evidence for
and against each model is discussed.

Schmitt's (1968) and Samson's (1971) models can be
considered together since they both postulate that particles

move along microtubule tracks. Both of these models predict
a jerky motion of particles within axons. This motion
results from a sequential binding, movement, and release of
particles from bonds formed in the vicinity of microtubules.
However, while the predicted motions of particles would be
discontinuous, this motion could not explain the observed
variations in motion (Koles *et al.* 1982a). The predicted
jumps in both Schmitt's and Samson's theories would have to
occur over intervals similar to intermolecular distances,
while the observed variations in motion occurred over
several micrometers.

One major assumption of Schmitt's and Samson's theories
is that microtubules function as guides. Circumstantial
evidence does exist for some form of longitudinally directed
guide within axons (Smith and McLeod 1979). The evidence
comes from the correlation of paths taken by particles with
the arrangement of microtubules within axons. However, the
role of microtubules in axonal transport remains
controversial (Grafstein and Forman 1980). If a structural
constraint exists for particle movements, it does not
necessarily have to be microtubules.

Neither Schmitt's nor Samson's models could explain how
different materials were transported at similar speeds. As
noted previously, this problem led Ochs (1974) to propose
his transport filament model. Conceptually, Ochs's model is
appealing since it is analogous to the generally accepted
model for muscle contraction. Several predictions follow

from Ochs's model (Ochs 1981):

1. Transport filaments should be isolable.

2. Filaments should bind to the variety of materials
    transported.

3. Crossbridges between filaments and their tracks should
    be demonstrable.

None of these predictions has yet been confirmed by
experiment.

Besides the fact that diverse materials are transported
at similar speeds, materials are also transported at
different speeds. Ochs's model could not account for this
finding without modification. Kerkut (1975) modified the
transport filament model with his "coded vesicles theory".
Kerkut's model is considerably more complicated than Ochs's
model— this reflects the complexity of axonal transport.
Kerkut makes specific predictions regarding the encoding of
vesicles, an actin filament network, and the existence of
transport filaments. None of these features has been
confirmed by experiment.

One other problem with both Ochs's and Kerkut's models
is the nature of the resulting motion. Recent observations
demonstrate a low frequency variation in velocity for any
individual particle (Koles *et al*. 1982a). There is no
feature of the transport filament models that allows for a
variation in velocity. Further modifications of both
theories are necessary to agree with observations.

Goldberg's (1978) and Rubinow's (1980) theories both have similar predictions. The first prediction is a dependence of transport speed on concentration of particles (Mackey *et al.* 1981). Goldberg used this prediction to explain the behavior of pulses of [³H] serotonin in neurons from *Aplysia californica*. However, a dependence of speed on concentration has not been found by other investigators (Brimijoin 1979; Snyder 1982), and this prediction remains controversial.

A second prediction from Goldberg's and Rubinow's theories was saltatory motion. This results as individual particles interact with carriers. A jerky motion of particles has not been observed with more advanced cinemicrographic techniques (Koles *et al.* 1982a). On the contrary, the motion is smoothly varying. The alternation from moving to nonmoving states in both of these theories was originally used to account for saltatory motion within axons. Now that saltatory motion is known not to occur within certain axons, modifications to both theories are required.

A third prediction from the two theories was a bimodal velocity distribution. This results from the alternation of particles between moving and nonmoving states. However, this prediction is not supported by observation. The observed velocity distributions are unimodal (Koles *et al.* 1982a).

Major problems arise from Weiss's (1970) theory of peristalsis within microtubules. There is no evidence that

microtubules are capable of peristaltic changes in their structures. Furthermore, 0.2 micrometer diameter particles have been observed to transport within axons; they cannot move within 25 nm diameter microtubules. A significant flow would have to exist outside the microtubules in order to move these particles.

In Gross's and Weiss's (1977) model of transport, a significant flow occurs in the vicinity of microtubules. The microstream model is supported by the observed faster transport speeds for particles relative to soluble material. However, this effect is predicted by other theories (Odell 1976). More specific support would result if dyes were shown transporting within microstreams, but this has not been demonstrated (Grafstein and Forman 1980). In addition, neighbouring particles within a single microstream should move in a coordinated manner since they are passively carried by the stream. Quite the opposite has been observed (Cooper and Smith 1974; Breuer *et al*. 1975); motion between particles is uncoordinated.

Odell's (1976) model for transport has some testable features:

1. Speed of transport should depend on molecular mass. This has not yet been verified.

2. A maximal speed of transport is predicted. This is 56,000 cm/d (Rubinow and Blum 1980), and it is much too high.

3. Neighbouring particles should demonstrate some

correlation in movement. As noted above, this has not been observed.

Evidence for involvement of smooth endoplasmic reticulum with transport is based on electron micrographs of radioautographs taken from axons (Droz and Rambourg 1975). This indirect method shows a close relationship of transported radiolabel with SER. However, the association does not automatically imply that transport occurs within SER (Schwartz 1979). There is also some controversy about whether SER forms a continuous system within axons (Porter et al. 1979), although the lack of continuity found by some may be due to staining techniques (Rambourg and Droz 1980). Rambourg's and Droz's (1980) model invokes an additional mechanism to transport vesicles from the axonal terminals to the cell body. Since anterograde transport of vesicles is known to exist (Cooper and Smith 1974), it seems much simpler to rely on one mechanism for both anterograde and retrograde transport rather than to introduce a new mechanism for anterograde transport.

The physical form of the material transported is important in some models. In Schmitt's model material is packaged within vesicles. In the transport filament model it is bound to carriers, and in the fluid flow models it can be either particulate or soluble. As noted previously, cell fractionation demonstrates a significant particulate component of transport.

Is there an advantage to transporting particles versus small molecules? The answer to this question might be found by studying the process of diffusion. The diffusion coefficient, D, is given by:

$$D = kT/(6 \pi \eta a)$$

<div align="right">(1.1)</div>

Here, k is Boltzman's constant (1.38×10^{-23} J/°K), η is viscosity, a is the radius of a particle, and T is temperature. For a particle moving as a result of diffusion, the time required to move a distance x is approximately x^2/D. However, for a particle moving as a result of directed transport, the time to move the same distance is x/u. Here u is the particle's average speed. The ratio of the time to move a given distance by transport versus that by diffusion is called the stirring number, s (Purcell 1977):

$$s = x \bullet u/D.$$

<div align="right">(1.2)</div>

The stirring number essentially indicates the effectiveness of directed transport in situations where diffusion has a significant influence on transport.

When $s < 1$, the movement of material is dominated by diffusion. It will take less time to move a given particle a distance x by diffusion, than by directed transport. If

large numbers of similar particles are observed, then any changes in the concentration of the particles, that are caused by directed transport, are dissipated by diffusion.

The diffusion coefficient of the particle has a major influence on the stirring number. Small molecules generally have diffusion coefficients of about 10^{-9} m^2/s. A particle of 0.2 micrometers radius in water at 294°K has a diffusion coefficient [Eq. (1.1)] of 1×10^{-12} m^2/s. With all other conditions being equal, the stirring number is three orders of magnitude larger for the particle than for small molecules. The dissipative effect of diffusion would be 10^3 times greater for the small molecules. Directed transport is thus more effective with larger particles than with small molecules.

Mechanisms whereby particles are transported through a motionless fluid can be compared to mechanisms whereby particles are carried in a fluid stream, on the basis of theoretical considerations. Before this can be done it is necessary to understand some basic particle and fluid dynamics.

The motion of a particle within a fluid is governed by the balance between driving forces and viscous resistance. For a spherical particle of mass, m, moving through a fluid and subject to a driving force, F, the equation of motion is (McQuarrie 1976):

$$m \, du/dt = -6\pi a\eta u + F(u,x,t).$$
$$(1.3)$$

Here the driving force is a function of velocity, u, position, x, and time, t. The viscous resistance affecting the particle is given by Stokes' relation:

$$\text{resistance} = 6\pi a\eta u.$$
$$(1.4)$$

The power required to move the particle is simply:

$$P^+ = 6\pi a\eta u^2.$$
$$(1.5)$$

Within a cell, the viscosity should not be less than that of water. Even when within water, microscopic particles will experience different forces than macroscopic bodies (Purcell 1977). The ratio of inertial forces to viscous forces is termed the Reynolds number, R.

$$R = au\rho/\eta.$$
$$(1.6)$$

Here ρ is the density of the surrounding fluid. For axonal particles of radius 0.2 micrometers, travelling at one micrometer per second, and within water of viscosity 1×10^{-3} Pa•s, and density 1×10^3 kg/m^3, the Reynolds number is 2×10^{-7}.

Inertial forces on a particle are so small, they can be ignored. Then the equation of motion [Eq. (1.3)] becomes:

$$6\pi a \eta u = F(u,x,t).$$

(1.7)

A particle's velocity is directly proportional to its driving force.

Viscous resistance dissipates a particle's kinetic energy as heat. The energy and momentum of particles within a viscous system are not conserved.

Turning from particle dynamics to fluid dynamics, consider the laminar incompressible flow of fluids within circular tubes. Different equations govern the motion (Olson 1967). The average speed, v, of a fluid moving within a duct of radius, r, and length, L, is:

$$v = \Delta p r^2 / (8L\eta).$$

(1.8)

The pressure drop over the duct is Δp. The power required to move the fluid is:

$$P^- = \pi r^2 v \Delta p.$$

(1.9)

Eliminating Δp between Eq. (1.8) and Eq. (1.9) gives:

$$P^- = 8 \pi \eta L v^2.$$

(1.10)

This amount of power is dissipated as heat from the flow within the tube.

With these basic principles from particle and fluid dynamics, it is now possible to analyse some of the models. First, consider the forces necessary to propel a typical axonal particle through a motionless fluid. For a particle with a radius of 0.2 micrometers, moving at one micrometer per second through axoplasm of viscosity 5×10^{-3} Pa•s (Haak *et al.* 1976), the Stokes resistance is 2×10^{-14} N [Eq. (1.4)]. At this speed 2×10^{-20} J/s is dissipated as heat [Eq. (1.5)]. Kaminura and Takahashi (1981) measured the force between sliding microtubules of sea urchin sperm to be 2 to 9 $\times 10^{-12}$ N per each dynein arm that extends from the microtubules. This force is more than sufficient to propel axonal particles. The forces necessary to propel axonal particles are within the range of known intracellular processes.

The power required to transport optically detectable particles within an axon can be crudely estimated. Cooper and Smith (1974) measured a particle flux of 9 particles/min across a ten micrometer transverse diameter in *Xenopus laevis*. Assuming an optical depth of field of 1.5 micrometers (McLeod 1980), this flux becomes 1×10^{-2}

particles/$\mu m^2 \cdot$s. With an average speed of one micrometer per second, the density of moving particles is 1×10^{-2} particles/ μm^3. If the power required to move one particle is 2×10^{-20} J/s and the specific gravity of nerve is 1 g/cm^3, then the power required is 2×10^{-10} J/g$\cdot$s.

Rang and Ritchie (1968) measured the oxygen consumption of resting rabbit vagus nerve to be 9.03×10^{-8} mol/g$\cdot$min. If the main component of metabolism comes from oxidation of glucose then for every six moles of oxygen gas consumed, 2.87×10^6 J of energy is released (Lehninger 1972). Thus the basal energy consumption of rabbit vagal nerve is 7.2×10^{-4} J/g$\cdot$s.

The basal energy consumption for rabbit vagus nerve is several orders of magnitude greater than a rough estimate of the energy required to transport optically detectable particles. Even if only a small fraction of transporting particles were optically visible, the energy required to move them all would be much less than the basal rate of metabolism.

Is it more efficient to propel axonal particles through a motionless fluid, or to carry them in a microstream? Using Eqs. (1.5) and (1.10), assume similar speeds of transport ($u = v$), let L = the average length of microstreams, and a = the average radius of particles transported. Define:

k^+ = the number of particles moving per nerve,

k^- = the number of microstreams per nerve, and

$k^\circ = k^+/(k^-L)$ = the number of particles per unit length of

one microstream. The total power per nerve for each
mechanism is k^+P^+ and k^-P^-. The ratio of total power is:

$$R^+ = P^-k^-/(P^+k^+)$$

$$R^+ = 4/(3ak°)$$

<div align="right">(1.11)</div>

If microstream transport is to be more efficient than
particle transport, then $R^+ < 1$. More than $4/(3a)$ particles
must then be packed per unit length of each microstream.

Even if this degree of packing is not consistent with
observation, this does not rule out the microstream model.
If the energy required for transport is only a small
fraction of the basal rate, then efficiency may not be a
limiting factor. Moreover, microstream flow may not be
analogous to lamellar Newtonian flow within tubes; then Eqs.
(1.8), (1.9), and (1.10) would not apply.

Let us now consider Hejnowicz's (1970) model for axonal
transport. One aspect deserving examination is the energy
requirement for maintenance of the ionic gradients within
axons. He proposed a 3:1 concentration gradient of a
univalent cation across each fibril in order to produce a 30
mV potential. To maintain this gradient, a minimal pumping
rate of 3.5×10^{-17} mol/s was required for each ten micrometer
length of fibril. Hejnowicz also calculated that 15 fibrils
were needed to move one particle of 0.5 micrometers

diameter.

From Hejnowicz's figures certain conclusions can be drawn. If the paths of 0.5 micrometer particles are not to be restricted to certain areas of axons, a minimal density of 76 fibrils/μm^2 is required to move the particles. This number is within an order of magnitude of the neurofilament density in rat nerve— 180 filaments/μm^2 (Weiss and Mayr 1971). Now the free energy change, ΔG, required to maintain the electrical potential across each fibril is (Daniels and Alberty 1961):

$$\Delta G = RT \ln(a^+/a^-) + nFE.$$

(1.12)

Here the gas constant, R = 8.3 J/mol•°K; the Faraday number, F = 9.6x10^4 J/mol•V; T = 294°K; the voltage drop across each fibril's surface, E = 30mV; the valency of the cation, n = 1; and the concentration ratio, a^+/a^- = 3. The Gibbs free energy change is then 5.6x10^3 J/mol. If the mass density of nerve is 1.0 g/cm^3, then the power requirement for Hejnowicz's model is 1.5 J/g•s. This calculation was based on the minimal pumping rate, minimal fibril density, and the Gibbs free energy change. The resultant number is over three orders of magnitude greater than the observed basal energy rate within rabbit nerve.

Axonal transport is a continuous process. The energy required for transport must be continuously supplied from

the basal metabolism of nerves. Since the energy required for maintenance of the ionic gradients in Hejnowicz's model is so much greater than measured basal energy requirements of nerves, Hejnowicz's model is not feasible.

Axonal transport is a complicated process, with many diverse features. Each model presented in this section can explain some of these features, but fails to explain all aspects of transport. It is not difficult to create an abstract model explaining one aspect of transport very well. Problems arise when that model is applied to the whole process. Model construction should be based closely on experimentation rather than on abstraction.

1.7 Summary

In this chapter the subject of axonal transport was examined. A general classification for transport was introduced and the major methods for studying transport were noted.

Several agents, known to inhibit fast axonal transport, were discussed. The mechanisms of action of some of these agents suggested a dependence of transport on microtubules. This dependence on microtubules, however, remains controversial.

The motion of optically detectable organelles was discussed. This motion has been described as saltatory, however, recent studies have indicated that this term is

inadequate. Organelles within certain axons move smoothly rather than with discontinuous jumps. Also it was noted that optically detectable motion is inhibited by the same blockers that affect the transport of radiolabels.

Fast axonal transport and transport of intraaxonal organelles are one and the same. This conclusion is based on the following points:

1.   studies with cell fractionation showed a large particulate component of transported material,

2.   biochemical analysis showed an association between the material transported and membrane components,

3.   electron microscopy showed an accumulation of organelles near axonal lesions,

4.   optical studies showed movement of organelles within axons, and

5.   theoretical considerations showed that particulate material may be more effectively transported than diffusible material.

The few specific conditions causing intraaxonal organelles to oscillate back and forth about fixed positions were discussed. Either metabolic mechanisms or Brownian forces are responsible for these oscillations.

Intraaxonal structure was reviewed. In particular, the influence of structure on axoplasmic viscosity, and Brownian motion was discussed.

Finally, the major postulated mechanisms for fast axonal transport were discussed and criticized. None of

these mechanisms was entirely satisfactory in explaining axonal transport.

In the remaining chapters, the nature of the oscillatory motion of intraaxonal organelles is studied. First, the experimental methods used in this study are detailed, followed by the experimental results and conclusions.

2. METHODS

In this chapter, the experimental procedures used in this study are described. Two different sets of experiments were performed:

1. experiments dealing with the effects of certain agents that are known to inhibit axonal transport on the motion of organelles within axons, and

2. experiments dealing with the effects of freezing on both transport and fine structure of axons.

The first section of this chapter describes the experiments with inhibitors of axonal transport. The preparations for dark-field microscopy are detailed. Following this, the methods of quantitative measurement are given, along with a discussion of measurement error.

The second section of this chapter deals with the freezing experiments. The methods for freezing nerves and observing organelle motion are discussed. Also, the method of preparing thawed nerve for electron microscopy is detailed.

In the final section of this chapter, the analytical methods used in this study are described. First, a theoretical discussion on the analysis of random processes is given, followed by a description of how these techniques were adapted to this study.

2.1 General Procedures

2.1.1 Dark-Field Microscopy

In the first set of experiments, the motions of optically detectable organelles within axons were observed after nerves were exposed to agents known to inhibit axonal transport. Adult female *Xenopus laevis* were chosen as the animal model, since organelle transport has been well studied in this species (Cooper and Smith 1974; Koles *et al*. 1982a). The animals were decapitated, pithed, and their sciatic nerves were dissected free.

The isolated sciatic nerves were placed in solutions of 0.12 M potassium glutamate, and 10 mM HEPES (N-2-hydroxy-ethylpiperazine-N'-2 ethanesulfonic acid), in deionized water with enough potassium hydroxide added to give a pH of 7.0. Potassium glutamate was chosen as the predominant constituent of the solutions for several reasons:

1. Some of the experiments allowed access of the external solution to cell interiors.

2. Standard Ringers solutions contain Ca^{+2} ions in millimolar concentrations.

3. There is evidence that Ca^{+2} ions in millimolar concentrations will profoundly alter the interior structure of cells (Porter *et al*. 1979; Rubinson and Baker 1979; Schliwa *et al*. 1981).

4. Calcium ions can also profoundly influence the movement of intracellular organelles (Shaw and Newby 1972).

5.   Solutions containing high potassium glutamate
     concentrations have been used sucessfully with permeable
     cells (Adams *et al.* 1982).

6.   Axonal transport is not influenced by potassium
     glutamate solutions (Smith 1980).

In summary, the solutions used in these experiments were
chosen to be compatible with the intracellular enviroment.

     Dissection and microscopy were performed with specimens
immersed in the basic potassium glutamate solution. The
isolated sciatic nerves were desheathed, teased apart, and
mounted in Dow-Corning 710 fluid on microscope slides. These
preparations served as controls, demonstrating uninhibited
axonal transport.

     In other preparations, nerves were exposed to solutions
containing different inhibitory agents prior to being
mounted on microscope slides. These agents were:

1.   1 mM colchicine,

2.   1.3 M dimethylsulfoxide (DMSO),

3.   1 mM dinitrophenol (DNP),

4.   10 mM calcium chloride.

The inhibitors were all dissolved in the potassium glutamate
solution previously described. Different incubation periods
for nerves with each agent were required before any effect
on organelle transport could be observed. The incubation
periods ranged from 15 minutes with DNP to four hours with
colchicine. Over 150 axonal segments in over 60 nerves were
studied.

The preparations with calcium chloride added to the basic solution require further explanation. These preparations were designed to ensure entry of Ca^{+2} ions into nerve cells. Other workers (Chan *et al.* 1980) have noted the presence of a diffusion barrier to Ca^{+2} ions in perineural sheaths. Another barrier, within cell membranes of monkey kidney cells, is known to prevent the entry of Ca^{+2} ions into these cells, unless the cell membranes are permeabilized by detergents (Schliwa *et al.* 1981). It is reasonable to expect a similar barrier against the entry of Ca^{+2} ions into axons. Thus crushed or severed areas of axons were observed with the expectation that Ca^{+2} ions would enter axons at these points more easily. Areas up to several hundred micrometers from the axonal lesions were observed for any effect on organelle transport. It was assumed that Ca^{+2} ions could eventually reach these regions as a result of diffusion from crushed regions. The areas observed were far enough from the axonal lesions that any local effects of these lesions could be assumed not to interfere with organelle transport.

In a different series of experiments, nerves were placed in one of two solutions prior to being mounted for microscopy. The first solution was 0.18 M potassium glutamate and 10 mM HEPES in deionized water with added KOH to give a pH of 7.0. This solution was 1.5 times hyperosmolar to axoplasm. The second solution was 0.12 M potassium glutamate in heavy water. The pD of the heavy

water solutions was adjusted to 7.4 using a glass electrode
(Glasoe and Long 1960). Nerves were incubated in these
solutions for ten minutes before being examined.

The preparations were examined with dark-field
microscopy. A Zeiss Ultradarkfield condenser with a 100x
planachromatic objective and 1.25 intermediate lens was
used. Light from a 12 volt quartz iodide lamp was filtered
of infared rays before reaching the condenser.

2.1.2 Measurement Technique

Within the microscope's field of view, distances were
calibrated with a ten micrometer grid. Calibration with this
grid gave a magnification factor of 1.0×10^4. A fine wire was
placed in the light path proximal to the eyepiece as a
positional reference. Permanent records of the motions of
intraaxonal particles were made with 16 mm 4X B&W (Kodak)
motion picture film. The motion picture camera was driven at
three frames per second with a calibrated servomotor.

Each 16 mm film was projected via a LW Photo-Optical
Data Analyser onto the ground-glass screen of a
Hewlett-Packard 9874A digitizer. The positions of
intraaxonal particles were digitized in frame by frame
sequence. The movements of individual organelles were thus
recorded by measurement of their positions at successive
0.33 second intervals. The data were compiled with a
Hewlett-Packard 9845B computer and stored in a
Hewlett-Packard 9845A Flexible Disk Memory. Over 100 sets of

data were obtained from over 3×10^4 separate measurements.

The measurements of organelle positions were made relative to a wire reference or to some motionless and well-defined intraaxonal structure. Only those particles that remained in focus for significant intervals and that had round images, 0.2 to 0.5 micrometers in diameter, were tracked. Each particle's position was estimated from the center of its image.

2.1.3 Measurement Error

There were several sources of measurement error:

1. The digitizer had limits to its accuracy. Here, the error introduced had a standard deviation of 1×10^{-3} micrometers. This was negligible.

2. A significant error was introduced by the estimation of each particle's position from its image. The center of each image had to be subjectively estimated. The standard deviations of these estimates ranged from 0.1 to 0.7 micrometers, depending on the size of each particle. This error was roughly the order of a particle's diameter.

3. Drift of some preparations on their microscope slides was at times excessive. These preparations were excluded from measurement.

4. Vibration from the motion picture projector was significant. To eliminate this error, positional measurements were made relative to the wire reference

point recorded on the motion picture film.

5. As individual particles were tracked, their images could change in shape and size and vary in degree of focus. Only those particles that had relatively constant images were subjected to positional measurement.

Owing to the small increments in positions being measured, the error from measurement was a significant factor. This error was minimized by repeated positional measurements and also by specific analytical techniques that are discussed later.

2.2 Freezing Experiments

2.2.1 Preparations For Light Microscopy

In the second group of experiments, the effects of freezing on both organelle transport and intraaxonal structure were observed. Isolated sciatic nerves of *Xenopus laevis* were desheathed and placed for 15 minutes in a solution of: 0.12 M potassium glutamate, 0.13 M DMSO, and 10 mM HEPES. The pH was adjusted to 7.0 with KOH. We used this solution because of anticipated changes in cell permeability after thawing (Daw *et al*. 1973). The DMSO was added as a cryoprotectant (Menz 1975): at the concentrations used, it was not expected to inhibit axonal transport (Donoso *et al*. 1976).

After treatment in the glutamate-DMSO solutions, nerves were frozen in liquid nitrogen. In less than fifteen seconds the nerves were cooled down to liquid nitrogen temperatures. These nerves were then rapidly thawed in either a glutamate-DMSO solution or in a similar solution with 10 mM colchicine added. The solutions used for thawing nerves were kept at 21°C. When thawed, the nerves were teased apart and mounted on microscope slides in their respective solutions.

Dark-field microscopy was used to examine movements of intraaxonal organelles within thawed nerve. Film records of these movements were made, and measurements of their positions were obtained. as was previously described.

2.2.2 Preparations For Electron Microscopy

Nerves were similarly prepared for electron microscopy in a glutamate-DMSO solution prior to being frozen. The nerves were thawed in either a glutamate-DMSO solution or in a similar solution with 10 mM colchicine added. After specific time intervals from thawing, the nerves were fixed in 3% glutaraldehyde with 0.05 M cacodylate and 0.13 M DMSO. Segments from the middle of each specimen were treated with 2% buffered osmium tetroxide prior to being dehydrated and embedded in Epon. Transverse sections of each nerve were obtained. The sections were stained with lead citrate and uranyl acetate. A Siemens transmission electron microscope was used to examine the specimens.

The numbers of microtubules and neurofilaments per unit area of nerve were counted from photographs (Hammond and Smith 1977). Nerves that had not been frozen were similarly prepared for electron microscopy as a control.

2.3 Analytical Methods

2.3.1 Analysis Of Random Processes

The movement of intraaxonal organelles is complicated and likely has a significant random component. In order to analyse the motion of individual organelles, certain averaging methods were required to deal with any random component of motion and with the measurement error. Let $x(t)$ be a continuous random function of t. Define a probability distribution, $p(t)$, so that $p(x)dx$ is the probability of $x(t)$ satisfying $x \leq x(t) \leq x + dx$. The nth moment of the distribution can thus be defined (McQuarrie 1976):

$$\langle x^n \rangle = \int_{-\infty}^{\infty} x^n \, p(x) \, dx.$$

$$(2.1)$$

If the probability distribution does not change over the period of time, $2T$, that $x(t)$ is examined, then the moments

can be calculated via time averages:

$$\langle x^n \rangle = \overline{x^n} = \int_{-T}^{T} x^n(t) \, dt \, /(2T).$$

(2.2)

The first and second moments are the mean value and mean squared value, respectively. The standard deviation, σ, and variance, σ^2, of the process are given by:

$$\sigma^2 = \int_{-T}^{T} (x(t) - \langle x \rangle)^2 \, dt \, /(2T).$$

(2.3)

The data can be further studied using Fourier analysis. The Fourier transform is defined:

$$X(f) = F\{x(t)\} = \int_{-\infty}^{\infty} x(t) \, \exp[-j2\pi ft] \, dt,$$

$$x(t) = F^{-1}\{X(f)\} = \int_{-\infty}^{\infty} X(f) \, \exp[j2\pi ft] \, df.$$

(2.4)

Here $X(f)$ and $x(t)$ are Fourier transforms of each other. The first function is in the frequency domain, f; the second is in the time domain, t. The Fourier transform is complex, that is, it involves imaginary numbers. Here, j denotes the square root of minus one. The usefulness of the Fourier

transform becomes apparent in the following text.

With Fourier analysis, it is possible to calculate the normalized power spectrum, $G_x(f)$, for the function $x(t)$:

$$G_x(f) = |X(f)|^2 / \int_{-\infty}^{\infty} |X(f)|^2 \, df. \tag{2.5}$$

For an oscillating function $x(t)$, the power spectrum measures the relative intensity of the components of $x(t)$ at different frequencies. The resultant power spectrum indicates the particular frequencies of oscillation which predominate in a given process.

Given two processes $x(t)$, and $y(t)$, it is possible to compare their components at specific frequencies by calculating their cross spectral density function. Take the Fourier transforms,

$$X(f) = F\{x(t)\} = \text{Re } X + j \text{ Im } X,$$

$$Y(f) = F\{y(t)\} = \text{Re } Y + j \text{ Im } Y, \tag{2.6}$$

and then calculate:

$$X* \bullet Y = [\text{Re } X \bullet \text{Re } Y + \text{Im } X \bullet \text{Im } Y] + j[\text{Re } X \bullet \text{Im } Y - \text{Im } X \bullet \text{Re } Y],$$

$$X* \bullet Y = A + jB. \tag{2.7}$$

Here the real and imaginary components are denoted by the prefix Re and Im, respectively. The cross spectral density has a magnitude,

$$|G_{xy}(f)| = (A^2 + B^2)^{1/2},$$

(2.8)

and phase,

$$\Theta_{xy}(f) = \text{Arctan } [B/A].$$

(2.9)

These calculations allow the frequencies shared by both $x(t)$ and $y(t)$, along with their phase relationship, to be determined. The result is that if both $x(t)$ and $y(t)$ have large components of oscillation at a specific frequency, then the cross spectral density will show a large intensity at that frequency. If, at that particular frequency, both $x(t)$ and $y(t)$ are oscillating in phase with each other, then the phase shift will be zero there.

Further information regarding a process can be obtained by calculating its spectral moments (Vanmarke 1977). These moments, $^{(n)}S$, are defined by:

$$^{(n)}S = \int_{0}^{\infty} f^n G_x(f) \, df.$$

(2.10)

The spectral moments are abstract parameters that describe the form of a given power spectrum. They can be combined to calculate three other parameters that are useful in characterizing power spectra:

$$f^+ = {}^{(1)}S / {}^{(0)}S,$$

$$f^- = ({}^{(2)}S / {}^{(0)}S)^{1/2}, \text{ and}$$

$$\delta = [1 - ({}^{(1)}S)^2 / ({}^{(0)}S \bullet {}^{(2)}S)]^{1/2}.$$

$$(2.11)$$

Here ${}^{(0)}S$ is the variance of the process; f^+ is the *center of spectral mass*; f^- is the *radius of gyration*; and δ is the variability of the frequency. The center of spectral mass is an estimate of the predominant frequency within a given process. The spectral parameter, δ , is also quite useful. For a sinusoidal process $\delta = 0$, indicating no variability of frequency. However, for a random process, δ approaches unity. This indicates a high degree of variability of the process's frequency.

2.3.2 Data Management

Analysis of data followed the methods of Koles *et al.* (1982b). For each particle, a series of discrete measurements in the x-y plane, $(\overset{\circ}{x}_a, \overset{\circ}{y}_a)$, were obtained at intervals of 0.33 seconds. The x-axis was aligned with the longitudinal axis of the axon that was being observed. A

line was fitted to the raw data using linear regression. The linear trend was then subtracted:

$$x_a = \mathring{x}_a - \mathring{v}_x t_a - b_x,$$

$$y_a = \mathring{y}_a - \mathring{v}_y t_a - b_y.$$

(2.12)

The slopes, $(\mathring{v}_x, \mathring{v}_y)$, gave the mean velocity for each particle while (b_x, b_y) were the intercepts. The first and second moments were computed from the trend-free data [Eq. (2.1)]:

$$\langle x \rangle = \sum_{n=1}^{N} x_n/N,$$

$$\langle x^2 \rangle = \sum_{n=1}^{N} (x_n)^2/N.$$

(2.13)

N is the number of data points. Because the linear trends were removed, both $\langle x \rangle$ and $\langle y \rangle$ were essentially zero. The standard deviations for each sequence were:

$$\sigma_x = (\langle x^2 \rangle N/(N-1))^{1/2},$$

$$\sigma_y = (\langle y^2 \rangle N/(N-1))^{1/2}.$$

(2.14)

Both measurement error and particle movements contributed to the standard deviations.

Instantaneous velocities, (x'_a, y'_a), for the trend-free data were calculated using a 21-term differentiating filter (Koles *et al.* 1982b):

$$x'_a = [\sum_{\varphi=-10}^{10} c_\varphi x_{a-\varphi}]/(g\,\Delta t),$$

$$y'_a = [\sum_{\varphi=-10}^{10} c_\varphi y_{a-\varphi}]/(g\,\Delta t).$$

(2.15)

Here $\Delta t = 0.33$ s; the gain factor $g = 3044$; and the coefficients, $c_\varphi = c_{-\varphi}$, are given in Table 2.1. This filter limited differentiation to signals with frequencies below 0.3 Hz. Frequencies above 0.3 Hz were suppressed from the signal. On the basis of previous work (Koles *et al.* 1982a), the significant oscillations were expected to occur with frequencies below 0.3 Hz.

Next, the first and second moments were calculated from the instantaneous velocities:

$$\langle v_x \rangle = \sum_{\phi=1}^{N} x'_\phi /N,$$

$$\langle v_x^2 \rangle = \sum_{\phi=1}^{N} (x'_\phi)^2/N.$$

(2.16)

TABLE 2.1

Differentiating Filter Coefficients

j	c_j	j	c_j
0	0	6	-50.5
1	-76.8	7	-5.8
2	-132.9	8	22.0
3	-155.0	9	30.7
4	-141.2	10	24.8
5	-101.0		

Again, $\langle v_x \rangle$ and $\langle v_y \rangle$ were negligible, thus the standard deviations of instantaneous velocity were:

$$\sigma_{x'} = (\langle v_x{}^2 \rangle N/(N-1))^{1/2},$$

$$\sigma_{y'} = (\langle v_y{}^2 \rangle N/(N-1))^{1/2}.$$

$$(2.17)$$

These standard deviations measured the variability of the trend-free instantaneous velocities.

The probability density functions for the instantaneous velocities were also calculated (Bendat and Piersol 1971). This was accomplished with a digital sorting program that evaluated:

$$p(v) = N_v/(2N \Delta v),$$

<div align="right">(2.18)</div>

for the N points in the sequences (x'_ϕ) and (y'_ϕ). Here N_v is the number of points with velocities in the interval $v \pm \Delta v$. When this distribution was shifted along the velocity axis by an amount equal to the mean velocity, $\overset{\lor}{v}$, then

$$\overset{\circ}{p}(v) = p(v - \overset{\lor}{v}),$$

<div align="right">(2.19)</div>

the overall velocity distribution resulted.

Periodograms for the trend-free positional deviations were calculated (Tretter 1976). A rectangular data window was used. Each sequence was packed with zeros to 512, 1024, or 2048 points and then a *Fast Fourier Transform* (FFT: Tretter 1976) was performed:

$$X_\phi = X(f_\phi) = FFT\{x_\phi\}.$$

<div align="right">(2.20)</div>

The resultant periodogram was an estimate for the power spectral density (Bendat and Piersol 1971). The periodogram was calculated using:

$$G(f_\phi) = |X(f_\phi)|^2/\langle x^2 \rangle.$$

<div align="right">(2.21)</div>

A typical periodogram could be represented by a graph showing a number of peaks at various frequencies. Each peak would then represent an oscillatory component that was limited to a specific frequency. If, instead, there were no significant oscillatory components in a process, then the corresponding periodogram would show only an even distribution of narrow peaks of random heights over the entire range of frequency. This latter periodogram would indicate noise.

It is useful to estimate the probability of the largest peaks of a periodogram arising as a fluctuation of noise. For this purpose, Fisher's test of significance for harmonic analysis was used (Shimshoni 1971). This test could be applied to the normalized periodograms, and by comparing the amplitudes of the larger peaks to values within a table, this probability could be estimated.

Cross periodograms between the sequences (x_φ) and (y_φ) were calculated:

$$|G_{xy}(f_\varphi)| = |X_\varphi^* \cdot Y_\varphi|,$$

$$\Theta_{xy}(f_\varphi) = \text{Arctan} \, [\text{Im} \, (X_\varphi^* \cdot Y_\varphi)/\text{Re} \, (X_\varphi^* \cdot Y_\varphi)]. \tag{2.22}$$

The moments of periodograms were also estimated

(Vanmarke 1977):

$$^{(n)}S = \sum_{a=1}^{N} f_a^n \, G(f_a) \, \Delta f.$$

(2.23)

These moments were then used to calculate the following parameters:

$$f^+ = {}^{(1)}S / {}^{(0)}S,$$

$$f^- = ({}^{(2)}S / {}^{(0)}S)^{1/2},$$

$$\delta = [1 - ({}^{(1)}S)^2 / ({}^{(0)}S \bullet {}^{(2)}S)].$$

(2.24)

These quantities were the spectral parameters defined in Eq. (2.11).

3. RESULTS: ORGANELLE MOVEMENTS AFTER TRANSPORT INHIBITION

In this chapter, the effects of specific agents on organelle transport are described. First, a brief description of the observations from the control preparations is given. Then the effects of colchicine, DMSO, DNP, calcium chloride, hypertonic solutions, and heavy water on organelle transport are documented.

An analysis of the motion of intraaxonal organelles follows next. Particular attention is directed to those motions not found in the control preparations. The analytical methods are used to their full extent. Periodograms, phase diagrams, instantaneous velocity, probability distributions, and periodogram moments are calculated.

3.1 Control Preparations

The transport of organelles was observed in axons not exposed to any inhibitory agents. Generally, organelles travelled longitudinally within axons; most organelles moved in a retrograde direction. These organelles had round profiles, and varied from 0.2 to 0.5 micrometers in diameter. Also occasional rod-shaped organelles (0.3 x 1-8 micrometers) were observed to move longitudinally over short distances.

The round particles exhibited certain characteristic movements. As any individual organelle was transported

within an axon, a wavy variation was noted in both position

and velocity. Figure 3.1 contains data from a typical

organelle's movements. Part *a* shows the particle's

longitudinal displacement within an axon plotted versus

time— note the undulations. Part *b* shows the displacements

after the least squares trend was subtracted. The

fluctuations are more apparent in part *b*. Part *c* is a plot

of the longitudinal component of the particle's total

velocity versus time. In this thesis total velocity is

defined as the sum of the mean velocity [Eq. (2.12)] and the

instantaneous velocity [Eq. (2.15)]. Note the smooth

variations in velocity. Part *d* is the periodogram obtained

from the data in part *b*. As Koles and associates (1982a) had

noted, there was a definite low frequency component to the

positional fluctuations. Figure 3.1*d* demonstrates a wide

peak centered at 0.06 Hz. This peak was significant by

Fisher's test (p < 0.01). That is, the probability of the

peak arising as a random perturbation of noise was less than

0.01. This low frequency variation in displacement and

velocity was found to be characteristic of particles moving

within the control axons. The nonzero value for intensity at

0.0 Hz in Fig. 3.1*d* resulted from the two micrometer net

displacement in Fig. 3.1*b*.

Several other qualitative features of organelle

transport were noted in the control axons:

1. No correlation between the movements of individual
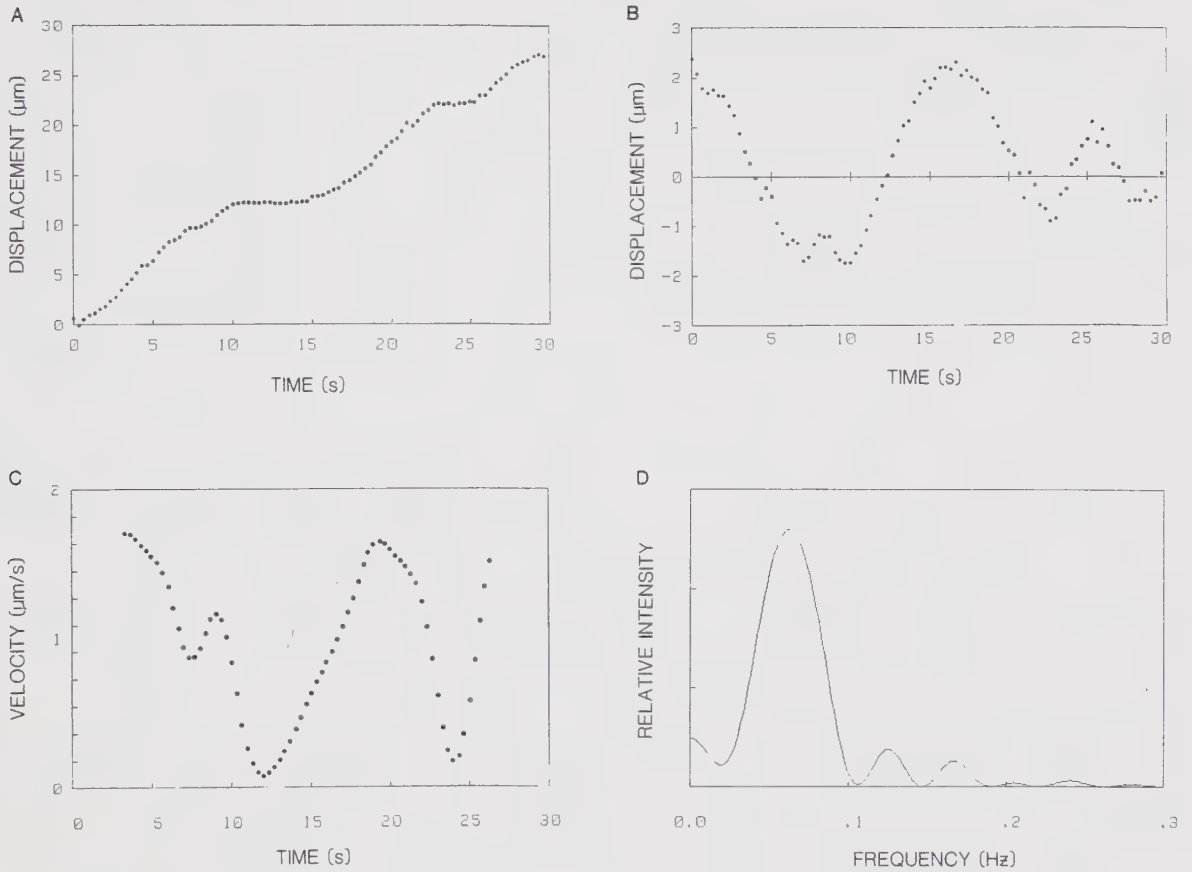
    particles was observed.

Figure 3.1 Axonal transport within uninhibited nerve:
a. Position-time plot of a transporting particle. *b*. The
positional deviations about the linear trend, plotted versus
time. *c*. The velocity-time plot for the particle. *d*. The
periodogram for the particle's movement.

2.   Individual particles travelled with different speeds.

3.   The majority of particles were moving.

4.   If two particles were initially very close together they
     could diverge apart with time.

     The motions of organelles within the control group of
axons were similar to those observed by Cooper and Smith
(1974) and Koles *et al.* (1982). The preparations used in
this study were kept in potassium glutamate solutions, while
those of other investigators were kept in Ringers solution.
Thus no noticeable adverse effect of potassium glutamate on
transport was observed.

3.2 The Action Of Inhibitors

     All of the inhibitory agents used in this study
affected the transport of organelles. Generally, as the time
of exposure to the inhibitor increased, fewer particles were
transported. The particles stopped translating and then
oscillated back and forth about fixed positions. The effects
of specific inhibitors on transport are reviewed in the
following section.

3.2.1 Colchicine

     Rapid axonal transport was inhibited within four hours
of exposure to colchicine. By that time most particles were
motionless, but some were observed to wobble, and others
still were translating. All three forms of movement occurred

simultaneously in the same region of many axons.

Several other features of organelle movement were found repeatedly within axons treated with colchicine:

1. The back and forth movement was aligned with the longitudinal axes of axons.

2. The amplitude of wobble varied for different particles, but generally it was of the order of a particle diameter.

3. Pairs of oscillating particles, located within two to three micrometers of each other, showed no correlation in their movements that was visually perceptible.

4. Similarly, pairs of particles transporting along axons showed no correlation in their movements.

5. The motion of some particles was discontinuous. An occasional particle moved over several micrometers, abruptly stopped and wobbled, and then resumed transport.

One example of the effect of colchicine on a particle's movement is given in Fig. 3.2. In Fig. 3.2*a* the displacement of an organelle is plotted versus time. The organelle had three relatively motionless periods during the time of observation. Interspersed between the motionless periods there were rapid displacements of up to four micrometers, occurring at velocities of about 0.4 micrometers per second. Within the relatively motionless periods the positional measurements were scattered over about 0.3 micrometers. This scatter was the result of random measurement error. However,
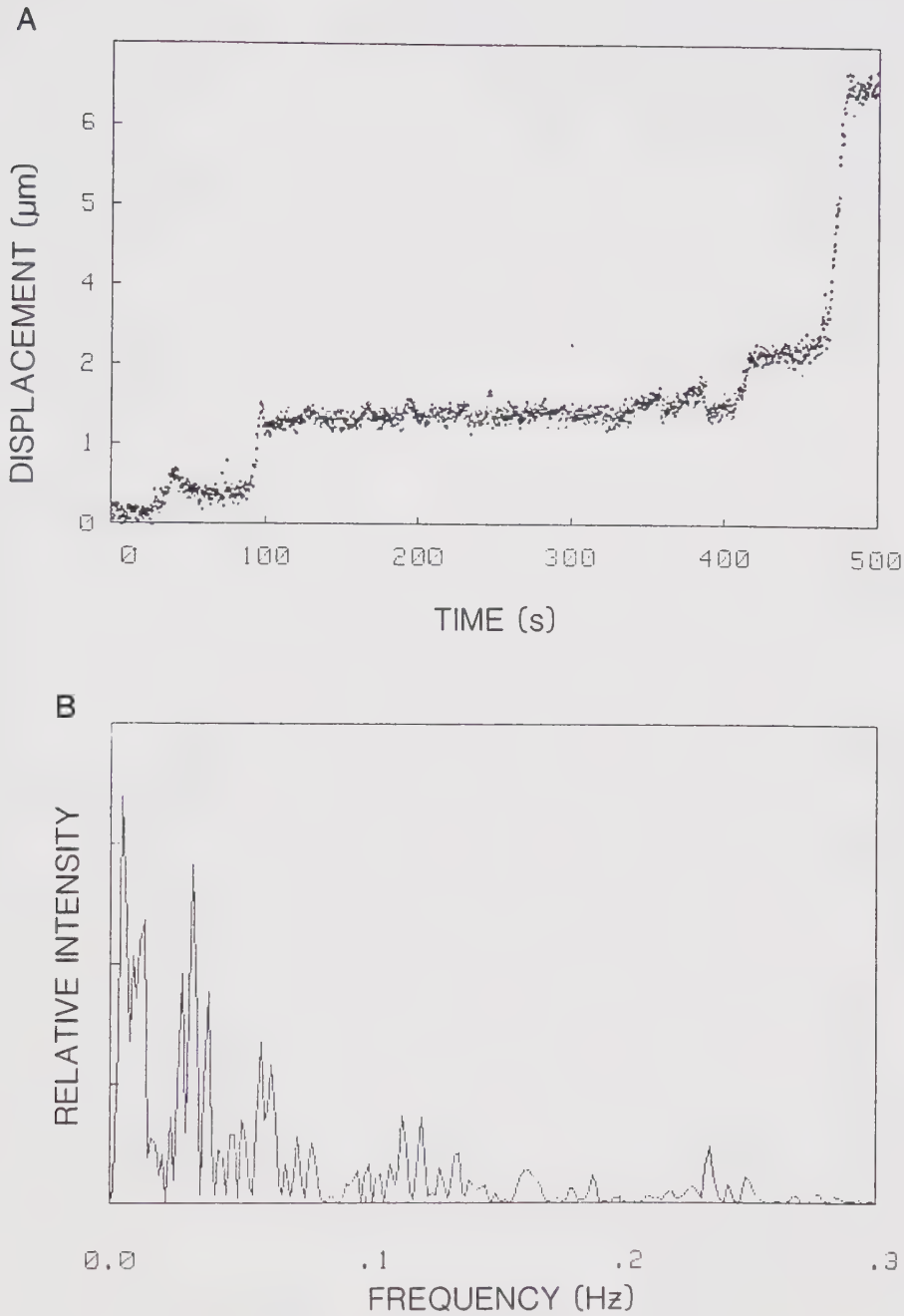
Figure 3.2 Transport of a particle within an axon exposed to colchicine: *a*. Position-time plot. *b*. The periodogram obtained from the segment of data from 100 to 400 s.

a low frequency wobble also was discernible from the random scatter. The movements during the period from 100 to 400 seconds were used to calculate a periodogram. The resultant periodogram is shown in Fig. 3.2b. Here, there were large peaks of oscillatory activity below the frequency of 0.1 Hz. The three tallest groups of peaks were all significant (p < 0.01), indicating a definite low frequency variation. This wobble about fixed positions shall be described by the term *stationary* in the remaining text.

3.2.2 Dimethylsulfoxide

Dimethylsulfoxide also inhibited transport. Within twenty minutes of exposure, particles exhibited stationary wobbles. As with the colchicine preparations, translating, wobbling, and motionless particles were present within regions of individual axons. With time, the proportion of motionless particles increased. The behavior of organelles within the preparations treated with DMSO was qualitatively similar to that within the colchicine preparations.

An example of a particle's motion is given in Fig 3.3. Figure 3.3a shows the displacement of the particle plotted versus time. The movement of the particle was irregular. There were short jumps interspersed with partial reversals in direction. The particle eventually became stationary. However, this stationary period (from 170 to 300 s) contained a low frequency fluctuation. The data from this later segment were processed into a periodogram (Fig 3.3b).
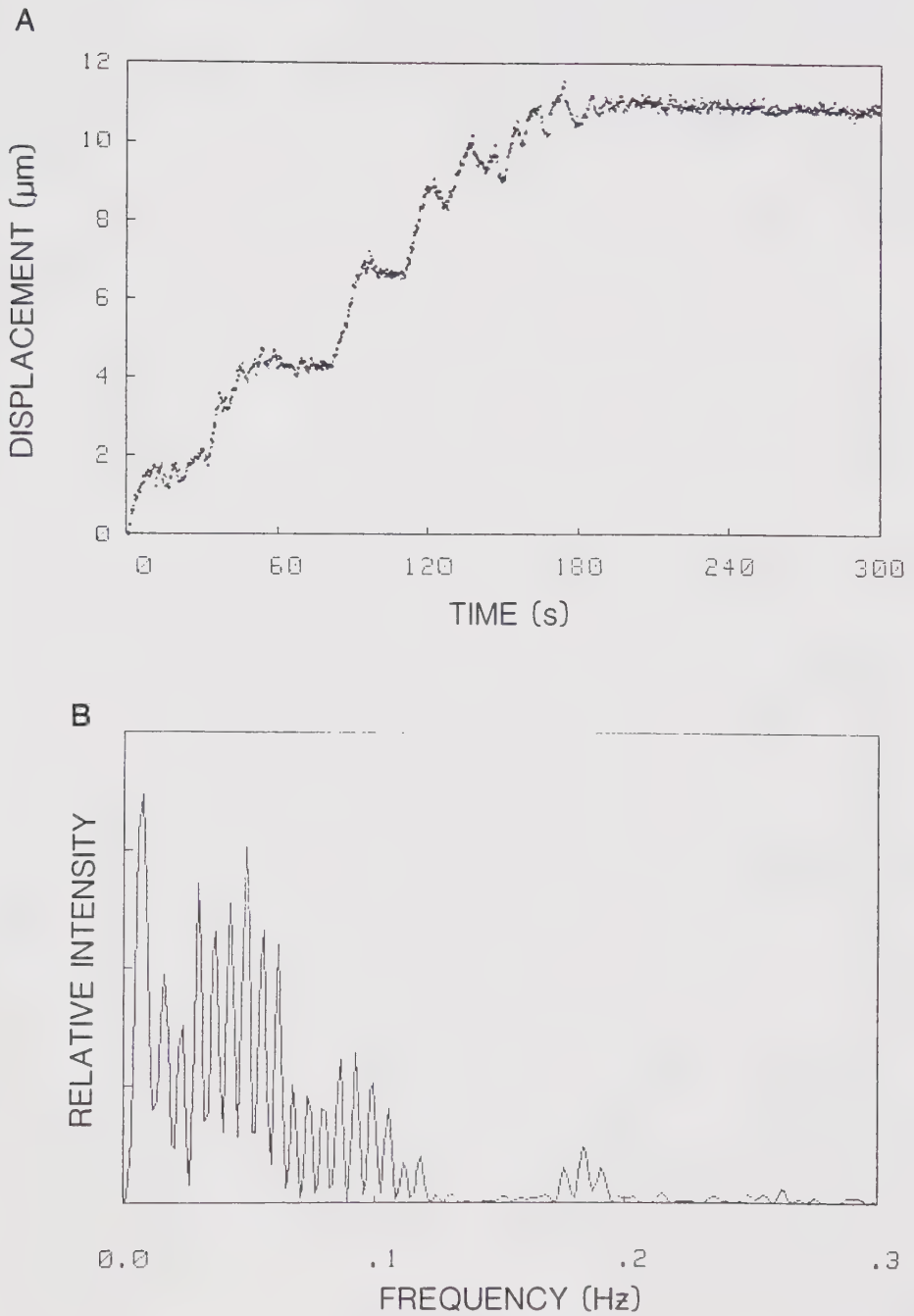
Figure 3.3 Transport of a particle within an axon exposed to DMSO: *a*. Position-time plot. *b*. The periodogram for the data from 170 to 300 s.

The fluctuations were most intense below 0.1 Hz. Within this region of frequency there were three groups of peaks, all of which were significant (p < 0.01). A significant residual oscillation persisted after the particle stopped translating.

3.2.3 Dinitrophenol

Similar longitudinal oscillations occurred in preparations which were treated with DNP, as occurred in those treated with colchicine or DMSO. Dinitrophenol began to inhibit transport within five minutes of exposure. Initially, after exposure to DNP, the transport was grossly normal, but with time the motion changed. First transport was slowed, then the particles wobbled about fixed positions, and finally they stopped moving entirely. The larger particles generally stopped first. By one hour only a few particles were translating— most were wobbling. After 1.5 hours even the oscillatory motion ceased.

A few particles moved longitudinally back and forth over large distances with no net displacement. The amplitude of these movements approached seven micrometers. Figure 3.4 shows the displacement of such a particle plotted versus time. However, most of the oscillating particles moved over smaller distances as was observed in the previous two preparations.
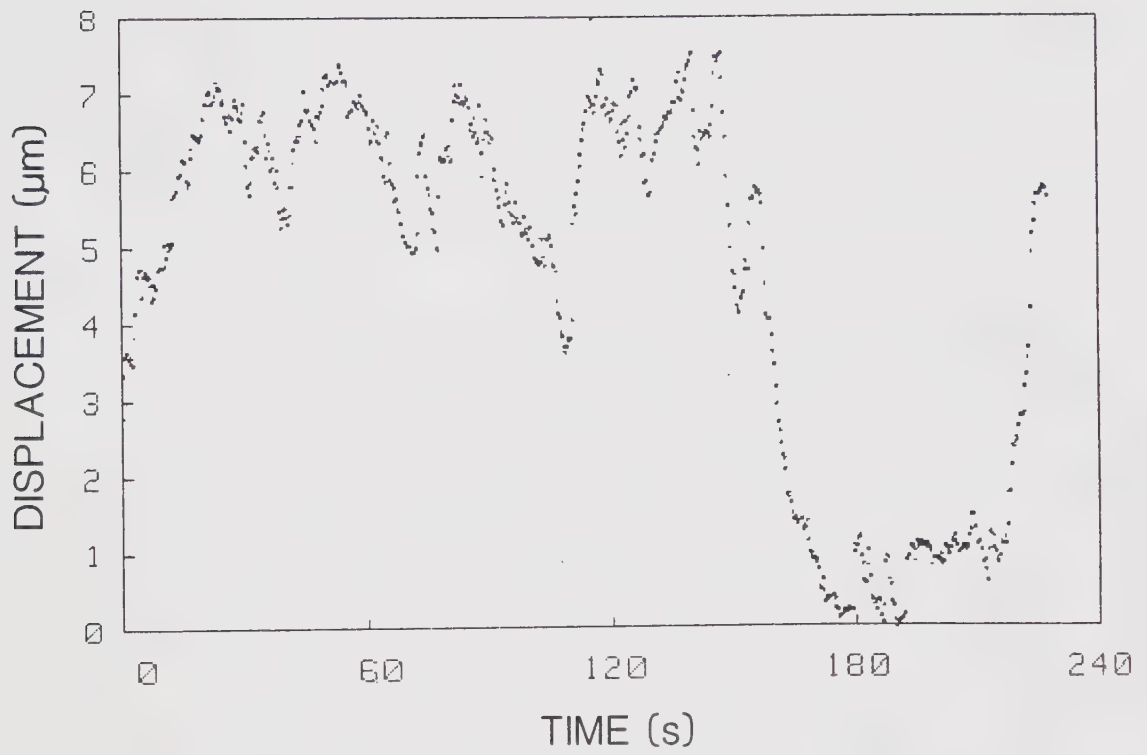
Figure 3.4 DNP: Large Amplitude Oscillations

3.2.4 Calcium Chloride

Calcium chloride affected organelle transport only in damaged or severed axons. Initially, in these axons, transport was grossly normal. With time, the particles began to oscillate about stationary positions. These movements first occurred in the immediate locality of damage to axonal walls. At later time periods, the regions of axons containing oscillating particles spread away from the areas of damage. Eventually, oscillations could be observed up to 100 micrometers away from a given axonal lesion. Those axons, without any lesions, remained unaffected by the calcium chloride.

The oscillatory movements of particles were generally similar to those observed in the three types of preparations described above. However, oscillations over relatively large amplitudes also occurred. Figure 3.5a shows the displacements of a particle moving back and forth over relatively large distances. This particle oscillated rapidly over distances of up to seven micrometers. These oscillations appeared random. Figure 3.5b is a periodogram calculated from Fig. 3.5a. The largest peak in the periodogram corresponded to a fluctuation with a period of 67 seconds. Since the period of observation was only 180 seconds, the permanence of the largest peak cannot be established. By Fisher's test, the six largest peaks in the periodogram were all significant ($p < 0.01$).
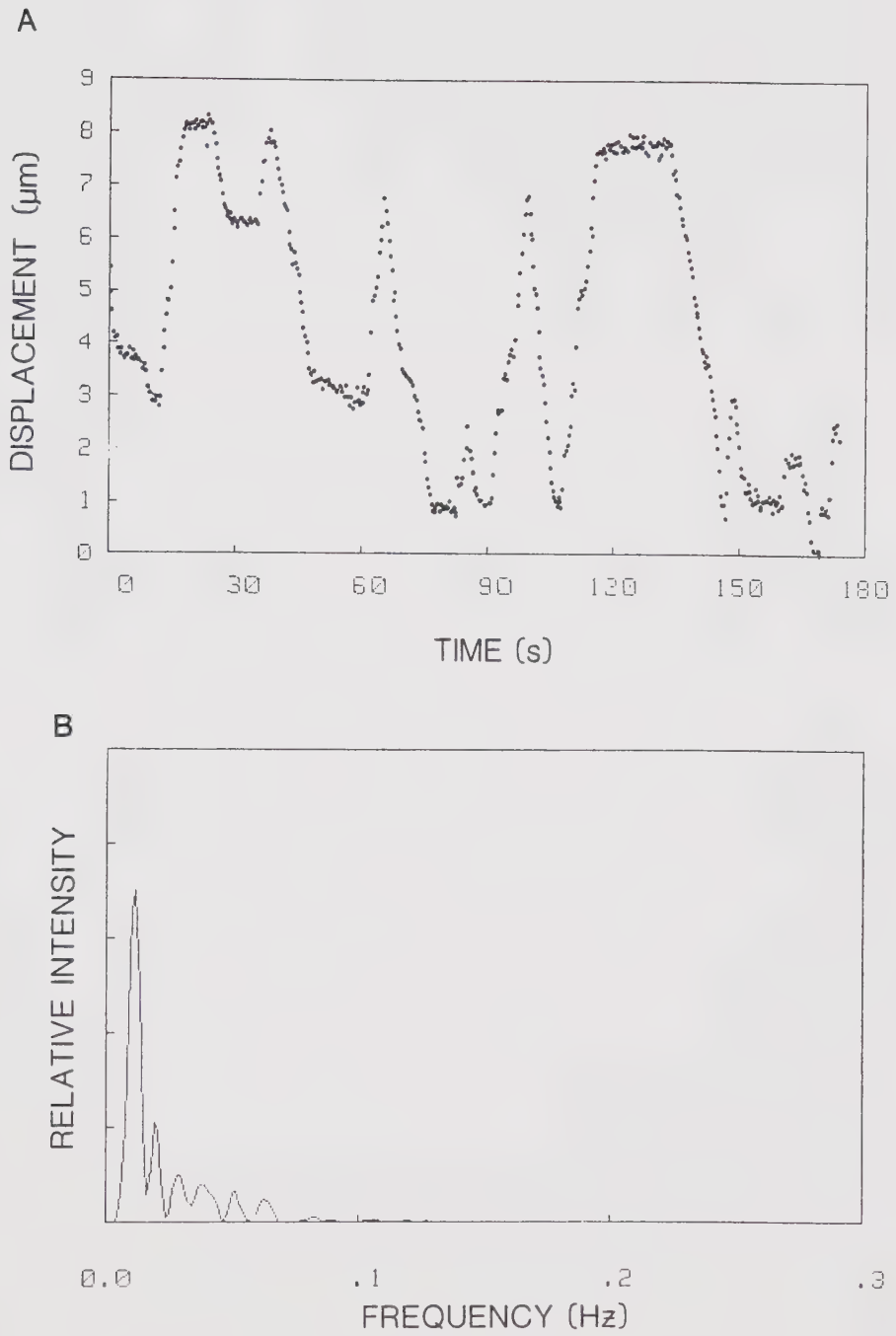
Figure 3.5 Large amplitude oscillations induced by calcium chloride: *a*. Position-time plot. *b*. Periodogram for the particle's motions.

3.2.5 Hypertonic Solutions

Organelle transport within axons treated with 0.18 M potassium glutamate was affected within ten minutes of exposure. The hypertonic solutions affected transport similarly to the agents described above. Translating particles, wobbling, particles, and motionless particles were all present simultaneously within axons. With longer exposure periods, the proportion of moving particles decreased.

Figure 3.6 shows data obtained from a translating particle in a hypertonic preparation. While stationary particles were observed in the preparations treated with hypertonic solutions, data from a translating particle were chosen for Fig. 3.6. This was done to compare the translation of a particle in a partially inhibited preparation to those in the control preparations. Part *a* of this figure shows displacement plotted against time. The characteristic undulating motion was present. There was no qualitative difference between the motion of this organelle and the motions of particles in the control preparations (Fig. 3.1*a*). The periodogram for the data in Fig. 3.6*a* is given in Fig. 3.6*b*. Most of the oscillations occurred at about 0.05 Hz. The three largest peaks occurred at about 0.05 to 0.1 Hz. They were all significant ($p < 0.01$). The particle tracked in Fig. 3.6 had transport that was indistinguishable from particles in the control preparations. However, impaired motion also occurred in the
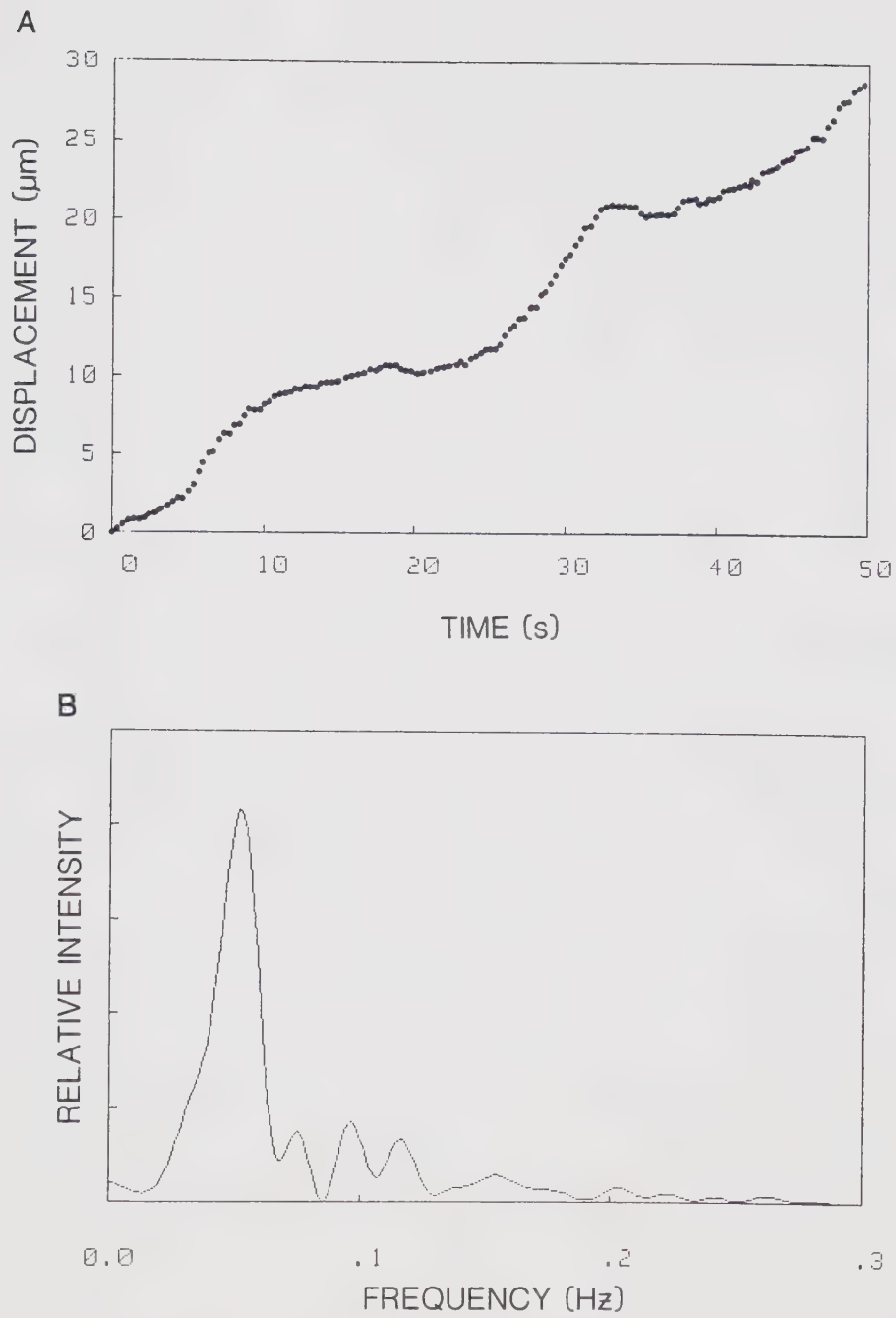
Figure 3.6 Transport of a particle within an axon exposed to a hypertonic solution: *a*. Position-time plot. *b*. Periodogram for the particle's motion.

hypertonic preparations.

3.2.6 Heavy Water

Heavy water inhibited axonal transport within five minutes of its application to nerves. The transporting particles moved more slowly than in the control preparations, and oscillatory motion also developed. The oscillations were grossly similar to those in previous experiments. As time progressed more disruption of transport occurred. These changes were more severe than could be attributed to the slightly increased viscosity of heavy water relative to that of water.

The displacement of an oscillating particle in heavy water is plotted in Fig. 3.7a, and its corresponding periodogram is given in Fig. 3.7b. The four largest peaks, within this periodogram, were significant $(p < 0.01)$. However, the largest peak at 0.015 Hz had a period of 66 seconds. This particular component could have been a transient process; thus its significance must be cautiously interpreted. The major point here is, however, that significant oscillatory components were present in the motion of this particle.
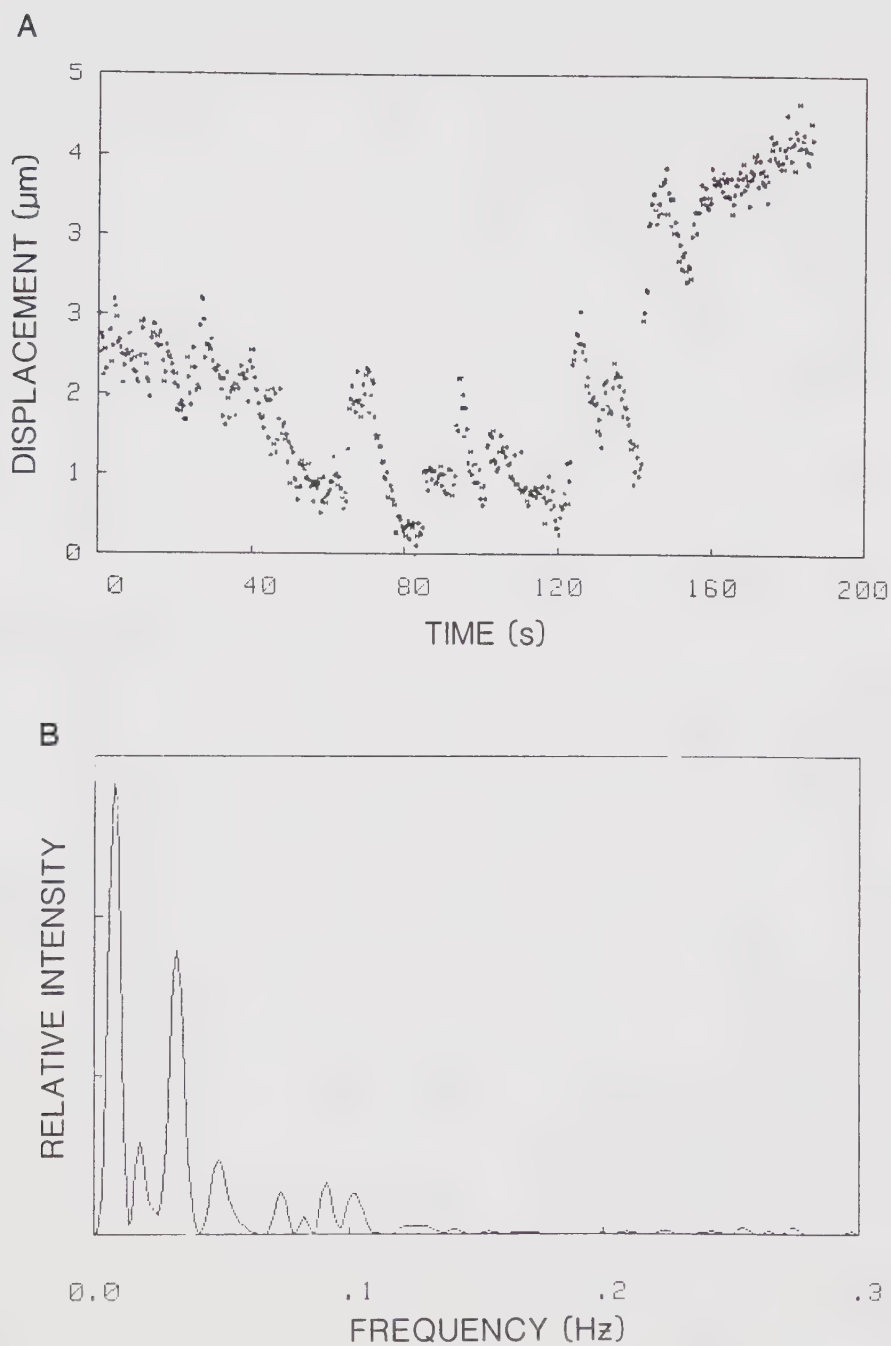
Figure 3.7 Wobbling of a particle exposed to heavy water:
a. Position-time plot. *b*. The corresponding periodogram.

3.3 Detailed Analysis Of Results

The oscillatory motions of organellles within axons
treated with colchicine, DMSO, DNP, hypertonic potassium
glutamate, and heavy water were similar. Despite the
different agents used to inhibit transport, the resultant
motion seemed to share common characteristics. In order to
further test this hypothesis, the data were analysed using
the more sophisticated methods detailed in chapter two. The
results of this detailed analysis follow. Other features of
the motion of organelles were also revealed by these
analyses.

3.3.1 Periodogram Evolution

Because of the difficulty with tracking particles for
long periods, it was difficult to quantitate how constant
the low frequency processes were. One pair of particles in a
nerve treated with colchicine was tracked for 500 seconds as
the particles wobbled. Figure 3.8 demonstrates periodograms
calculated from five successive segments of this data. Each
segment was 100 seconds long. They are placed in order of
increasing time— from the bottom to top of Fig. 3.8. There
was a persistent component of oscillation below 0.05 Hz,
although the form of each tracing changed, and transient
peaks emerged. These results indicated an apparently random
oscillation that generally occurred below 0.1 Hz. While the
oscillations behaved as random perturbations, they occurred
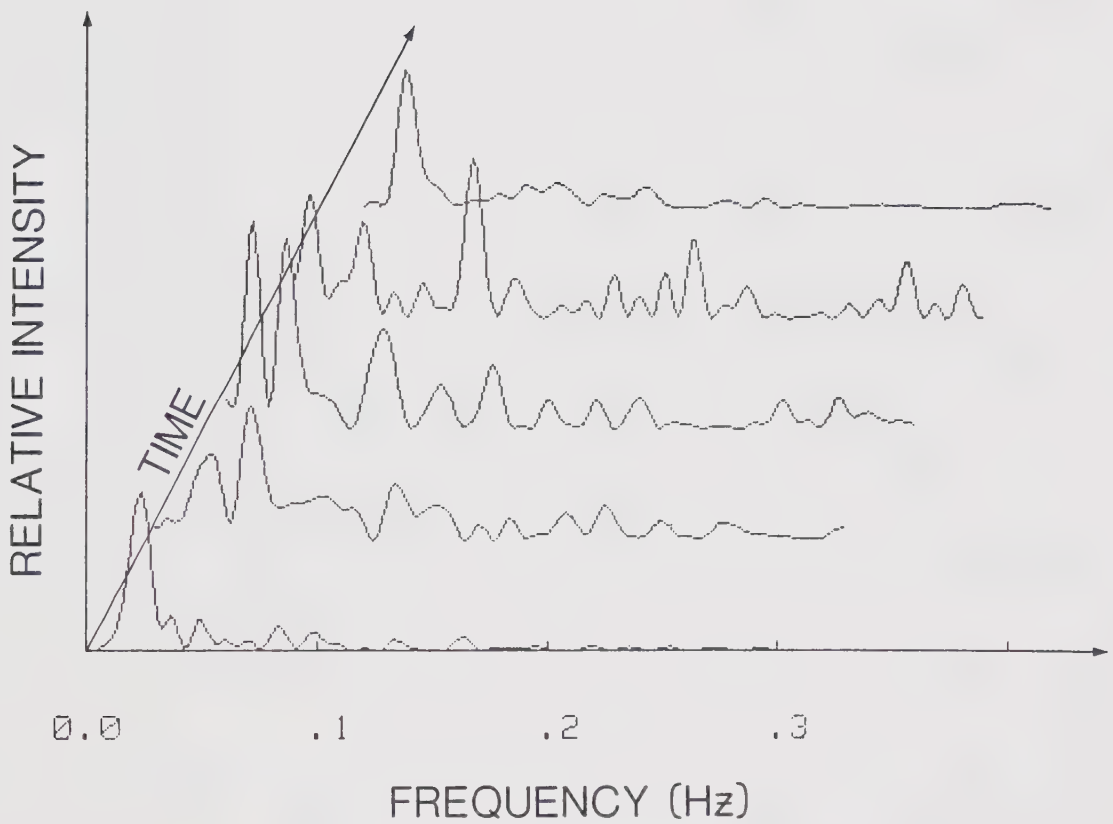over a relatively narrow range of frequency.

Figure 3.8 Evolution of a periodogram with time. Each periodogram was calculated from successive 100 s segments of data from a pair of particles. The five segments are placed from bottom to top, in sequential order, as time increases.

3.3.2 Phase Diagrams

Phase diagrams were constructed by plotting total velocity of a particle versus the particle's position within its axon. Figure 3.9 is the phase diagram for the particle treated with colchicine that was tracked in Fig 3.2. The particle oscillated within different regions of its axon for variable time periods and then jumped to new positions. The jumps occurred unexpectedly, and generally had higher velocities than when the particle was oscillating.

Another phase diagram of a particle oscillating about a fixed position is shown in Fig. 3.10. This particle was from a preparation exposed to DNP. The phase diagram here contained a self-intersecting two dimensional curve. This curve meandered over its phase plane with no apparent pattern. No stable equilibrium points developed. The oscillations diagramed in Fig. 3.10 had apparently random and nonlinear properties.

3.3.3 Anisotropic Motion

All of the organelles that wobbled about fixed positions had the major component of their motion aligned with the longitudinal axis of their axons. This effect occurred in all preparations regardless of the inhibitor used. Similarly, translating particles had a superimposed wobble that was aligned with the longitudinal axis. In order to study this alignment further, the standard deviations of the trend-free displacements were calculated. The x and
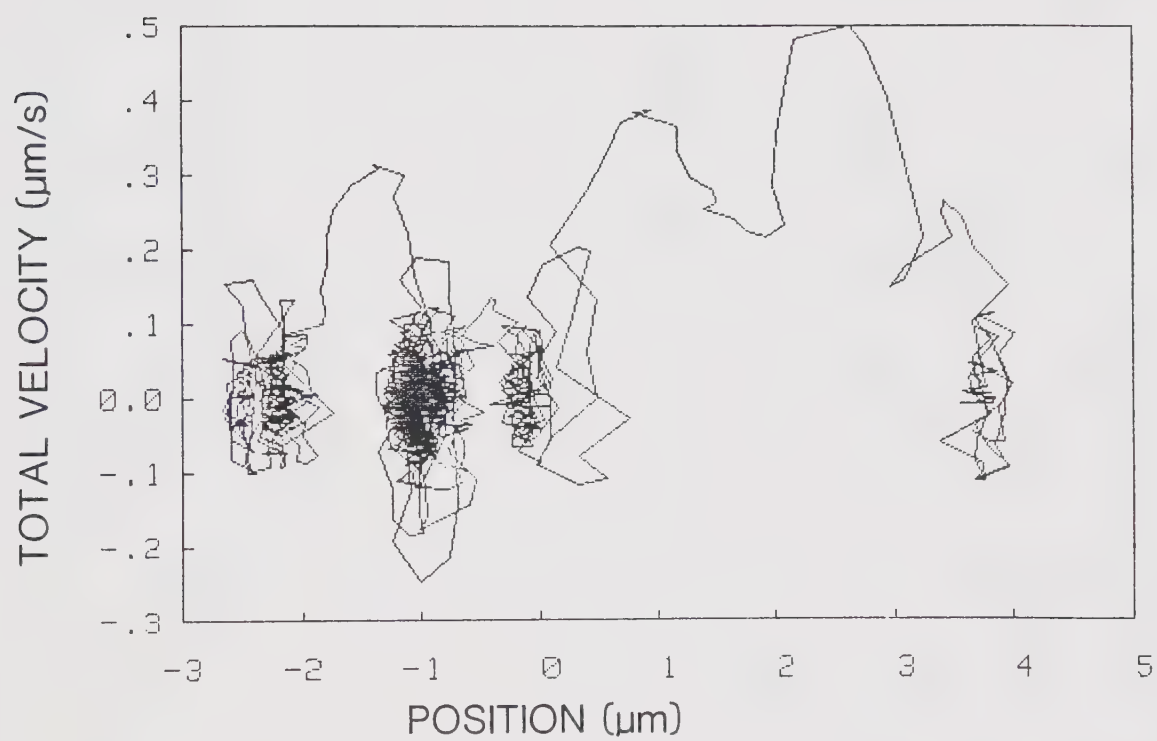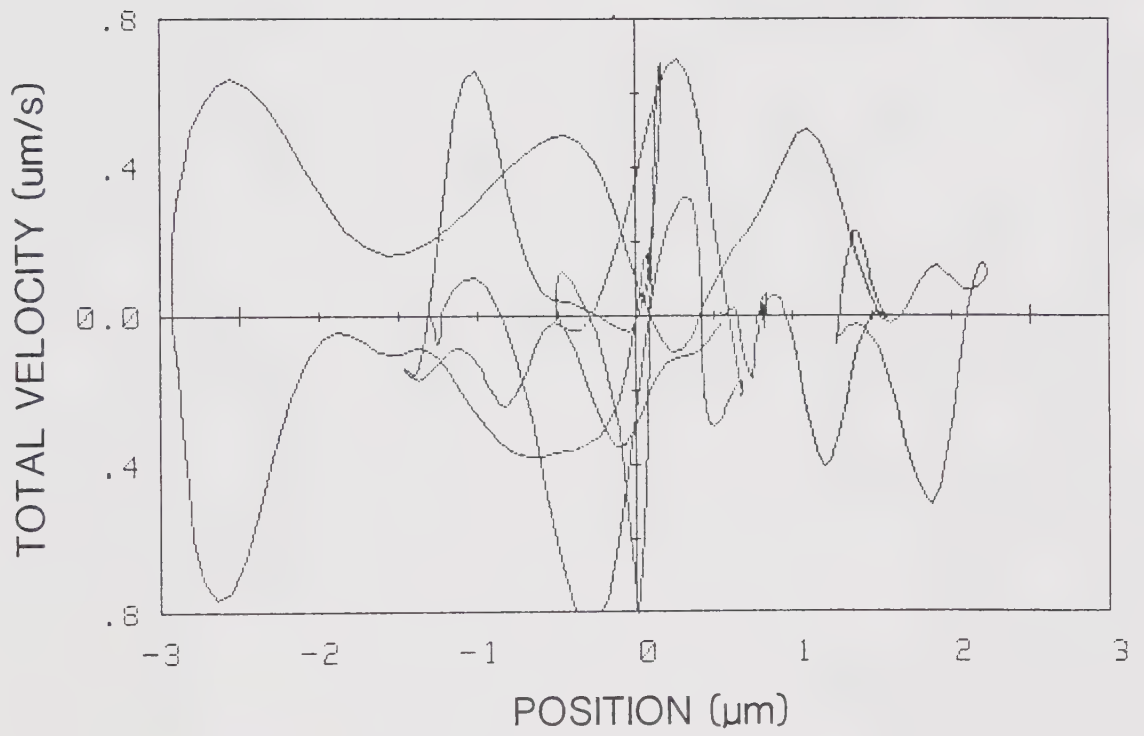
Figure 3.9 Phase Diagram: Jumping Particle

Figure 3.10 Phase Diagram: Oscillating Particle

y-components of these standard deviations were plotted against each other for each individual particle. Data from all of the preparations were used. Both translating particles and those wobbling about fixed positions were included in these calculations. Figure 3.11 gives the results; each point represents a single axonal particle. The standard deviation was a convenient measure of the amplitude of wobble along the x and y-axes. A continuous distribution of points, extending over two orders of magnitude of displacement, resulted. There was no separation of translating particles from stationary particles. Neither was there any separation on the basis of the specific inhibitor used. These results suggested that oscillations were part of one general process.

Figure 3.11 also emphasized the anisotropy of the wobble. The standard deviations along the x-axis were greater than the y-component. Thus the oscillations appeared to be aligned with the general direction of transport.

The y-axis oscillations were a significant component of motion for some of the particles. Did the y-oscillations result from a process independent to the x-oscillations? A cross-periodogram was calculated from some typical data. This is shown in Fig. 3.12.

The cross-periodogram is a measure of how synchronized two signals are. In this case, the oscillations of a particle along the x and y-axes were compared to each other. From Fig. 3.12, the x and y-components had a common
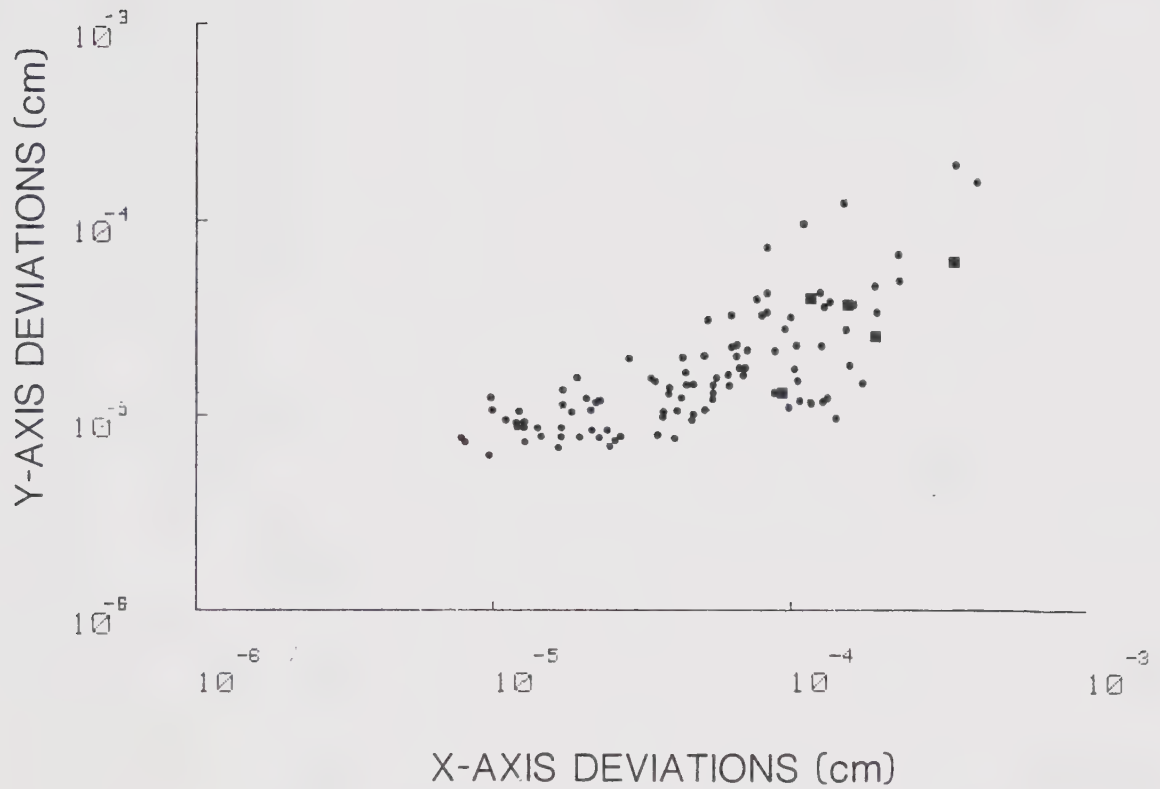
Figure 3.11 Graph comparing the magnitude of positional
oscillations along the transverse axonal (y) axis to those
occurring along the longitudinal axis. Each point represents
data obtained from a single particle. Both stationary and
translating particles were used. The squares indicate
data from the control preparations.
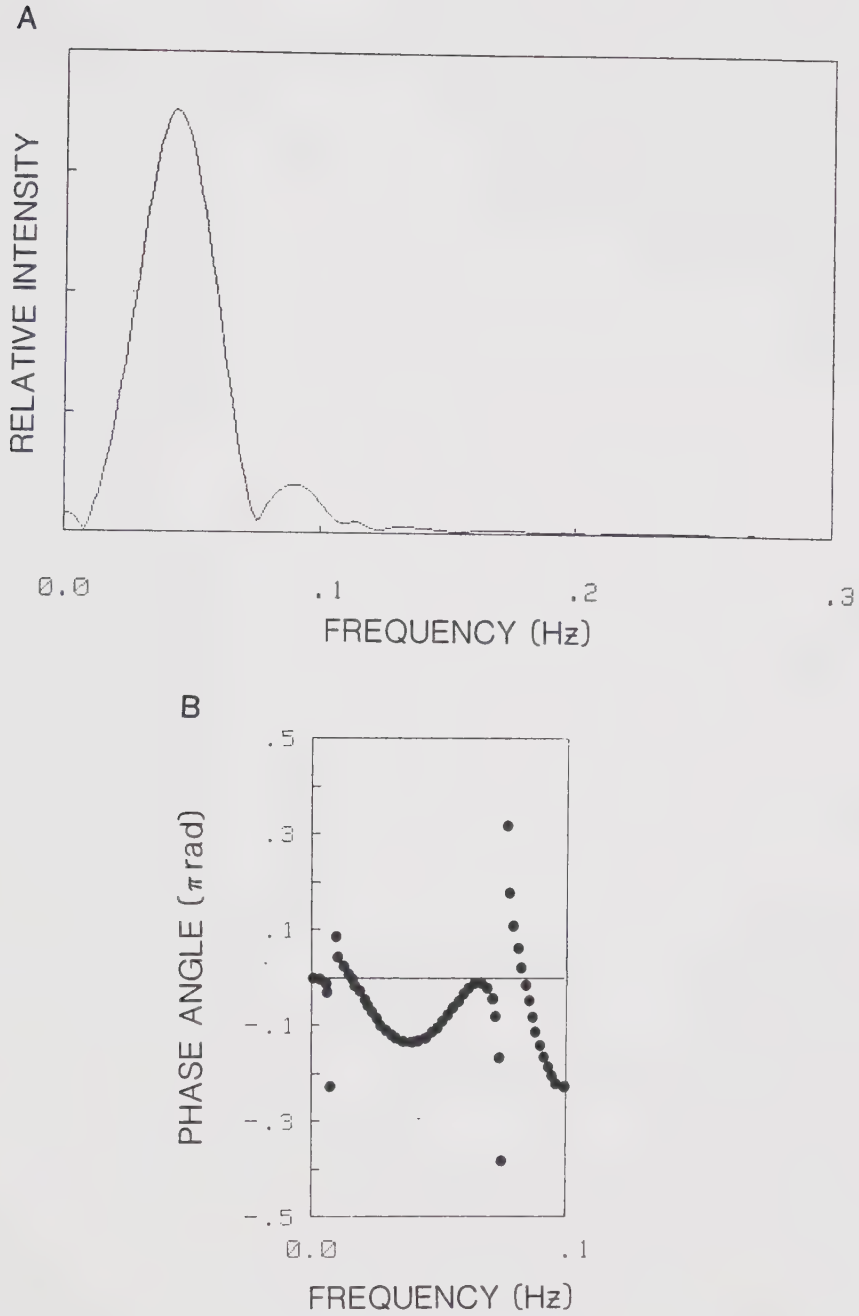
Figure 3.12 Cross periodogram comparing the component of motion of a particle along the transverse axis to the longitudinal axis: *a*. Magnitude. *b*. Phase shift.

frequency of oscillation at 0.03 Hz. At this frequency the
two components were separated by a phase lag of only 0.15 pi
radians. The two processes were essentially in phase with
each other.

It is reasonable to conclude that the y-axis
oscillations were a component of the x-axis process. The
y-component resulted in part from difficulty with aligning
the digitizer's x-axis with the major axis of motion. Also
it resulted from perturbations of the major axis of particle
motion that occurred with time.

3.3.4 Mean Velocity And Velocity Fluctuations

Along any axis there were two components of velocity:

1. the mean velocity, $\dot{V}$, calculated from the least squares
    slope [Eq. (2.12)], and

2. the instantaneous velocity, (x'_a , y'_a), calculated from
    the trend-free fluctuations [Eq. (2.15)].

The standard deviations of the instantaneous velocities were
calculated in order to measure the magnitude of fluctuations
of velocity [Eq. (2.17)]. The mean velocities were plotted
versus the standard deviations in Fig. 3.13. Only the
longitudinal components were used. Each point represented
one particle. All particles, whether fixed or translating,
and irrespective of preparation, were included in these
calculations.

The data points were spread over a continuous spectrum
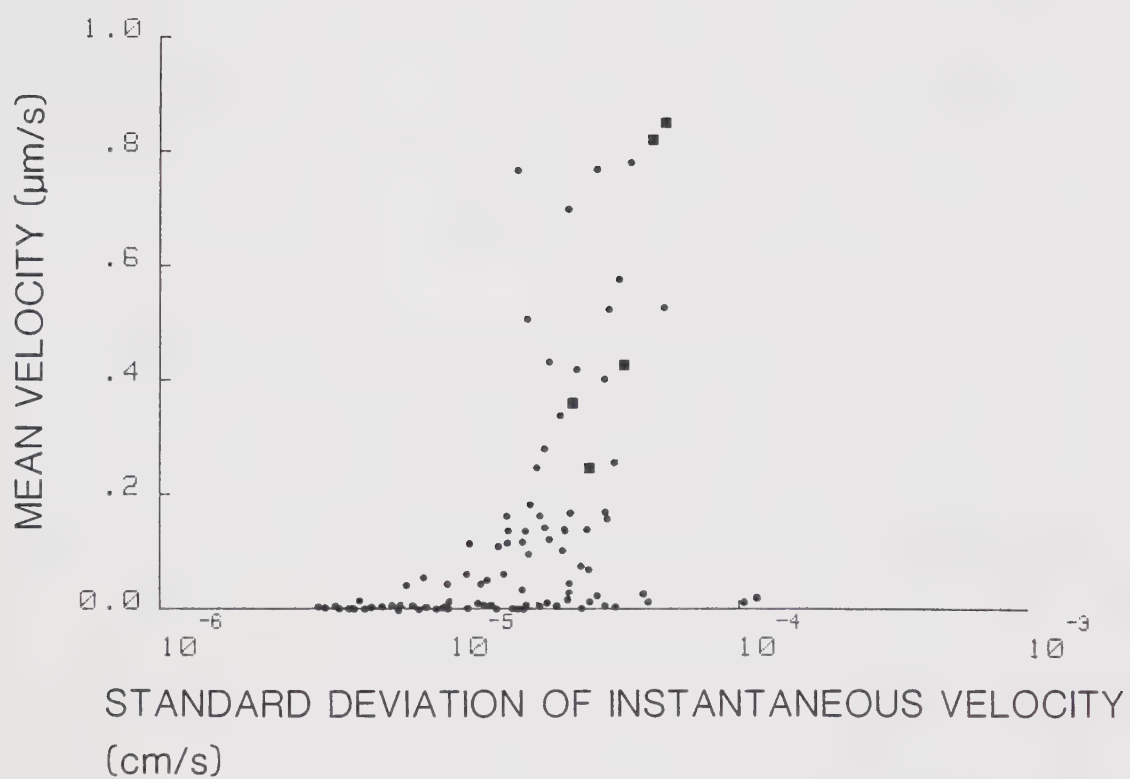in Fig. 3.13. Most of the particles translated at speeds

Figure 3.13 Graph comparing mean velocity to the magnitude of the velocity fluctuations about the mean. Each point represents data from one particle.The squares denote data from the controls.

much lower than the average speed of one micrometer per second found for uninhibited particles (Cooper and Smith 1974: Koles *et al.* 1982a). Many particles had no significant net velocity. Some of the stationary particles had velocity fluctuations of a size similar to those of translating particles.

The main finding from Fig. 3.13 was the continuous distribution of mean velocities from about 0.0 to 0.8 micrometers per second. The process of inhibition did not separate the data into two groups: one of particles moving at a constant speed, the other of stationary particles.

3.3.5 Probability Distribution For Velocity

Probability distributions for instantaneous velocities were calcuated for particles oscillating about fixed positions. Only the longitudinal components of velocity were used. A resultant histogram, for data from one particle, is shown in Fig. 3.14. The velocity distributions were essentially unimodal. The distribution for the data in Fig. 3.14 ranged from about -1 to 1 micrometers per second. These data were similar to data obtained from translating particles (Koles *et al.* 1982a).

3.3.6 Periodogram Moments

The periodogram moments for each particle were calculated. All particles were analysed irrespective of their preparation or motion. The first moment was plotted
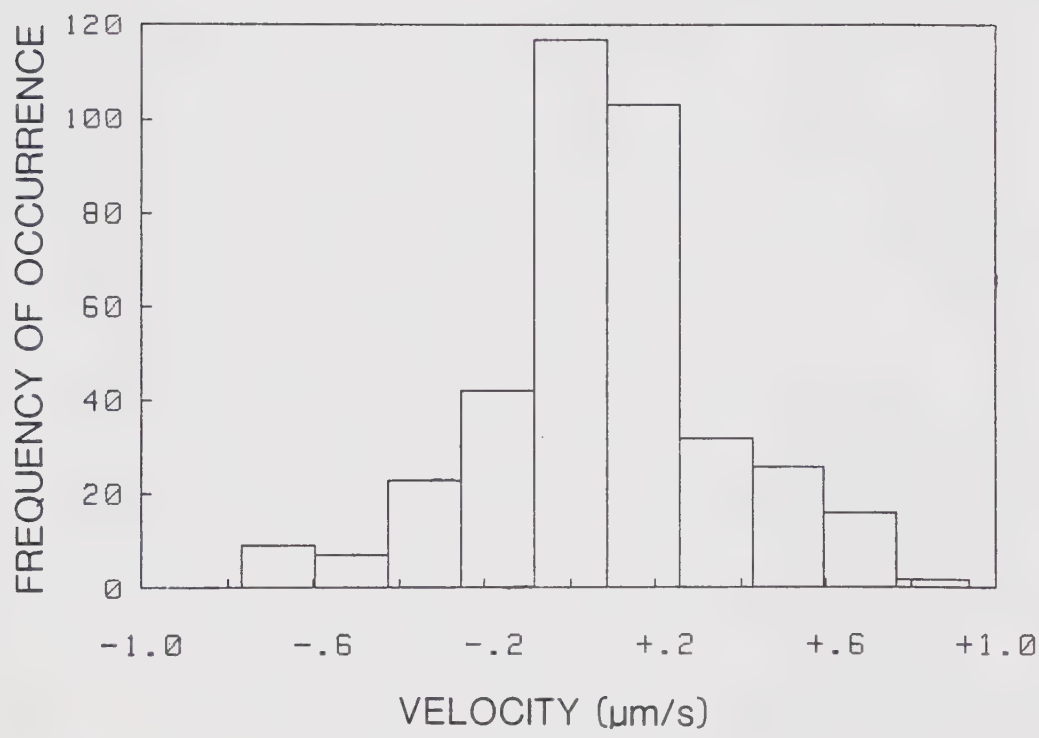
Figure 3.14 Distribution of instantaneous velocities obtained from a particle oscillating about a fixed position.

versus the zeroth moment in Fig. 3.15. As mentioned previously, the ratio of the first moment to the zeroth moment gives the center of spectral mass. The zeroth moment is proportional to the variance of its signal.

The data points were continuously distributed over about five orders of magnitude. There was no clear division of translating particles from stationary particles. Nor was there a division according to the specific treatment.

The relationship in Fig. 3.15 was approximately linear. The slope gave an average value for the center of spectral mass. The oscillatory activity was centered on a frequency range of 0.18 ± 0.02 Hz (SEM).

Next the spectral parameter δ was plotted versus the zeroth moment (Fig. 3.16). The parameter δ is a measure of the variability of frequency content for each process. The values for δ were clustered near 1.0, being more concentrated there for the stronger signals. An average value for δ was 0.84 ± 0.01 (SEM). These data demonstrated a highly variable frequency content for the oscillations.

Finally, the standard deviations of the positional fluctuations along the longitudinal axis were plotted versus the center of spectral mass, f^+ (Fig. 3.17). The center of spectral mass was a crude estimate of the predominant frequency within each signal. The major problem with using f^+ was that for weaker signals, the magnitude of f^+ was increased (Fig. 3.17). For these oscillations the values of f^+ were larger because of the larger contribution from
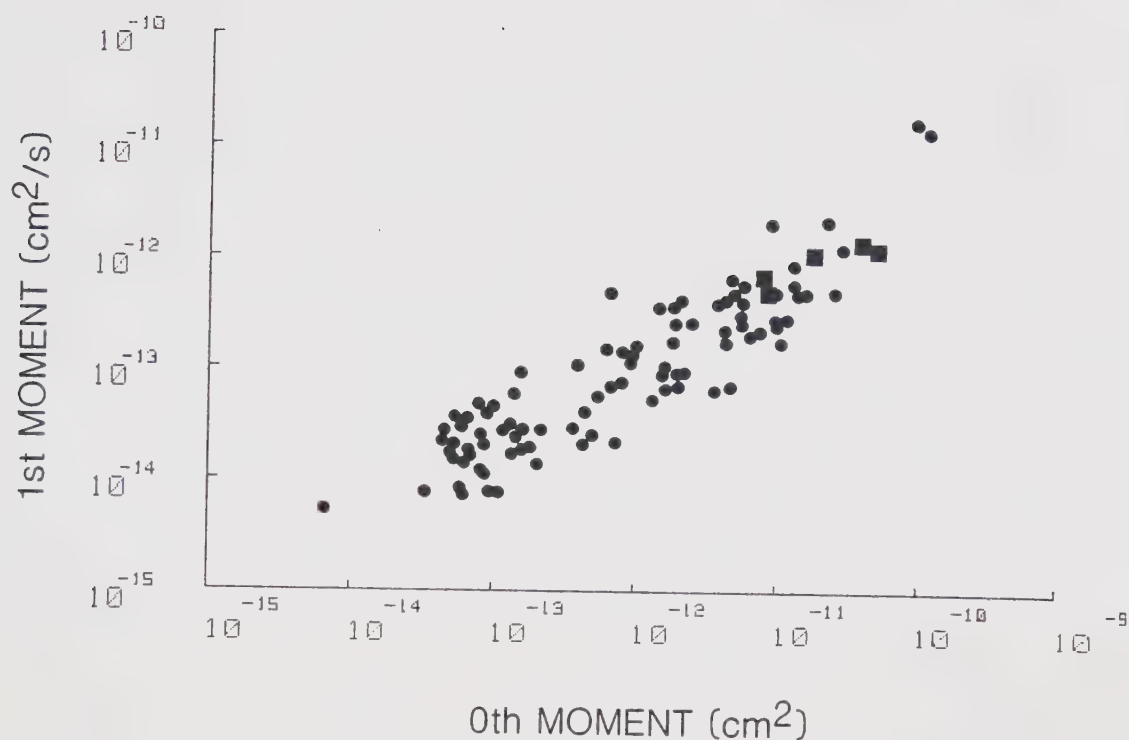
Figure 3.15 Plot of first periodogram moment versus zeroth moment. Each point represents data obtained from one particle. The slope of this graph gives an overall frequency for oscillatory motion of particles at 0.18 ± 0.02 Hz (SEM). The squares represent data from the controls.

measurement error. For stronger signals with standard deviations above 3×10^{-5} cm, the centers of spectral mass were generally about 0.1 Hz. This value of 0.1 Hz was a reasonable estimate for the characteristic frequency of the positional oscillations.
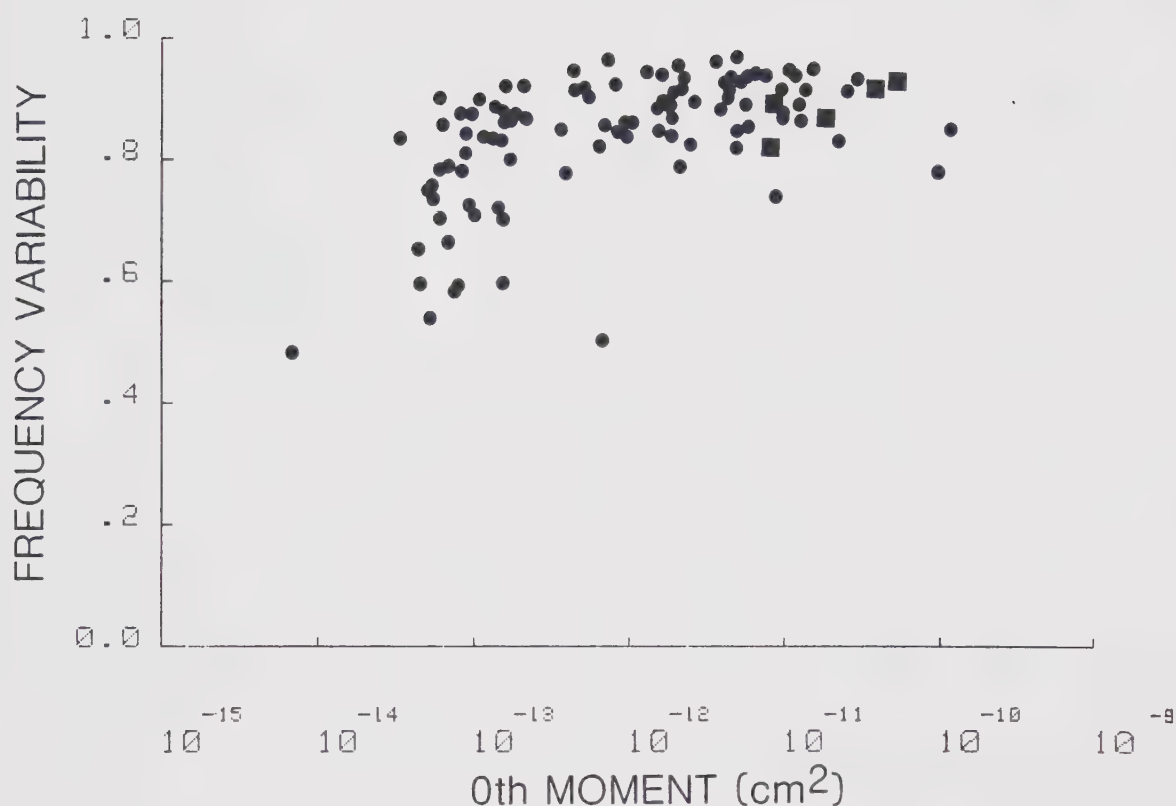
Figure 3.16 Variability of frequency plotted against the zeroth moment. Each point represents data obtained from one particle. As the magnitude of the zeroth moment increases the signal becomes stronger, and the variability approaches unity. A frequency variability of unity indicates a highly variable signal. The squares represent the controls. Both translating and stationary particles are represented here.
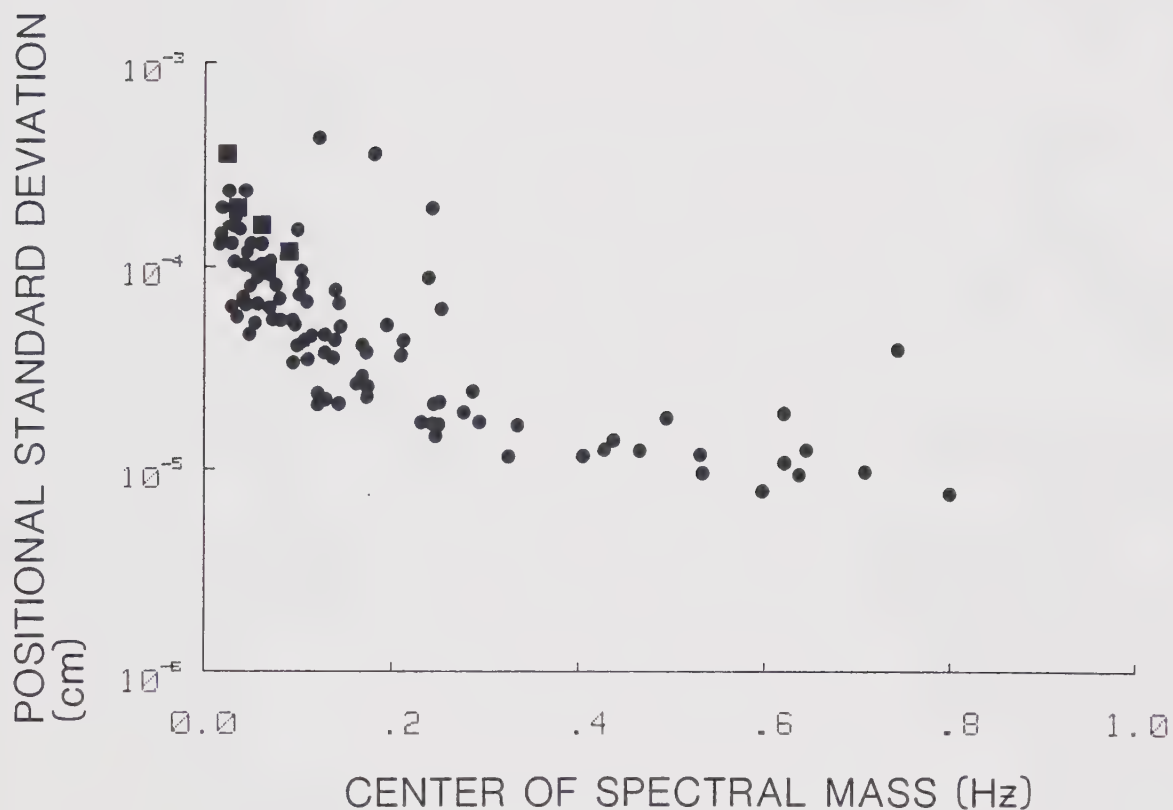
Figure 3.17 Plot of positional fluctuations versus center of spectral mass. For the larger fluctuations the center of mass is below 0.2 Hz, indicating that the stronger signals have a lower frequency. The squares represent the controls. Both translating and stationary particles were used here.

4. RESULTS: FREEZING EXPERIMENTS

In this chapter the effects of rapidly freezing and thawing axons are described. First the effect on organelle transport is detailed, followed by the results of morphological studies.

4.1 Dark-Field Microscopy

Axons, frozen in liquid nitrogen and then rapidly thawed, initially showed no evidence of organelle movement. After about five minutes from thawing, the particles began to wobble along the longitudinal axis. During the next five to ten minutes they began to translate. Transport was mainly retrograde, but anterograde motion occurred too. After 15 to 20 minutes from thawing, the proportion of transporting particles gradually decreased. At about 45 minutes, motion of organelles was rarely detectable. These results were easily reproduced.

The longitudinal displacement of two organelles after thawing is plotted in Fig. 4.1. In Fig. 4.1a a previously stationary particle moved back and forth, and then was transported in the typical undulating manner. The particle tracked in Fig. 4.1b initially wobbled back and forth over distances of up to four micrometers, then it was transported about 14 micrometers, and finally it came to rest. These data demonstrated the sequence of recovery after a freezing and thawing. Initially motionless particles began to wobble,

95
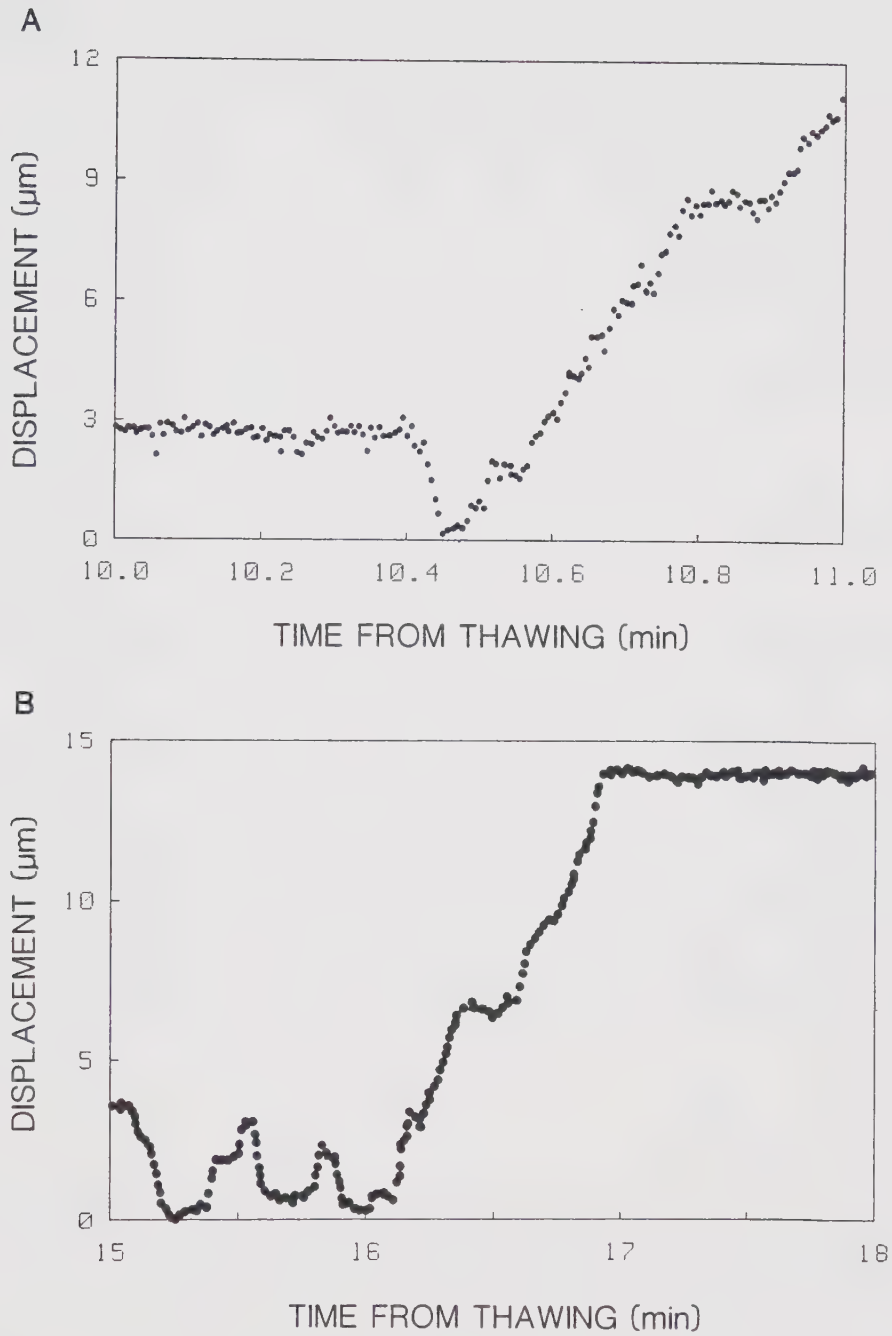
Figure 4.1 Recovery of transport after thawing:
a. Position-time plot for an intraaxonal particle.
b. Position-time plot for a second particle.

then translated, and finally stopped moving.

Oscillations over relatively large amplitudes were observed within the thawed preparations. The displacement of an organelle performing such large oscillations is plotted in Fig. 4.2*a*. These oscillations spanned over six micrometers and appeared random. The instantaneous velocities corresponding to these data were plotted in Fig. 4.2*b*. Note the smoothly varying velocity with respect to time. These variations were also apparently random. However, a random appearance does not always imply that the underlying process is indeed stochastic. This point shall be discussed in a later chapter.

With the addition of 10 mM colchicine to the solutions used for thawing, transport never resumed. Only very rarely did an occasional particle wobble. When this wobble did occur it was transient and it was over distances of less that one micrometer. This effect of colchicine was easily reproducible. Colchicine prevented the recovery of transport after thawing.

4.2 Morphological Studies

Could any submicroscopic intraaxonal structures be influencing the recovery of transport after thawing? To answer this question, electron microscopy was performed on segments of axons fixed at specific time intervals after thawing.
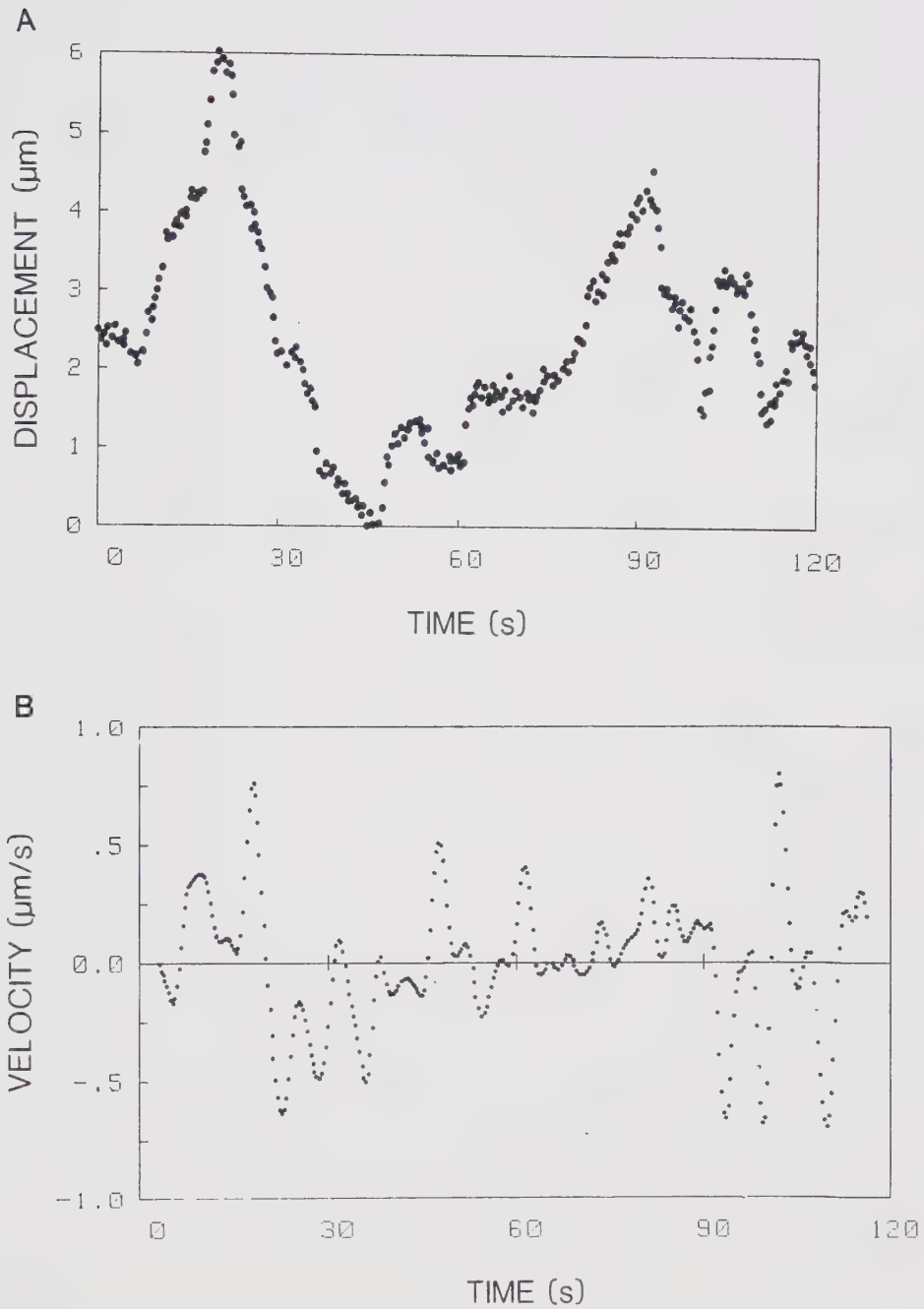
Figure 4.2 Large amplitude wobble after thawing:
a. Position-time plot for a particle. *b*. Velocity-time plot
for the same particle.

The structure of thawed nerves was generally well preserved on electron microscopy. While the mitochondria did appear swollen, the endoplasmic reticulum, microfilaments, and microtubules individually appeared unaltered. The axoplasm appeared more condensed, with an increased density of microfilaments and endoplasmic reticulum. Plate 4.1 demonstrates three transverse sections of thawed nerve. Part *a* is a low power view of nerve that was thawed and immediately fixed; parts *b* and *c* are higher power views of transverse sections of nerves fixed at 12 minutes after thawing. Occasional convolutions and cracks in the axonal membrane were evident in parts *b* and *c*. In general, these features suggested a slight shrinkage of the axons after freezing and thawing.

Plate 4.2 contains high power views of three transverse sections of axons. Part *a* was taken from control nerves, not treated in liquid nitrogen. Parts *b* and *c* were from frozen and thawed nerves that were fixed at 0 and 12 minutes after thawing, respectively. Comparison of the three micrographs reveals one conspicuous difference between them. In part *a* the numerical density of microtubules was normal. For emphasis, the microtubules have been circled in these photographs. In part *b* the numerical density of microtubules was noticibly decreased while in part *c* the density appeared normal.

To investigate the changes in numerical density of microtubules after freezing, these densities were measured

Plate 4.1 Electron micrographs of transverse sections of myelinated axons which were frozen and thawed as described in the text: *a*. Low power view of two axons. Their myelin is disrupted. The intraaxonal organelles individually are grossly normal. *b*. and *c*. High power views to show abnormal folding and possible defects of the axolemma (arrowheads). Scale bar: *a*. 5 micrometers; *b*. and *c*. 1 micrometer. Time following thawing: *a*. 0 min; *b*. and *c*. 12 min.
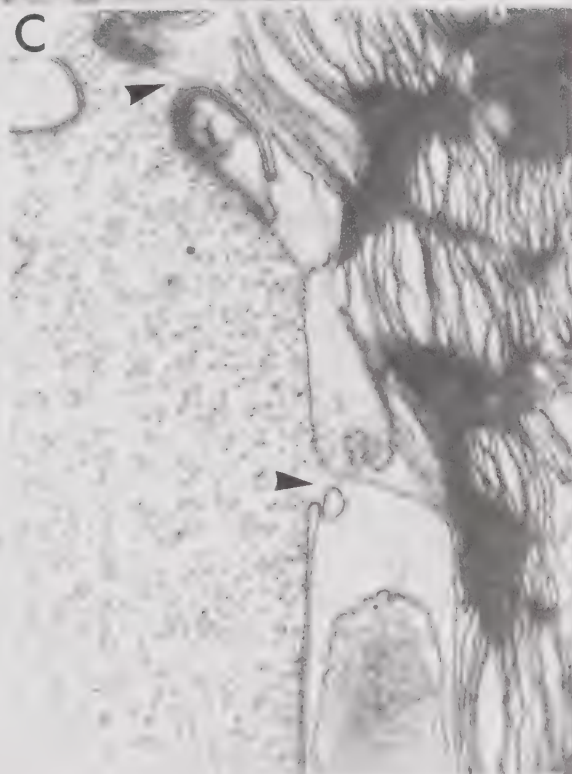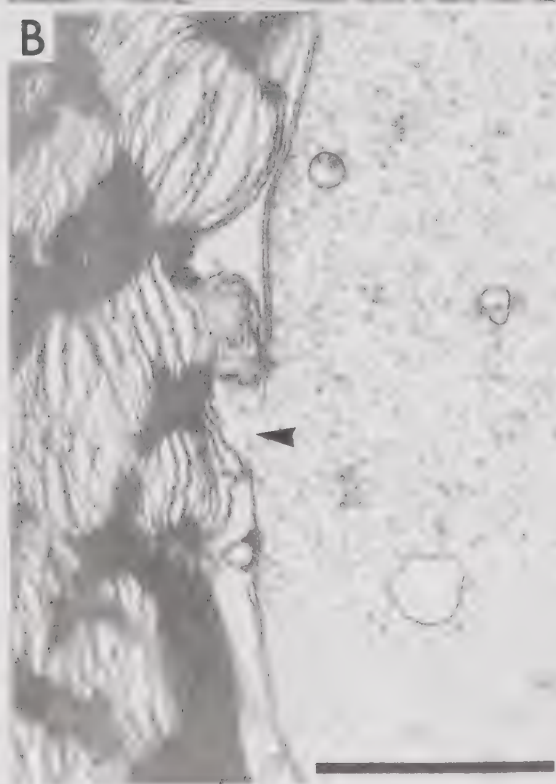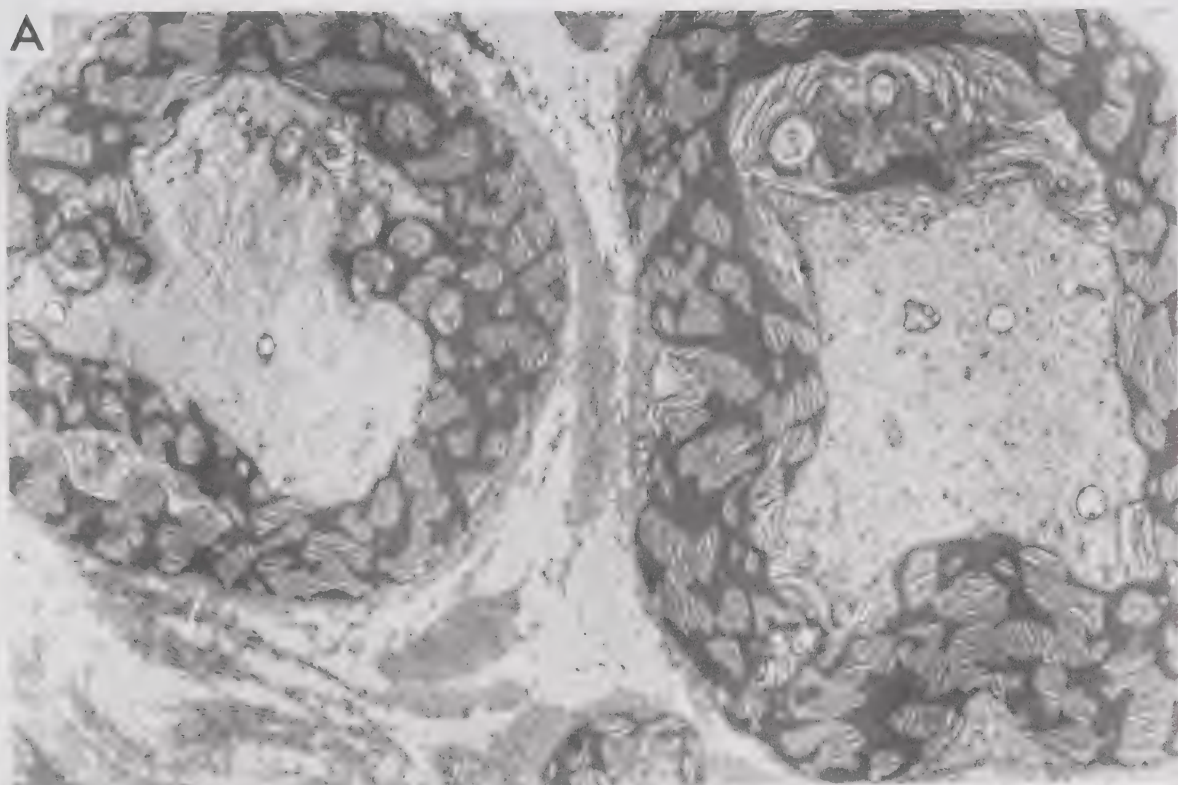
Plate 4.2 High power electron micrographs of transverse sections of axons: *a*. Control axon that was not subjected to freezing and thawing. The microtubules have been circled for ease of identification. *b*. Axon that was frozen and thawed in fixative. The numbers of microtubules are decreased. *c*. Axon that was frozen and fixed 12 minutes after thawing. The numbers of microtubules have returned to normal. Scale bar: 1 micrometer.
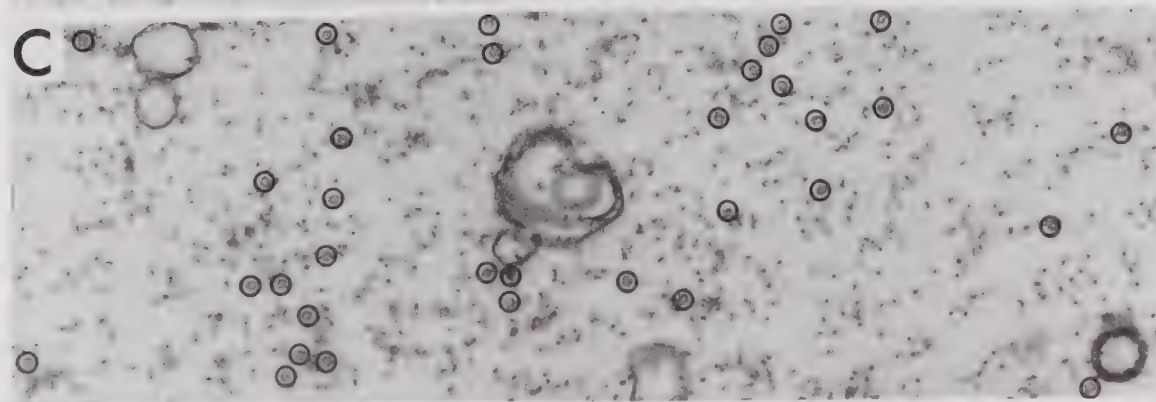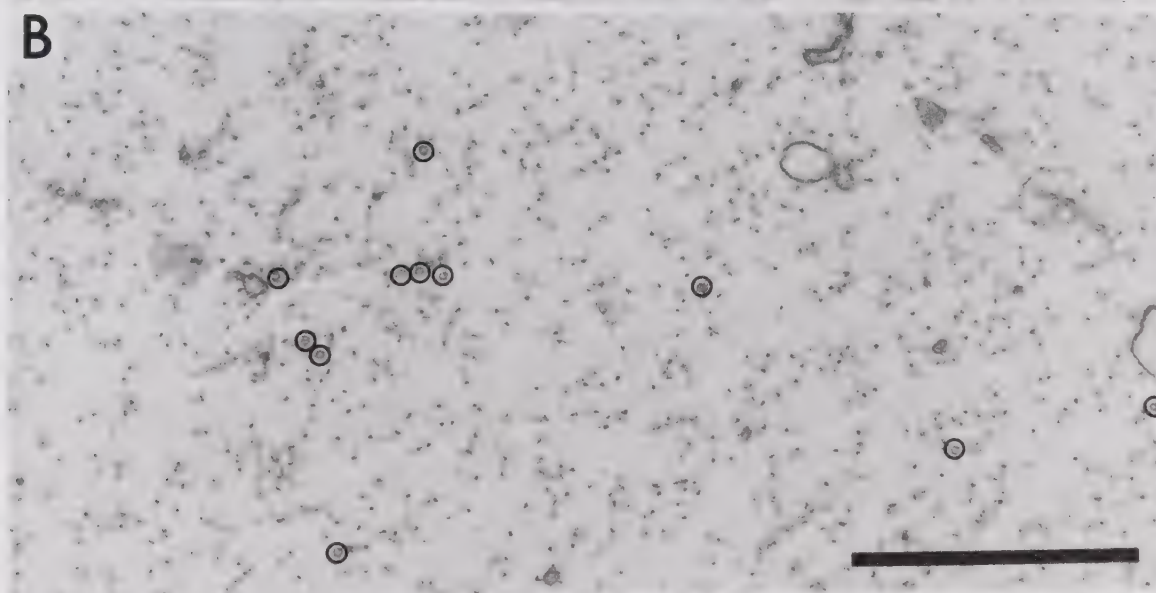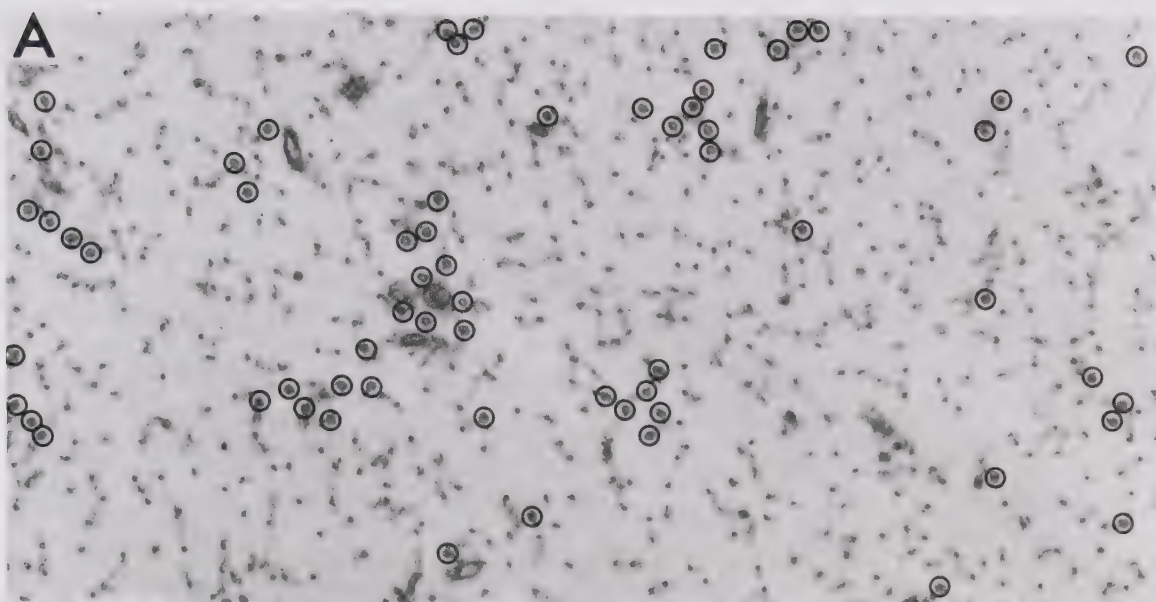
from specimens that were fixed at specific time intervals after thawing. These data were compared to the number of transporting particles at sequential periods from thawing. Figure 4.3a shows the total number of transporting particles, within five thawed axons, plotted versus time. A ten micrometer segment of each axon was observed. Groups of particles were placed in the microscope's field of view, and then observed. During the initial four minutes after thawing, no particles were transported. From four to seven minutes after thawing the number of transporting particles rapidly increased. Thereafter, the groups of particles dispersed out of the field of view, and a lower frequency of transporting particles resulted.

In Fig. 4.3b the numerical density of microtubules is plotted against the time from thawing. Initially, few microtubules were present. Paralleling the increase in number of particles being transported, there was an increase of microtubule density to control levels. Thereafter, the density of microtubules remained constant. The addition of colchicine to the solution used for thawing kept the density of microtubules limited to about 40% of control levels.

In Fig. 4.3b the numerical density of microtubules in the colchicine preparations is represented by a black square. The solid dots are data from preparations that were not exposed to colchicine. These data were averages, obtained from nine to eleven preparations. The error bars define one standard deviation above and below each data
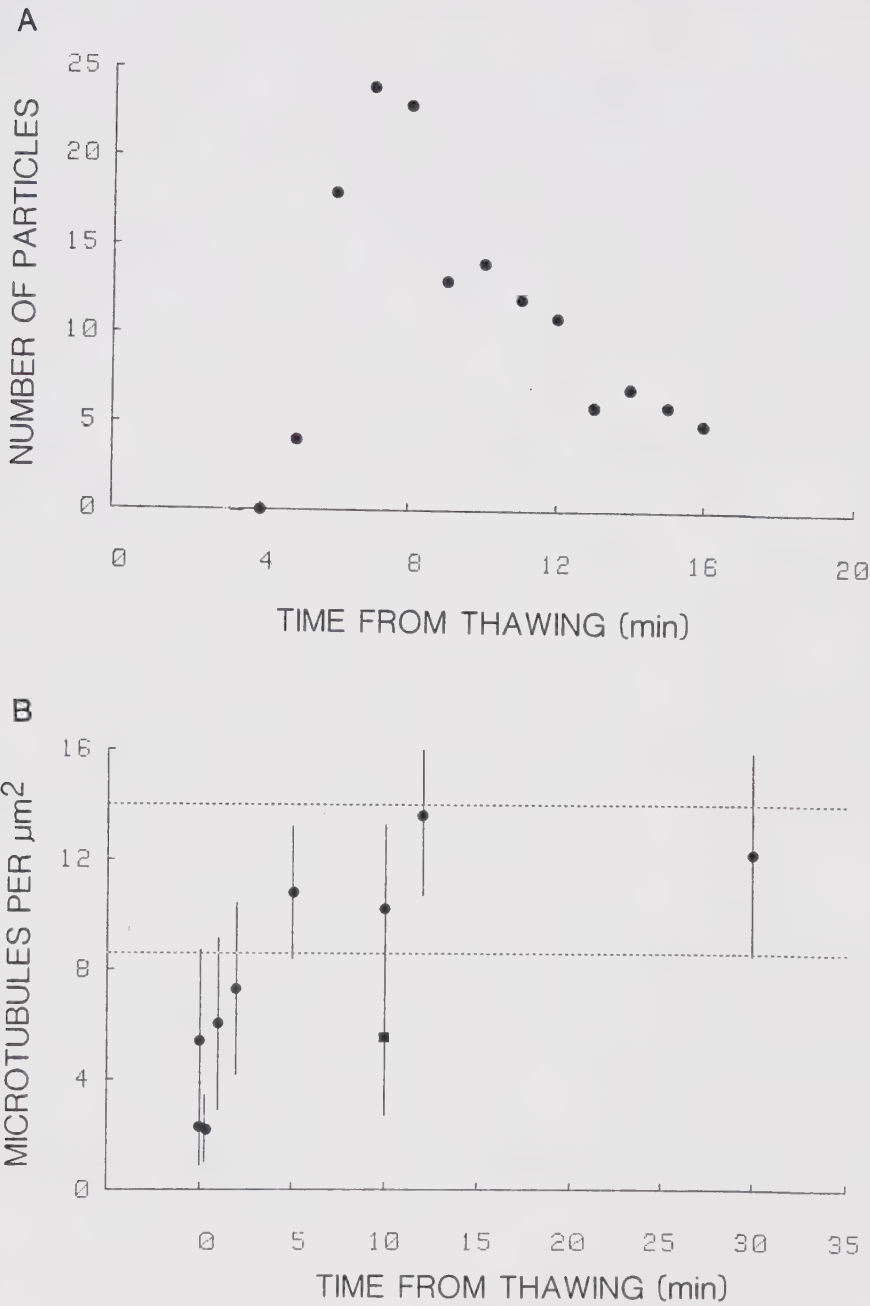
Figure 4.3 Recovery of transport and microtubules after thawing: *a*. Total number of transporting particles in five 10 m axonal segments, plotted versus time from thawing. *b*. Average number density of microtubules within about ten preparations, plotted versus time from thawing. The error bars represent one standard deviation about each point. The dotted lines define one standard deviation about control levels. The square point is data from preparations treated with colchicine.

point. The dotted lines represent one standard deviation about the control levels.

In Fig 4.4 the numerical density of neurofilaments is plotted versus time from thawing. Again, the dotted lines define one standard deviation about the control levels, and the error bars represent one standard deviation about each point. Each point is an average taken over nine to eleven preparations. The neurofilament density remained elevated by about 50% above control levels during the period it was observed. There was no significant change in neurofilament density with time. Nor was there any significant difference in neurofilament density in the specimens treated with colchicine. These changes were probably caused by axonal shrinkage after freezing and thawing.

The relative numbers of particles that were transporting after 30 minutes appeared to be decreased. As previously mentioned, motion of organelles appeared to cease after about 45 minutes. However, no structural changes could be found within axons that corresponded to the decreased numbers of transporting particles.
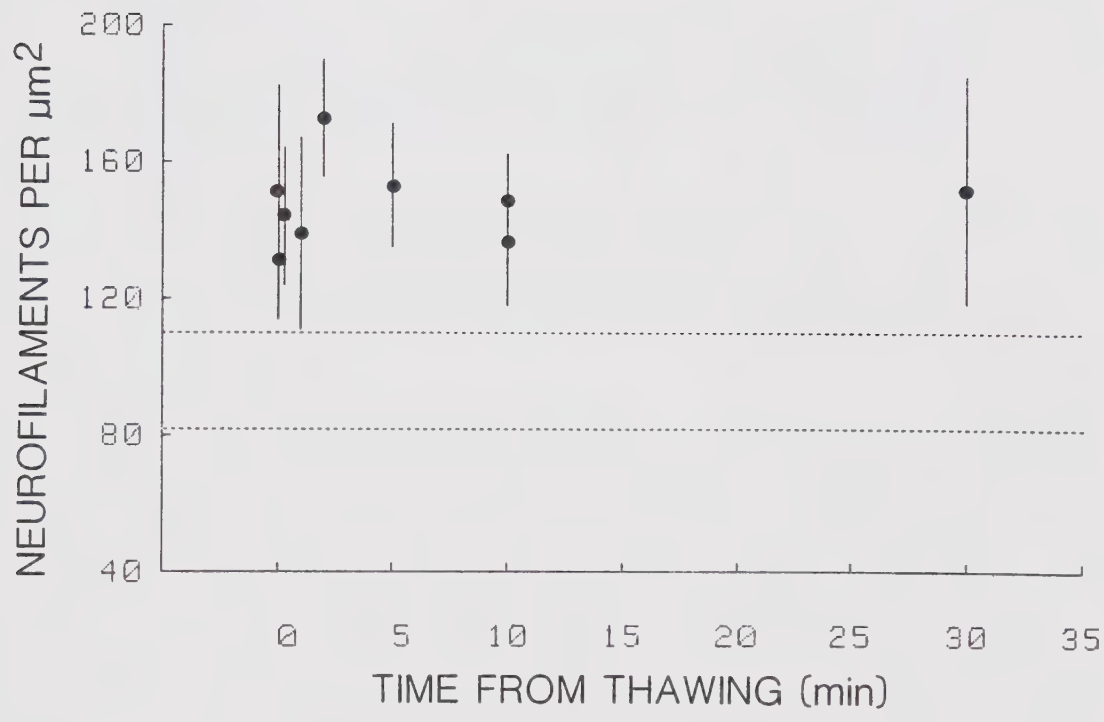
Figure 4.4 Numerical density of neurofilaments plotted versus time from thawing. Each point represents an average over about 10 preparations. The error bars represent one standard deviation about each point. The dotted lines define one standard deviation about control levels.

5. DISCUSSION

5.1 Overview

In this thesis, the subject of axonal transport was reviewed. Several general features of transport were emphasized:

1. the classification of axonal transport into fast and slow components,

2. the diverse nature of the material transported,

3. the different speeds of transport for different materials,

4. the bidirectional nature of fast transport, and

5. the large particulate component of the material transported.

Methods of observing axonal transport were also discussed and, in particular, optical techniques were emphasized.

Several agents, known to inhibit axonal transport, were reviewed. The postulated mechanisms of action of these agents had two interesting implications. First, the action of dinitrophenol implied a dependence of fast transport on oxidative metabolism. Second, the action of agents such as colchicine implied a possible dependence of transport on microtubules. This latter aspect was recognized as being controversial.

Next the transport of optically detectable organelles was reviewed. This transport of organelles was equated with

fast axonal transport. The motion of individual organelles was complicated. Early, more qualitative, observations of organelle movements were perceived as being irregular and discontinuous— thus the term saltatory was applied to these movements. However, with the advent of more sophisticated experimental techniques, the motions of organelles were found to be uniform. Thus, the term saltatory may no longer be applicable to describing the transport of organelles within axons.

Several features of the uninhibited transport of organelles within axons were:

1. the fluctuations in position superimposed on the linear displacement of normal transport,

2. the rare complete reversals in net direction of an individual particle's movement,

3. the rare occasion when a particle would oscillate back and forth about a fixed position in normal axons.

These features perhaps indicated the tendency with which a particle could reverse direction— albeit for variable periods of time.

In certain preparations, sustained back and forth movements of organelles could be produced. Colchicine and local crushing of axons could both cause these motions. The significance of these motions was unknown. It was suggested that these motions were due to either active or thermal forces.

Intraaxonal structure was reviewed. An orderly arrangement of submicroscopic and fibrillar elements exists within axons. These structures could possibly affect the motion of organelles by acting as barriers to movement, by altering the local viscosity of axoplasm, or by participating in the mechanism of transport.

Brownian motion within cells was discussed, since this was a possible mechanism for oscillatory motion. Within cells of higher organisms, Brownian motion has not been easily observed. This is because of the increased amount of structure within highly developed cells; this restricts the motions of organelles and damps out Brownian motion.

Several postulated mechanisms for axonal transport were described and criticized. A general classification was introduced: ratchet mechanisms, fluid flow mechanisms, and mechanisms dependent on smooth endoplasmic reticulum. None of these mechanisms was entirely satisfactory in explaining observations of axonal transport.

In the second chapter, the methods used in this study were introduced. This study proceeded along two directions:

1. the study of organelle transport within axons exposed to inhibitory agents, and
2. the study of organelle motion and fine structural changes in axons that had been rapidly frozen and thawed.

A sophisticated means of analysing the motion of organelles was also introduced.

The aim of this study was to answer the following
questions concerning the transport of organelles within
axons:

1.   What are the conditions producing oscillatory motion of
     organelles about fixed positions?
2.   What are the characteristics of the oscillatory motion
     of organelles?
3.   What is the action of metabolic blockers on this
     oscillatory motion?
4.   What is the driving force of the oscillatory motion? Is
     it Brownian motion or is it an active process?
5.   Do axonal microtubules have a role in fast axonal
     transport?

These questions are discussed in detail in the following
sections.

Before proceeding with this discussion several
frequently used terms are defined here. A process is called
random if it is unpredictable. The opposite of a random
process is a deterministic process. It is possible to
predict the behavior of a deterministic process with
equations. The term oscillatory is used in the general sense
to describe a process which fluctuates back and forth about
a mean value. An oscillatory process may be either
deterministic or random. A periodic process is one which can
be described by the summation of a finite number of
sinusoidal terms in an equation. If a process cannot be
represented by the summation of sinusoids then it is

referred to as aperiodic.

5.2 Conditions Producing Oscillatory Motion

All of the inhibitors of axonal transport used in this study produced oscillatory motion of organelles. As noted by previous workers (Hammond and Smith 1977; Horie *et al*. 1981), oscillatory motion of organelles about fixed positions was produced by colchicine. In addition dimethylsulfoxide, dinitrophenol, high calcium ion concentrations, hypertonic potassium glutamate, and heavy water could all produce oscillatory motion. These motions also occurred during the recovery phase of transport within axons that had been frozen.

Since such a wide variety of agents produced oscillatory motion of organelles, this motion must be a fundamental process. Brownian motion is one possibility. On the other hand, the oscillatory motion could be caused by metabolically driven forces. This question of whether Brownian or active forces caused the oscillatory motion is examined in the next section.

5.3 Brownian Versus Active Forces

The primary aim of this study was to understand the forces causing residual oscillatory motion of intraaxonal particles. It is argued here that oscillatory motion is caused by metabolic processes rather than by thermal

motions.

Oscillatory motion was a characteristic feature of organelle movements. Not only was this motion present in the inhibited preparations but it also was pervasive in normal transport. The undulatory variation in displacement of control particles (Fig. 3.1) was essentially an oscillatory motion. Koles and associates (1982a) similarly found low frequency perturbations superimposed on the linear displacements of transporting particles. The average frequencies of both the oscillatory motion when stationary, and when translating was about 0.18 ± 0.02 Hz (Fig. 3.15). When data from stationary oscillating particles were combined with those from translating particles a continuous distribution of data points resulted (Figs. 3.11, 3.13, 3.15, 3.16). On this basis there was no clear separation of translating organelles from stationary organelles. Moreover, the graph of mean velocity versus velocity fluctuations (Fig. 3.13) showed oscillations present at all transport velocities. Clearly, the transporting organelles had a superimposed oscillatory motion. Inhibitory agents might stop a particle from translating, but a residual oscillatory motion could persist. Either Brownian or active forces could cause these residual motions.

Dinitrophenol eventually stopped all particle movement—even the residual oscillation. Since DNP is known to inhibit oxidative phosphorylation it could be concluded that the residual oscillation depended on oxidative metabolism. The

implication here is that active, not Brownian forces, produced the oscillatory motion.

However, this argument is oversimplified. Although DNP eventually inhibited the oscillatory motion, this does not automatically imply that the residual oscillation depends upon oxidative phosphorylation. One way to illustrate the flaw in the preceding argument is with a counterexample: Suppose the residual oscillation was driven by Brownian forces. With the application of DNP, oxidative metabolism within cells was inhibited. As a result, transport ceased along with many other functions dependent on oxidative metabolism. If the maintenance of intraaxonal structure was dependent on oxidative metabolism then structural changes could have resulted after exposure to DNP. These structural changes could increase the resistance to organelle motion. Thus the disappearance of residual oscillation could have resulted from structural changes within axons that damped out Brownian motion.

It was thus pertinent to investigate any structural changes paralleling changes in organelle motion. The studies on frozen and thawed nerves were directed to this end. In these studies the return of transport after thawing, paralleled the reappearance of microtubules (Fig. 4.3). The slow disappearance of all motion after 30 minutes had no corresponding morphologic change. The possibility of thermal motions being damped out by structural changes was not supported by electron microscopy of thawed nerve.

In order to consider Brownian motion as a possible
cause of the oscillatory motion, the quantitative
observations in this study should be compared to predictions
from Brownian theory. It is thus necessary to digress with a
short discussion of Brownian theory.

The Langevin equation (McQuarrie 1976) defines the
behavior of a particle in Brownian motion:

$$du/dt = -\lambda u + A(t).$$
$$(5.1)$$

Here, u is the velocity of the particle, t is time, and $A(t)$
is a Gaussian random, fluctuating, acceleration imparted to
the particle by surrounding molecular motion. The parameter
$\lambda = 6\pi a\eta/m$, where a and m are the particle's radius and
mass, and η is the viscosity of the surrounding medium.
Equation (5.1) is a stochastic differential equation that
can be solved for a distribution of displacements (Shea and
Karnovsky 1966):

$$F(|x|) = \int_{-x/\sigma}^{x/\sigma} \exp[-q^2/2]\, dq\, /(2\pi)^{1/2},$$
$$(5.2)$$

where,

$$\sigma^2 = kTt/(3\pi a\eta).$$
$$(5.3)$$

Here, T is the absolute temperature, and k is Boltzman's constant ($k = 1.38 \times 10^{-23}$ J/°K).

In free Brownian motion a particle's mean squared displacement, $\langle r^2 \rangle$, is proportional to time:

$$\langle r^2 \rangle = 6Dt.$$

(5.4)

The diffusion coefficient, D, is given by Eq. (1.1).

The probability for a given displacement occurring by means of free Brownian motion is obtained by evaluating the integral in Eq. (5.2). Figure 5.1 gives the probabilities of different displacements for particles of 0.2 micrometers radius during a three second interval. It was assumed that the particles were within water at 22°C. For example, in three seconds 75% of the particles will have moved less than three micrometers. Conversely, only 25% of particles will have moved more than three micrometers. These calculations were done for a viscosity of 1×10^{-3} Pa•s. The viscosity experienced by axonal particles is probably higher, and thus their mobility would be less.

Brownian particles vibrate in position because of the surrounding continual molecular bombardment. The intensity of positional vibration, $G(f)$, will depend upon the particular frequency, f, of Brownian motion (McQuarrie 1976).
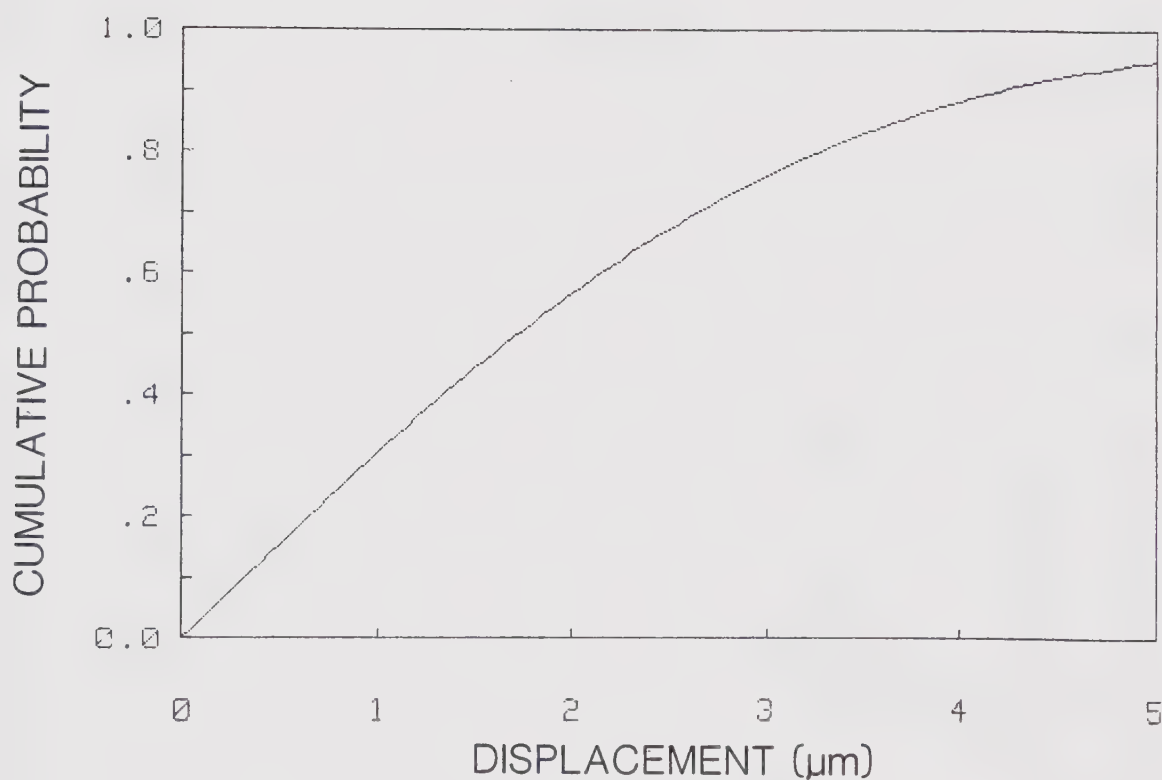
Figure 5.1 Probability of free Brownian displacements.
Calculations were for 0.2 micrometer radius particles
within water after three second intervals. During three
seconds 75% of particles will have moved less than three
micrometers.

$$G(f) = 4D/(\lambda^2 + 4 \; \pi^2 \; f^2).$$

$$(5.5)$$

The resultant power spectrum is plotted in Fig. (5.2). In this figure ^of is the relaxation frequency for the motion. It is given by the equation:

$$^of = kT/(2 \pi mD).$$

$$(5.6)$$

For particles of radius 0.2 micrometers and mass of $3x10^{-14}$ g at 22°C, the relaxation frequency is $2x10^7$ Hz.

Now, could free Brownian motion cause the oscillations in position that were superimposed upon the general linear trends? Since this oscillatory motion resulted in no net movement of the partices, free Brownian motion could not cause these oscillations. However, it is useful to compare the distances travelled by organelles to predictions from Brownian theory. This should indicate whether thermal motions could occur over similar distances.

A particle oscillating about a fixed intraaxonal position, or about a linear trend, could be expected to move a distance equal to one standard deviation of its displacement fluctuation within about one-quarter of its cycle. Refer now to the data in Fig. 3.17. The centers of spectral mass were generally greater than 0.2 Hz for the positional deviations below $3x10^{-5}$ cm. This indicated a greater influence of noise that shifted the spectral mass to
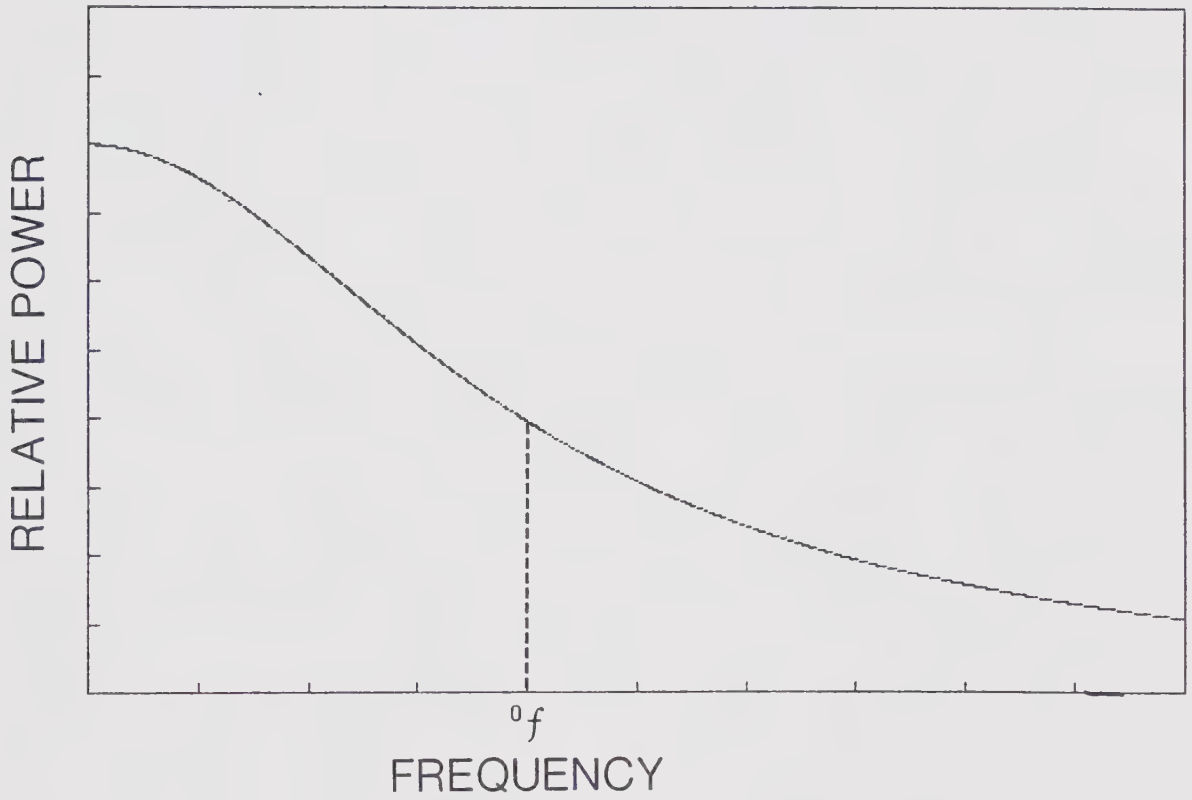
Figure 5.2 Theoretical power spectrum for free Brownian
motion: The frequency ^0f is called the relaxation frequency.
Here relative power is plotted versus relative frequency.

the right. For the signals not overly influenced by noise, the standard deviations ranged from 3×10^{-5} to 5×10^{-4} cm. These oscillations occurred with an average period of roughly 12 seconds. Thus an organelle could be expected to move 0.2 to 5 micrometers in about three seconds. Referring to Fig. 5.1, more than 95% of particles could be expected to move over 0.2 micrometers in three seconds. However, only about 5% could move over five micrometers. While the smaller displacements are within the range expected for Brownian motion, the larger displacements are much less probable. Indeed, the probability of Brownian forces moving a particle through one full cycle of motion is even smaller. Free Brownian motion was unlikely to occur over similar distances as did the larger oscillations.

Is there evidence that the larger fluctuations are a separate process from the smaller ones? The graphs of x versus y-axis standard deviations (Fig. 3.11), and first versus zeroth moments (Fig. 3.15) showed a continuous distribution of points over a wide range of values. There was no evidence for the larger fluctuations being a different process than the smaller ones. If Brownian motion were to explain the residual oscillation it would have to do so for all amplitudes of oscillation.

A further comparison of free Brownian motion to the data can be made. Figure 5.2 shows the theoretical power spectrum for the positional fluctuations of a free Brownian particle. The power shows a significant decrease at the

relaxation frequency. For typical intraaxonal particles, the relaxation frequency was estimated to be about 2×10^7 Hz. However, the frequencies of organelle oscillations occurred generally below 0.2 Hz, and thus the periodograms calculated from the data did not resemble the prediction for free Brownian motion (Figs. 3.1d, 3.2b, 3.5b, 3.7b, 3.8).

The predicted displacements and predicted power spectrum for free Brownian motion did not fit the experimental observations. Also, the anisotropy of oscillations could not be caused by free Brownian motion. The data given in Fig. 3.11 demonstrated a significantly larger component of oscillation along the x-axis than the y-axis. These data implied a spatial constraint on particle motion. While free Brownian motion, by definition, cannot have any constraints, there remain other thermally driven and constrained systems to be considered. One such constrained system is Brownian motion within small tubules (Brenner and Gaydos 1977).

In order to consider constrained thermal motion, it is necessary to digress from the present arguments and discuss some theoretical aspects of constrained motion. An idealized constrained system can be considered to have an input driving force, $y(t)$, causing an output motion, $x(t)$ (Bendat and Piersol 1971). In this discussion, this system is assumed to be linear, as a first approximation. The relation

between input and output is:

$$x(t) = \int_{-\infty}^{\infty} h(t°) \, y(t - t°) \, dt°,$$

(5.7)

where $h(t°)$ is the weighting function. Expressed in convolution algebra, the equation becomes:

$$X(f) = H(f) * Y(f).$$

(5.8)

$H(f)$ is the frequency response function. This response function determines the range of frequencies of input that can produce an output. With a narrow frequency response, the output will also.have a narrow frequency range— even with a wide range of input frequencies. The frequency response function is determined by the mechanical properties of the system.

For a system driven by thermal forces, the input is a broad band process, extending out to the relaxation frequencies of the surrounding molecules. In the case of intraaxonal particles, most of the driving force could be expected to come from water molecules. Using Eq. (5.6), the relaxation frequency for water is approximately 2×10^{13} Hz. Now the observed fluctuations of organelles had frequencies of about 0.1 Hz. In order for vibrations of water molecules to drive the organelle motions there must be some internal

axonal structure that damps out frequencies above the observed range. The frequency response of the system must therefore be relatively narrow.

It is unlikely that Brownian motion within tubules would possess such a narrow frequency response function without the addition of forces that could restrict the longitudinal movements of the particles within these tubules. A stronger interaction between organelles and internal axonal structures seems necessary. Such an interaction would result if organelles were bound by elastic forces to some internal axonal structure.

The application of a linear restoring force to a Brownian particle causes harmonic oscillations of the particle (Chandrasekhar 1943). The equation of motion [Eq. (5.1)] becomes:

$$du/dt = -\lambda u + A(t) - \omega^2 x.$$

(5.9)

Here, ω is the oscillator's undamped natural frequency. The observed frequency of the oscillator is:

$$f = (\omega^2 - \lambda^2/4)^{1/2}/(2\pi).$$

(5.10)

The parameter,

$$\beta = (\lambda^2 - 4\omega^2)^{1/2},$$

$$(5.11)$$

defines the resulting motion. If β is real, then the motion is overdamped; if imaginary, the motion is periodic; and if zero, the motion is aperiodic.

Chandrasekhar calculated the mean and mean squared values for the displacement and velocity of a harmonically bound Brownian particle:

$$\langle x \rangle = 0,$$

$$\langle u \rangle = 0,$$

$$\langle x^2 \rangle = kT/(m\omega^2),$$

$$\langle u^2 \rangle = kT/m.$$

$$(5.12)$$

These calculations are averages, taken over large time intervals.

The power spectrum for a harmonically bound Brownian particle is (Wang and Uhlenbeck 1945):

$$G(f) = 4D/|-(2\pi f)^2 + 2\pi j\lambda f + \omega^2|^2.$$

$$(5.13)$$

This spectrum is plotted in Fig 5.3. Note the narrow band of frequencies of the oscillator. This theoretical spectrum
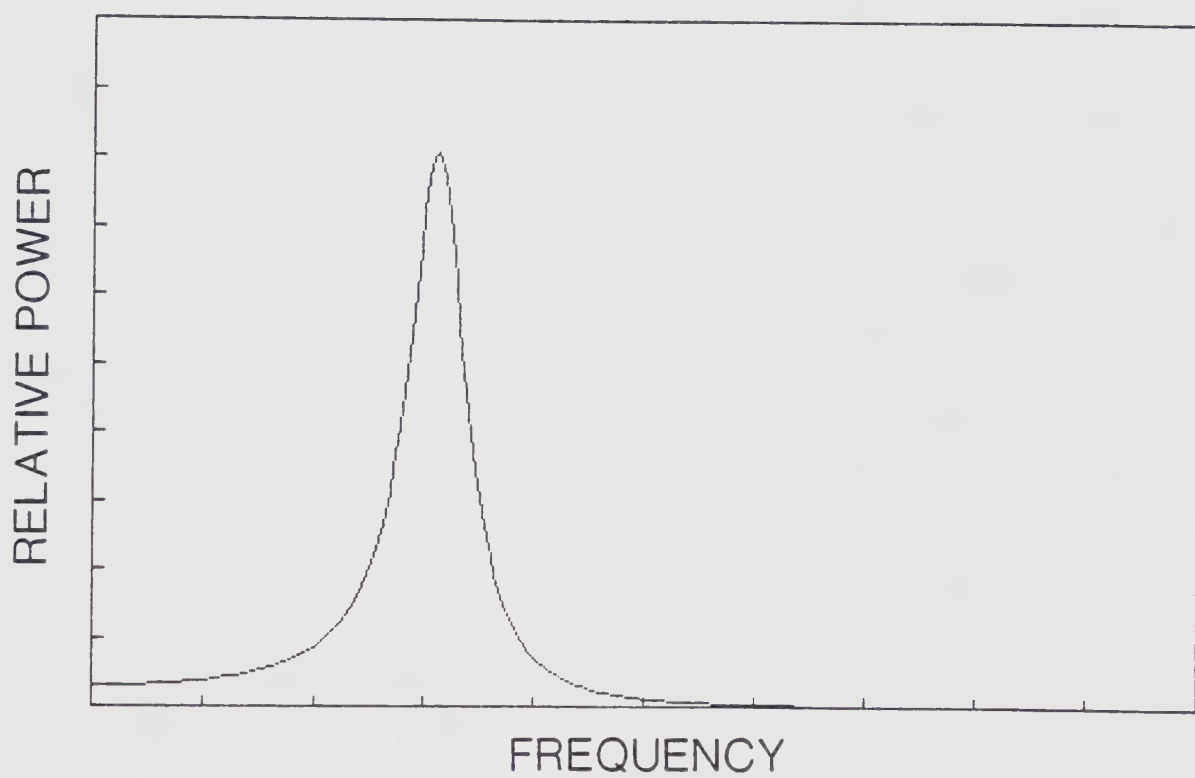
Figure 5.3 Power Spectrum For Harmonically Bound Brownian Motion

qualitatively resembles some of the observations (Figs. 3.1d, 3.5b, 3.6a, 3.7a).

A better comparison of organelle motion with predictions of harmonically bound Brownian motion results if Chandrasekhar's formulae are used [Eq. (5.12)]. Using these formulae, and assuming that the particles are of radius 0.2 micrometers, mass 3×10^{-14} g, with oscillations of 0.2 Hz, in water at 294°K gives the predictions outlined in Table 5.1. These predictions are not compatible with the observed motion. It is improbable that any form of Brownian motion could explain the oscillations of organelles.

Passive thermal forces are unlikely to cause the oscillations. An active, metabolically driven, force is more plausible. This force presumably also acts on translating particles. Transport inhibitors eliminate the translating component leaving a residual oscillation.

5.4 Involvement Of Microtubules In Axonal Transport

Whether axonal transport requires intact microtubules remains controversial (Grafstein and Forman 1980). Because of the small size of the system being investigated the arguments for and against involvement have necessarily been indirect. In this study more indirect evidence associating axonal transport with microtubules is presented.

In the experiments with rapidly frozen and thawed nerve, initially transport was completely inhibited. After a

TABLE 5.1

Harmonically Bound Brownian Predictions

	Predicted	Observed
$\langle u^2 \rangle$	$10^8 \ \mu m^2/s^2$	10^{-3} to $1 \ \mu m^2/s^2$
$\langle x^2 \rangle$	$3 \times 10^{-8} \ \mu m^2$	10^{-2} to $10 \ \mu m^2$

lag period of about five minutes from thawing, the organelles resumed transport. Concurrent with this, there was a reappearance of microtubules on transverse sections of axons (Plate 4.2). When these processes were closely compared, the recovery of axonal transport was found to parallel the reappearance of microtubules within axons (Fig. 4.3). In addition, colchicine prevented the recovery of transport and allowed only decreased numbers of microtubules to reappear.

These data were interpreted as follows: Freezing and thawing caused a rapid depolymerization of microtubules within axons. The microtubules disassociated into tubulin dimers. Rapid axonal transport, depending in some way on intact microtubules, was inhibited. Over the first ten

minutes after thawing the tubulin dimers were reassembled into microtubules. A threshold density of microtubules was reached, and axonal transport resumed. At first, transport was disjointed, occurring only over short intervals. With further repolymerization, larger segments of microtubules became available for transport. The motion then resembled normal transport.

Colchicine added to the thawing solutions bound the tubulin dimers; this inhibited any further reassembly of microtubules (Margolis and Wilson 1981). Without sufficient microtubules, axonal transport remained inhibited.

The reappearance of microtubules is explained by repolymerization of microtubules within ten minutes from thawing. Is this supported by the known behavior of microtubules? Depolymerization of microtubules within toad sciatic nerves has been observed at 2°C. This was followed by repolymerization after rewarming to 25°C (Rodriguez-Echandia and Piezzi 1968). Similar evidence for *in vivo* repolymerization of microtubules within *Actinosphaerium nucleofilum* was found to occur within four minutes of rewarming the specimen (Tilney and Porter 1967). Also, rates for tubulin formation and destruction have been measured at 50 micrometers per hour (Margolis and Wilson 1981). It is reasonable to conclude that microtubules could repolymerize within ten minutes of thawing.

Another interesting finding was that colchicine totally inhibited transport within ten minutes of its application to

thawing nerve. Yet, when applied to nonfrozen nerves,
colchicine required one to four hours to produce partial
inhibition (Hammond and Smith 1977). This discrepancy might
be explained by one of two mechanisms:

1.   Colchicine has a more rapid action with free tubulin
     than with intact microtubules.

2.   Cell permeability to colchicine is increased after
     thawing.

The first mechanism is reasonable. Colchicine inhibits
microtubule assembly by successively binding free tubulin
followed by the binding of this tubulin-colchicine complex
to the ends of microtubules (Margolis and Wilson 1981).
Thus, if the microtubules are already depolymerized, this
reaction should proceed more quickly. There is also evidence
for increased permeability of cell membranes after freezing
and thawing (Daw *et al*. 1973; Wellman and Pendyla 1979).
Indeed, the convolutions and clefts observed on the axonal
cell membranes after thawing, indicated damage that could
possibly have allowed entry of larger molecules into axons
(Plates 4.1*a*, 4.1*b*).

5.5 Characteristics Of Organelle Transport

     In this study the motion of organelles within axons was
analysed using sophisticated quantitative techniques. The
results obtained revealed certain basic features of
organelle movement. A closer examination of these features

might allow a better understanding of the mechanisms behind organelle movement.

In this section several properties of organelle transport are examined:

1. the oscillatory motion,

2. the anisotopic motion,

3. the fluctuations in velocity, and

4. the velocity distributions.

Each of these properties has possible implications concerning the mechanism of transport.

Next, the stochastic nature of organelle movements is discussed. Several questions are considered: Does the random appearance of the motion imply a mechanism with random features? Could an underlying deterministic process be responsibile for the apparently random motion of organelles? Could such a complicated behavior of particles occur in a fluid flow model? These questions are discussed in the context of the experimental observations.

Finally, the abrupt changes in motion of some particles are discussed. Possible explanations for this behavior are examined.

5.5.1 Oscillatory Motion

An oscillatory component of motion was superimposed on the movement of all particles. Both translating particles and stationary particles exhibited this motion. No difference could be found between the oscillatory motion of

translating particles and that of stationary particles. Indeed, these two processes were probably the same. Agents that inhibited axonal transport destroyed the translatory component leaving a residual oscillation. The oscillatory motion was pervasive in organelle transport. No moving organelles were observed without it. Moreover, oscillations were the last component of motion to disappear when transport was inhibited. It is possible that oscillatory motion is a necessary and fundamental component of transport. Since thermal motion could not cause these oscillations, they must result from a metabolic process. The oscillatory motion probably is a result of an underlying mechanochemical mechanism.

One further aspect of the oscillatory motion should be discussed. Was there any evidence that these oscillations were saltatory? Rebhun's (1972) definition of saltatory motion required that particles exhibit intermittent jumps of several microns at velocities of several micrometers per second. The velocity of particles undergoing saltatory motion must be discontinuous. While occasional abrupt movements of particles were observed, on the average, the observed movements were smooth. By smooth, it is meant that low frequency (<0.2 Hz) components of motion predominated. Abrupt motions would be indicated by by the presence of high frequency components. No such high frequency oscillations were discernible— within the limits of experimental accuracy.

There are precedents for oscillatory motion in other biological systems. Flagella, cilia (Brokaw 1975), and insect flight muscle (Jewel and Ruegg 1966) have oscillatory mechanisms. The mechanism for oscillations within neurons remains unknown. The oscillations of cilia are thought to result from interactions between microtubules that are contained within them. It may be that intraaxonal microtubules induce oscillatory movements of particles through a related mechanism.

5.5.2 Anisotropic Motion

Organelle movement had two anisotropic features:

1. The transport of organelles occurred longitudinally.
2. The oscillations of organelles were directed longitudinally.

Guiding tracks or channels could account for the longitudinal direction of transport (Leestma 1976). It is possible that similar structures could constrain oscillations to longitudinal directions.

5.5.3 Velocity Fluctuations

With the fluctuations in position of transporting particles, there corresponded fluctuations in velocity. Since the movement of organelles occurred with low Reynolds numbers, each organelle's velocity was directly related to the net force acting on it. A fluctuating velocity indicated a fluctuating force. Either variations in drag or variations

in driving force could have caused these fluctuations in velocity (Koles *et al.* 1982a).

Similar fluctuations in velocity occurred with particles moving about fixed positions. The drag experienced by such a particle is directly proportional to its velocity [Eq. (1.4)]. Since the particles that moved about fixed positions had no net velocity, they experienced no net drag. Thus, their back and forth motion could not result from fluctuations in drag. It seems more likely that a fluctuating driving force could be responsible.

The oscillations of both translating and stationary particles possibly resulted from the same process. Now, if a fluctuating driving force caused stationary particles to move back and forth then this could cause fluctuations of transporting particles too.

5.5.4 Velocity Distributions

The distribution of instantaneous velocity for organelles that moved back and forth about fixed positions was unimodal (Fig. 3.14). Translating particles also have unimodal distributions (Koles *et al.* 1982a). Goldberg and associates (1978) proposed a theory in which organelles alternated between moving and nonmoving states. Their theory predicted a bimodal distribution of velocity. In the present study, there was no evidence to support this theory.

5.5.5 Complicated Nature Of Particle Movements

The motion of individual organelles within axons had several characteristic features:

1. Each particle moved independently of its neighbours.
2. Particles within one micrometer of each other took divergent paths.
3. The motion of individual particles was punctuated by unpredictable changes in speed and direction.
4. The oscillatory motion of individual particles varied in amplitude and frequency in an apparently random manner, although these variations occurred within narrow bounds.
5. Particles that were oscillating about fixed positions could unexpectedly start transporting and *vice versa*.

Three possible hypotheses for these rather complex motions are discussed here.

First, the motion might result from a periodic process with a superimposed random noise (Bendat and Piersol 1971). Basically, some deterministic mechanochemical process could drive particles while the added noise could result from random perturbations introduced by neighbouring intracellular processes. Is this hypothesis of organelle movement supported by the experimental data? The theoretical power spectrum for this hypothetical process would consist of a discrete delta function with a surrounding smooth and broad spectrum. In this study the periodograms obtained showed large peaks generally below about 0.1 Hz. Within the limits of experimental accuracy, a discrete delta function

cannot be ruled out. This sort of process is one of several that could be considered.

Second, the motion may result from a narrow band random process. Here, the motion of an individual particle would be random. However, these oscillations would be restricted to a narrow band of frequencies. This restriction on frequency could result from physical constraints to particle movements, or from mechanochemical limitations on the driving forces. When the data from this study were reviewed, the periodograms were qualitatively consistent with narrow band random processes.

While the complicated motion of individual organelles could result from an underlying stochastic mechanism, this is not necessarily so. It is possible for a deterministic mechanism to produce a complicated and apparently random motion (May 1976). The resultant power spectrum from such a process could mimic narrow band or even wide band random data. This third hypothesis is examined in detail in the following text.

The term *chaotic* can be used to describe the complicated movements of particles governed by deterministic equations (Ott 1981). Chaotic motion, while apparently random, is not necessarily so (Eckmann 1981). Three criteria for chaotic motion are:

1. *a sensitive dependence on initial conditions*,

2. the power spectrum of such a process consists of a relatively broad band, and

3.   the motion is aperiodic.

The motion of intraaxonal organelles generally appeared to
satisfy these criteria.

How could chaotic motion occur within axons? If we
consider fluid flow models then is it reasonable to assume
that the motion of organelles results from turbulent fluid
flow? This latter question might be answered by considering
the flow of fluids within tubes. The Reynolds number for
this type of flow is (Geankoplis 1978):

$$R = a v \rho / \eta .$$

(5.14)

where a is the diameter of a tube. Substitute in values to
maximize the Reynolds number, for the case of flow within
axons: the diameter of the tube cannot be larger than the
diameter of its axon thus let a = 10 μm; the speed of the
flow should be about the usual speed for particles thus v =
1 μm/s; the density of axoplasm, ρ = 10^3 kg/m^3; and the
viscosity of axoplasm should not be less than that of water
thus η = 1×10^{-3} Pa•s. The resultant Reynolds number is
1×10^{-5}. A flow within a straight circular tube is always
laminar when the Reynolds number is less than 2100. Thus
turbulence cannot occur within any conceivable flow within
axons. Chaotic motion of intraaxonal organelles cannot
result from turbulence of fluids.

We are still left with the question of how chaotic motion could arise within axons. For fluid flow models to be feasible, it is necessary for a complicated system of channels or guides to exist within axons. These channels would necessarily be about one micrometer wide so that a channel could be individualized to each particle. On the other hand we could abandon the microstream hypothesis for a mechanism that moves particles through a stationary fluid. This mechanism probably would have to be individualized to each particle.

The complicated motion of organelles can be further analysed by constructing phase diagrams. A phase diagram consists of the curve defined by plotting $x'(t)$ versus its corresponding function, $x(t)$. The resultant curve in phase space is termed an orbit (Hofstadter 1981). A phase diagram was produced from observations of a moving intraaxonal organelle in Fig. 3.10. The resultant self-intersecting orbit describes the complicated motion of an organelle within an axon.

How can the phase diagram in Fig. 3.10 be interpreted? The orbit meanders over its phase plane in an apparently random manner. One simplistic interpretation is that some random influence perturbed the motion of the particle. However, if the particle's motion is chaotic, its motion could be entirely deterministic. The meandering orbit could then result from a sensitive dependence of the process on initial conditions.

While the orbit in Fig. 3.10 has a complicated pattern, it is confined to a bounded region of its phase plane. When such limits are imposed on phase orbits an *attractor* is said to be present (Eckmann 1981). Often orbits around attractors have well-defined ovoid patterns. However, the orbit in Fig. 3.10 shows no such pattern. This sort of behavior could indicate the presence of a *strange attractor*. Again, such properties arise from nonlinear equations of motion.

The main point of this section is that while the oscillatory motion was complicated and had apparently random properties, it could also be deterministic. It is possible for a very complicated motion to be deterministic. If the process were deterministic, then the complicated motion of organelles would be a reflection of underlying nonlinear processes.

5.5.6 Abrupt Changes In Motion

One other type of movement was observed within axons. In certain preparations some particles alternated between stationary and translating states. A particle could oscillate about a fixed position then abruptly start translating. This motion was only rarely observed within the control preparations. Only those preparations with inhibited transport commonly exhibited this motion.

It must be emphasized that these abrupt changes in motion were not the saltatory motions described by earlier workers (Leestma and Freeman 1977; Forman *et al.* 1977a).

These early studies were observations on the uninhibited transport of organelles, while the abrupt movements discussed here resulted from partially inhibited transport.

What are the factors that cause these abrupt movements? No association was found with frequency of oscillation, total velocity, nor amplitude of oscillation. Perhaps these transitions resulted from the initiation of a driving force, or the removal of a resistive force.

Another possible explanation for these movements involves chaotic motion. Under certain conditions a particle moving in the chaotic regime may take an orbit that diverges from a region of attraction. For example, suppose the equation of motion of an organelle resembled the Duffing equation (Davis 1962):

$$x'' + x + ax^3 = b \sin(kt).$$

(5.15)

Here, the position of an organelle is $x = x(t)$; a, b, and k are constants. A particle moving according to the Duffing equation may oscillate about an attractor or it may take a divergent path. A numerical solution of the Duffing equation is shown in Fig. 5.4. This solution exhibits a typical divergence.

The point to be emphasized here is that a deterministic process could produce the abrupt changes in motion of organelles. The complicated motion of organelles may be the
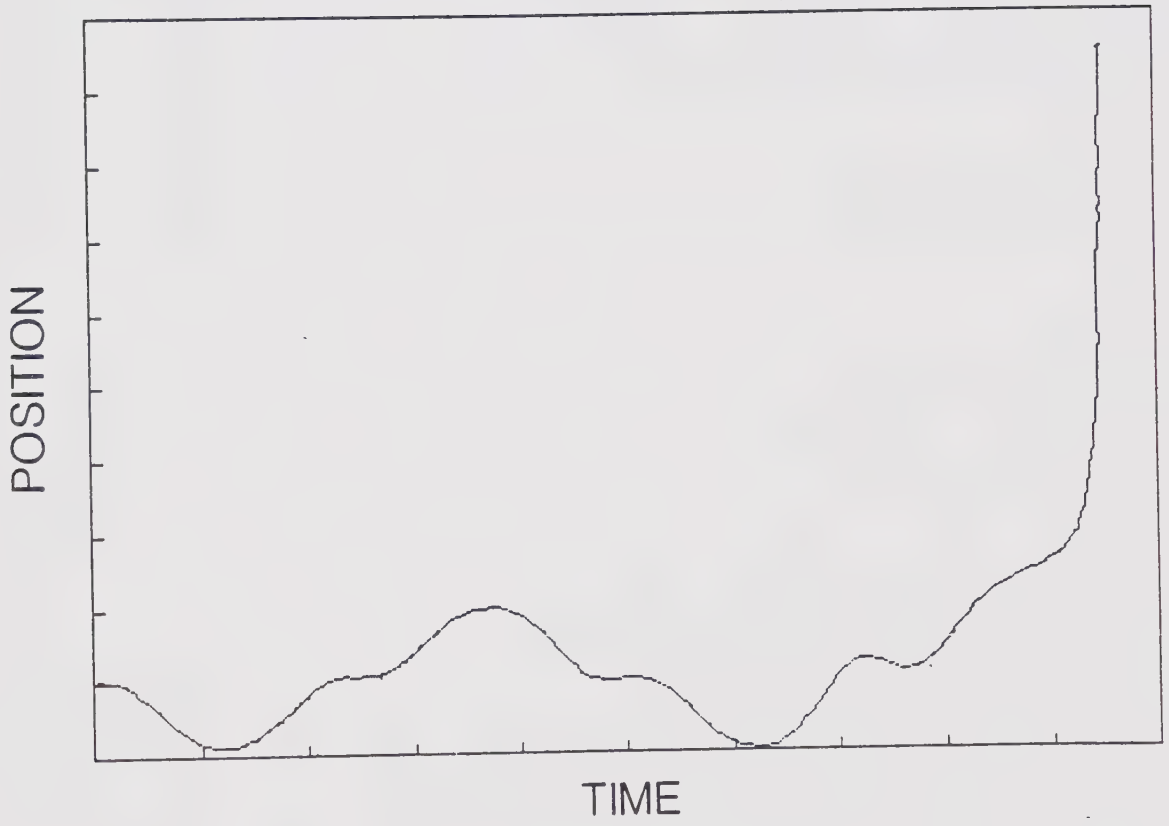
Figure 5.4 A Solution Of Duffing's Equation

result of a relatively simple, but nonlinear, mechano-
chemical process.

5.6 Conclusion

The primary aim of this study was to investigate the
residual motion of intraaxonal organelles. Much work was
devoted to demonstrating that thermal forces could not
produce this motion. Since Brownian motion was an improbable
cause of this motion, then the motion should be secondary to
a metabolic process.

Normal axonal transport consisted of two components:
1. a translatory component, and
2. an oscillatory component.
The inhibition of rapid transport eliminated the translatory
component leaving residual oscillations. With further
inhibition even these oscillations ceased.

The oscillatory component of transport was quite
complicated. Either a stochastic process or a nonlinear and
deterministic process could produce this motion. This
distinction, while apparently abstract, does have
implications concerning the driving mechanism. The mechanism
could either be a stochastic process, analagous to Brownian
motion, or a highly coordinated and complicated
mechanochemical process. It is probable that the
oscillations are caused by the underlying mechanism for
transport. Perhaps these oscillations are a result of an

oscillatory chemical reaction, or some cyclical control
mechanism governing a mechanochemical process.

A secondary aim of this study was to investigate the
recovery of axonal transport after freezing and thawing.
This stress inhibited transport, and destroyed intraaxonal
microtubules. Both of these actions were spontaneously
reversible. Recovery of transport paralleled the
reappearance of microtubules. Furthermore, colchicine
prevented both recovery of transport and reappearance of
microtubules. Because of this circumstantial evidence, it
was concluded that axonal transport likely depended on
microtubules.

The final goal was to study the motion of organelles in
order to evaluate several postulated models for transport.
Unfortunately, none of the currently popular models could
explain all aspects of transport.

From the observations and theoretical considerations
examined in this thesis, several hypotheses concerning
transport can be proposed:

1. Fast axonal transport involves primarily particles.

2. The driving force is individualized to each particle.

3. The driving force is both oscillatory and bidirectional.

4. Some mechanism exists to convert bidirectional
   oscillations to unidirectional movement.

5. There is a recognition system that determines the speed
   and direction of travel for each particle.

6. Transport requires oxidative metabolism.

7. Rapid axonal transport could possibly depend upon intact
    microtubules: as structural supports, as guides for
    movement, or as components of the driving mechanism.

    To go any further and construct a detailed model would
require several assumptions. Any one of these assumptions
would likely be incorrect. Rather than constructing an
abstract model, the best way to understand the mechanism of
axonal transport would be to perform well designed
experiments that are aimed at elucidating this mechanism.
Any understanding of the mechanism of transport must be
closely based on experimental results.

REFERENCES

Adams, R., Baker, P. F., and Bray, D. 1982. Particle movement in crustacean axons that have been rendered permeable by exposure to brief intense electric fields. Proc. Physiol. Soc. in: J. Physiol. 321:16P-17P.

Allen, R. D., David, B. F., Nomarski, G. 1969. The Zeiss-Nomarski differential interference equipment for transmitted light microscopy. Zeitschr. F. Wiss. Mikr. und Mikrotech. 69:193-221.

Anderson, K. E., Edstrom, A., and Hanson, M. 1972. Heavy water reversibly inhibits fast axonal transport of proteins in frog sciatic nerves. Brain Res. 43:299-302.

Appeltauer, G. S. L., and Korr, I. M. 1975. Axonal delivery of soluble, insoluble, and electrophoretic fractions of neuronal proteins to muscle. Exp. Neurol. 46:132-146.

Arhem, P. 1975. Diffusion of sodium in axoplasm of myelinated nerve fiber: potential clamp analysis. Acta. Physiol. Scanc. 97:415-425.

Bendat, J. S. and Piersol, A. G. 1971. *Random data: analysis*

and measurement procedures. New York: John Wiley & Sons, Inc.

Biondi, R. J., Levy, M. J., and Weiss, P. A. 1972. An engineering study of the peristaltic drive of axonal flow. Proc. Natl. Acad. Sci. USA 69:1732-1736.

Brady, S. T., Crothers, S. D., Nosal, C., and McClure, W.O. 1980. Fast axonal transport in the presence of high Ca^{2+}: evidence that microtubules are not required. Proc. Natl. Acad. Sci. USA. 77:5905-5913.

Bray, D., and Bunge, M. B. 1981. Serial analysis of microtubules in cultured rat sensory axons. J. Neurocytol. 10:589-605.

Bray, D. and Gilbert, D. 1981. Cytoskeletal elements in neurons. Ann. Rev. Neurosci. 4:505-523.

Bray, J. J., Kon, C. M., and Brekenridge, B. McL. 1971. Reversed polarity of rapid axonal transport in chicken motoneurons. Brain Res. 33:560-564.

Brenner, H., and Gaydos, L. J. 1977. The constrained Brownian movement of spherical particles in cylindrical pores of comparable radius. J. Colloid Interface Sci. 58:312-356.

Breuer, A. C., Christian, C. N., Henkart, M., and Nelson, P.
    G. 1975. Computer analysis of organelle translocation in
    primary neuronal cultures and continuous cell lines. J.
    Cell. Biol. 65:562-576.

Brimijoin, S. 1979. On the kinetics and maximal capacity of
    the system for rapid axonal transport in mammalian
    neurones. J. Physiol. 292:325-337.

Brimijoin, S., Olsen, J., and Rosenson, R. 1979. Comparison
    of the temperature dependence of rapid axonal transport
    and microtubules in nerves of the rabbit and bullfrog.
    J. Physiol. 287:303-314.

Brokaw, C. J. 1975. Molecular mechanism for oscillation in
    flagella and muscle. Proc. Natl. Acad. Sci. USA.
    72:3102-3106.

Byers, M. R. 1974. Structural correlates of rapid axonal
    transport: evidence that microtubules may not be
    directly involved. Brain Res. 75:97-113.

Cancalon, P., and Beidler, L. M. 1975. Distribution along
    the axon and into various subcellular fractions of
    molecules labeled with [^{3}H] leucine and rapidly
    transported in the garfish olfactory nerve. Brain Res.

89:225-244.

Casley-Smith, J. R. 1964. The Brownian movements of
    pinocytic vesicles. J. Roy. Microscop. Soc. 82:257-261.

Chan, S. Y., Ochs, S., and Worth, R. M. 1980. The
    requirements for calcium ions and the effect of other
    ions in axoplasmic transport in mammalian nerve. J.
    Physiol. 301:477-504.

Chandrasekhar, S. 1943. Stochastic problems in physics and
    astronomy. Rev. Mod. Phys. 15:1-89.

Cooper, P. D., and Smith, R. S. 1974. The movements of
    optically detectable organelles in myelinated axons of
    Xenopus laevis. J. Physiol. 242:77-97.

Daniels, F., and Alberty, R. A. 1961. *Physical Chemistry*.
    2nd ed. London: John Wiley & Sons, Inc.

Davis, H. T. 1962. *Introduction to nonlinear differential
    and integral equations.* New York: Dover Publications,
    Inc.

Daw, A., Farrant, J., and Morris, G. J. 1973. Membrane
    leakage of solutes after thermal shock or freezing.
    Cryobiology 10:126-133.

Donoso, J. A., Illanes, J. P., and Samson, F. 1976. Dimethylsulfoxide action on fast axoplasmic transport and ultrastructure of vagal axons. Brain Res. 120: 287 301.

Droz, B., and Leblond, C. P. 1962. Migration of proteins along the axons of the sciatic nerve. Science 137:1047-1048.

Droz, B., Rambourg, A., and Koenig, H. L. 1975. The smooth endoplasmic reticulum: structure and role in the renewal of axonal membrane and synaptic vesicles by fast axonal transport. Brain Res. 93:1-13.

Eckmann, J. P. 1981. Roads to turbulence in dissipative dynamical systems. Rev. Mod. Phys. 53:643-654.

Edstrom, A. 1974. Effects of Ca^{++} and Mg^{++} on rapid axonal transport of proteins in vitro in frog sciatic nerves. J. Cell. Biol. 61:812-818.

Edstrom, A., and Mattsson, H. 1972. Fast axonal transport *in vitro* in the sciatic system of the frog. J. Neurochem 19:205-221.

Elam, J. S., and Agranoff, B. W. 1971. Rapid transport of

protein in the optic system of the goldfish. J.
Neurochem. 18:375-387.

Forman, D. S., Padjen, A. L., and Siggins, G. R. 1977a.
Axonal transport of organelles visualized by light
microscopy: cinemicrographic and computer analysis.
Brain Res. 136:197-213.

Forman, D. S., Padjen, A. L., and Siggins, G. R. 1977b.
Effect of temperature on the rapid retrograde transport
of microscopically visible intra-axonal organelles.
Brain Res. 136:215-226.

Geankoplis, C. J. 1978. *Transport processes and unit
operations.* Boston: Allyn and Bacon, Inc.

Glasoe, P. K., and Long, F. A. 1960. Use of glass electrodes
to measure acidities in deuterium oxide. J. Phys. Chem.
64:188-190.

Goldberg, D. J., Schwartz, J. H., and Sherbany, A. A. 1978.
Kinetic properties of normal and perturbed axonal
transport of serotonin in a single identified axons. J.
Physiol. 281:559-579.

Grafstein, B., and Forman, D. S. 1980. Intracellular
transport in neurons. Physiol. Rev. 60:1167-1283.

Gross, G. W., and Weiss, D. G. 1977. Subcellular
    fractionation of rapidly transported axonal material in
    olfactory nerve: evidence for a size-dependent molecule
    separation during transport. Neurosci. Lett. 5:15-20.

Gross, G. W., and Weiss, D. G. 1982. Theoretical
    considerations on rapid transport in low viscosity
    axonal regions. in: *Axonal Transport*. ed. D. G. Weiss.
    Berlin: Springer-Verlag.

Haak, R. A., Kleinhans, F. W., and Ochs, S. 1976. the
    viscosity of mammalian nerve axoplasm measured by
    electron spin resonance. J. Physiol. 263:115-137.

Hammond, G. R., and Smith, R. S. 1977. Inhibition of the
    rapid movement of optically detectable axonal particles
    by colchicine and vinblastine. Brain Res. 128:227-242.

Hanson, M., and Edstrom, A. 1977. Fast axonal transport:
    effects of antimitotic drugs and inhibitors of energy
    metabolism on the rate and amount of transported protein
    in frog sciatic nerves. J. Neurobiol. 8:97-108.

Hejnowicz, Z. 1970. Propagated disturbances of transverse
    potential gradient in intracellular fibrils as the
    source of motive forces for longitudinal transport in

cells. Protoplasma 71:343-364.

Hofstadter, D. R. 1981 Strange attractors: mathematical patterns delicately poised between order and chaos. Sci. Am. 245:22-43.

Horie, H., Takenaka, T., and Inomata, K. 1981. Effects of antimitotic drugs on axoplasmic transport in tissue cultured nerve cells. in: Abstracts, Soc. Neurosci. 11th annual meeting, Vol. 7. 1981 pp. 485, Bethesda Maryland: Society for Neuroscience.

Jewell, B. R., and Ruegg, J. C. 1966. Oscillatory contraction of insect fibrillar muscle after glycerol extraction. Proc. R. Soc London Ser. B 164:428-459.

Kaminura, S., and Takahashi, K. 1981. Direct measurement of the force of microtubule sliding in flagella. Nature 293:566-568.

Kerkut, G. A. 1975. Axoplasmic Transport. Comp. Biochem, Physiol. A. 51:701-704.

Kirkpatrick, J. B., Bray, J. J., and Palmer, S. M. 1972. Visualization of axoplasmic flow *in vitro* by Nomarski microscopy. Comparison to rapid flow of radioactive proteins. Brain Res. 43:1-10.

152

Koles, Z. J., McLeod, K. D., and Smith, R. S. 1982a. A study
    of the motion of organelles which undergo retrograde and
    anterograde rapid axonal transport. J. Physiol. London.
    (in press).

Koles, Z. J., McLeod, K. D., and Smith, R. S. 1982b. The
    determination of the instantaneous velocity of axonally
    transported organelles from filmed records of their
    motion. Can. J. Physiol. Pharmacol. (in press)

Lasek, R. 1968. Axoplasmic transport in cat dorsal root
    ganglion as studied with [³H]-L-leucine. Brain Res.
    7:360-377.

Leestma, J. E. 1976. Velocity measurements of particulate
    neuroplasmic flow in organized mammalian CNS tissue
    cultures. J. Neurobiol. 7:173-183.

Leestma, J. E., and Freeman, S. S. 1977. Computer-assisted
    analysis of particulate axoplasmic flow in organized CNS
    tissue cultures. J. Neurobiol. 8:453-467.

Lehninger, A. I. 1972. *Biochemistry.* New York: Worth
    Publishers, Inc.

Lorenz, T., and Willard, M. 1978. Subcellular fractionation

of intra-axonally transported polypeptides in the rabbit visual system. Proc. Natl. Acad. Sci USA 75:505-509.

Lubinska, L., and Niemierko, S. 1971. Velocity and intensity of bidirectional migration of acetylcholinesterase in transected nerves. Brain Res. 27:329-342.

Mackey, S., Schuessler, G., Goldberg, D.J., and Schwartz, J.H. 1981. Dependence of fast axonal transport on the local concentration of organelles. Biophys. J. 36: 455-459.

Margolis, R. L., and Wilson, L. 1981. Microtubule treadmills— possible molecular machinery. Nature 293:705-711.

Marion, J. B. 1970. *Classical dynamics of particles and systems.* New York: Academic Press.

May, M. 1976. Simple mathematical models with very complicated dynamics. Nature 261:459-467.

McEwen, B. S., and Grafstein, B. 1968. Fast and slow components in axonal transport of protein. J. Cell. Biol. 38: 494-508.

McLeod, K. D. 1980. The dynamics of the motion of optically

detectable particles in nerve axons. M.Sc. thesis,
University of Alberta, Edmonton. Alberta.

McQuarrie, D. H. 1976. *Statistical Mechanics*. New York:
Harper & Row.

Menz, L. J. 1975. Effect of cryoprotective agents on rat
cutaneous nerves. Cryobiology 12:405-416.

Ochs, S. 1974. Systems of material transport in nerve fibers
(axoplasmic transport) related to nerve function and
trophic control. Ann. N. Y. Acad. Sci. 228: 202-223.

Ochs. S. 1982. On the mechanism of axoplasmic transport. in:
Axoplasmic Transport. ed. D. G. Weiss. Berlin:
Springer-Verlag.

Ochs, S., and Hollingsworth, D. 1971. Dependence of fast
axoplasmic transport in nerve on oxidative mechanisms.
J. Neurochem. 18:107-114.

Odell, G. M. 1976. A new mathematical continuum theory of
axoplasmic transport. J. Theor. Biol. 60:223-237.

Olson, R. M. 1967. *Essentials of engineering fluid
mechanics*. Scrandon Pennsylvania: International Textbook
company.

Ott, E. 1981. Strange attractors and chaotic motions of dynamical systems. Rev. Mod. Phys. 53:655-671.

Piddington, R. W. 1976. Laser measurement of Biological movement. in: *Calcium in Biological Systems.* SEB Symposia #30. Cambridge: Cambridge University Press.

Porter, K. R., Byers, H. R., and Ellisman, M. H. 1979. The cytoskeleton. in: *The neurosciences, 4th study program.* eds. F. O. Schmitt, and F. G. Worden, pp. 703-722. Cambridge, MA:MIT press.

Purcell, E. M. 1977. Life at low Reynolds number. Am. J. Phys. 45:3-11.

Rambourg, A., and Droz, B. 1980. Smooth endoplasmic reticulum and axonal transport. J. Neurochem. 35:16-25.

Rang, H. P., and Ritchie, J. M. 1968. The dependence on external cations of the oxygen consumption of mammalian non-myleinated fibers at rest and during activity. J. Physiol. 196:163-181.

Rebhun L. I. 1959. Studies of early cleavage in the surf clam, *Spisula solidssima*, using methylene blue and toluidine blue as vital stains. Biol. Bull. 117:518-545.

Rebhun, L. I. 1972. Polarized intracellular particle
    transport: saltatory movements and cytoplasmic
    streaming. Int. Rev. Cytol. 32:93-137.

Rodriguez-Echandia, E. L., and Piezzi, R. S. 1968.
    Microtubules in the nerve fibers of the toad *Bufo*
    arenarum Hensel. J. Cell Biol. 39:491-497.

Rubinow, S. I., and Blum, J. J. 1980. A theoretical approach
    to the analysis of axonal transport. Biophys. J.
    30:137-148.

Rubinson, K. A., and Baker, P. F. 1979. The flow properties
    of axoplasm in a defined chemical enviroment: influence
    of anions and calcium. Proc. Roy. Soc. Lond. B.
    205:323-345.

Sabri, M. I., and Ochs, S. 1973. Characterization of fast
    and slow transported proteins in dorsal root and sciatic
    nerve of cat. J. Neurochem. 4:145-165.

Samson, F. E. 1971. Mechanism of axoplasmic transport. J.
    Neurobiol. 2:347-360.

Schliwa, M., Euteneuer, U., Bulinski, J. C., and Izant, J.
    G. 1981. Calcium lability of cytoplasmic microtubules

and its modulation by microtubule-associated proteins.
Proc. Natl. Acad. Sci USA 78:1037-1041.

Schmitt, F. O. 1968. Fibrous proteins— neuronal organelles.
Proc. Natl. Acad. Sci. USA 60:1092-1101.

Schwartz, J. H. 1979. Axonal transport: components,
mechanisms, and specificity. Ann. Rev. Neurosci.
2:467-504.

Shaw, T. I., and Newby, B. J. 1972. Movement in a ganglion.
Biochim. Biophys. Acta. 255:411-412.

Shea, S. M., and Karnovsky, M. J. 1966. Brownian motion: a
theoretical explanation for the movement of vesicles
across the endothelium. Nature 212:353-355.

Shield, L. K., Griffin, J. W., Drachman, D. B., and Price,
D. L. 1977. Retrograde axonal transport: a direct method
for measurement of rate. Neurology 27: 393.

Shimshoni, M. 1971. On Fisher's test of significance in
harmonic analysis. Geophys. J. R. Astr. Soc. 23:373-377.

Smith, R. S. 1980. The short term accumulation of axonally
transported organelles in regions of localized lesions
of single myelinated axons. J. Neurocytol. 9:39-65.

158

Smith, R. S., and McLeod, K. D. 1979. Unusual particle
    trajectories and structural arrangements in myelinated
    nerve fibers. Can. J. Physiol. Pharmacol. 57:1182-1186.

Snyder, R. E., Reynolds, R. A., Smith, R. S., Kendal, W. S.
    1976. Application of a multiwire proportional chamber to
    the detection of axoplasmic transport. Can. J. Physiol.
    Pharmacol. 54:238-244.

Snyder, R. E. 1982. (private communication)

Taylor, E. W. 1965. Brownian and saltatory movements of
    cytoplasmic granules and the movement of anaphase
    chromosomes. in: *4th international congress on rheology,
    Proceedings part 4, Symposium on biorheology.* ed. A. L.
    Copley, New York: Interscience Publishers.

Tilney, L. G., and Porter, K. R. 1967 Studies on the
    microtubules in heliozoa. J. Cell. Biol. 34:327-343.

Tretter, S. A. 1976. *Introduction to discrete-time signal
    processing.* New York : John Wiley & Sons, Inc.

Vanmarke, E. H. 1977., Method of spectral moments to
    estimate structural damping. in: *Stochastic problems in
    dynamics*, ed. B.L. Clarkson, pp 515-524 London: Pitman

Publishing Limited.

Wang, M. C., and Uhlenbeck, G. E. 1945. On the theory of
    Brownian motion II. Rev. Mod. Phys. 17:323-342.

Weiss, P. A. 1970. Neuronal dynamacis and neuroplasmic flow.
    in: *The neurosciences: second study program*, ed. F. O.
    Schmitt, pp840-850. New York: Rockefeller University
    Press.

Weiss, P. A., and Hiscoe, H. B. 1948. Experiments on the
    mechanism of nerve growth. J. Exp. Zool. 107:315-395.

Weiss, P. A., and Mayr, R. 1971. Organelles in neuroplasmic
    ('axonal') flow: neurofilaments. Proc. Natl. Acad. Soc.
    USA. 68:846-850.

Wellman, A. M., and Pendyla, L. 1979. Permeability changes
    in membranes of *Neurospora crassa* after freezing and
    thawing. Cryobiology 16:184-195.

Willard, M., Cowan, W. M., and Vagelos, P. R. 1974. The
    polypeptide composition of intraaxonally transported
    proteins: evidence for four transport velocities. Proc.
    Natl. Acad. Sci. USA. 71:2183-2187.